DEVELOPMENT OF A T-LOOP ASSAY TO INVESTIGATE

T-LOOP DYNAMICS AND STRUCTURE

APPROVED BY SUPERVISORY COMMITTEE

Jerry W. Shay, Ph.D.
Professor of Cell Biology

Woodring E. Wright, M.D., Ph.D.
Professor of Cell Biology

Sandeep Burma, Ph.D.
Assistant Professor of Radiation Oncology

Hongtao Yu, Ph.D.
Professor of Pharmacology

DEDICATION

Dedicated to my mother Lai Yi Fan Mak, who passed away on June 2009, and my father Chun Po Mak, who passed away on February 2014, for their nurture and support that makes who I am today. Special dedication to my husband Gabriel Ho for his continuous support, love, and encouragements. To my mother-in-law Helen Ho for her prayers and encouragements. All of which have made this possible.

DEVELOPMENT OF A T-LOOP ASSAY TO INVESTIGATE T-LOOP DYNAMICS AND STRUCTURE

By

SIN MAN (SABRINA) MAK

DISSERTATION

Presented to the Faculty of the Graduate School of Biomedical Sciences

The University of Texas Southwestern Medical Center at Dallas

In Partial Fulfillment of the Requirements

For the Degree of

DOCTOR OF PHILOSOPHY

The University of Texas Southwestern Medical Center at Dallas

Dallas, Texas

May 2014

Copyright

by

SIN MAN MAK, 2014

All Rights Reserved

ACKOWLEDGEMENTS

I would like to acknowledge my two very insightful mentors Jerry and Woody, for their continuous support and resourceful guidance throughout these years. Thank you, Jerry, for your always optimistic view in science which has greatly inspired me to feel the same way. I will keep in mind the flexibility and positive attitude you have in moving research forward. Thank you, Woody, for allowing me to learn the basics of science and all the troubleshooting twists and turns a scientist must take to achieve an ultimate goal. I have really pushed myself over the limit in my experience of developing, validating, and utilizing such extremely high level of technicality type of research these past years.

I would also like to thank the Division of Basic Science at UTSW, the Cancer Biology Program, and my thesis committee: Dr. Sandeep Burma, Dr. Hongtao Yu, and Dr. Hui Zou for your support and scientific advices. Here I would also like to mention my undergraduate Chemistry department at Seattle University and my undergraduate research mentor Dr. Jamie Harmon and Dr. R. Paul Robertson at Pacific Northwest Research Institute (Seattle, WA) in motivating my scientific interest that went from being a Medical Technology major to pursuing a Ph.D. degree.

I'm blessed to have shared these past seven and a half years in graduate school with many wonderful people I have met and become great friends with. Thanks to Kevin Kennon for your professional and efficient administrative assistance all the time from arranging lab meeting lunch, booking conference rooms, to providing us with pens and tapes in the lab. Thank you to all past and present Shay/Wright lab members. Special acknowledgements to Dr. Tracy Chow, Dr. Guido Stadler, Dr. Quan (Nathan) Wang, and Dr. Yong Zhao for many past insightful scientific discussions and encouragements through rough times in the lab. Tracy, you were my best "twin" sister in the lab that also happened to be from Hong Kong as well out of thousands of graduate students, whom I have shared many laughter and tears with. Thank you for teaching me another difficult technique—Cesium Chloride Gradient. Guido, thank you for being there for me to share our special tea times and outings in our hiking excursions so we can enjoy life other than just science. Nathan, thank you for all your help with radioactivity while I was pregnant.

Most importantly, I would like to thank the person dearest to my heart. My husband, thank you for all your love, support, and trust in anything and everything that I do. Your always "it's okay" really puts my worrisome heart at ease during all the tidal waves that come one after another these past years. Thank you to the birth of our son, Emmanuel Man Hei Ho, for changing my entire perspective and priorities in life. There is nothing more important in this world than family support. Special thanks to my mother-in-law, Helen Ho, for always praying for my project, mentors, career paths, and my health so I am able to get as far as I could to this present day. Thank you to my Mom and Dad for bringing me up the way they did that mold me to who I am today. Mom, even though you have passed away from cancer a few years ago, I know you are smiling down from Heaven with joy to see what I have accomplished to this very day. Dad, your death was so sudden that makes it hard to believe you are no longer a phone call away. Pray that you are with God in Heaven now, enjoying your time with Mom.

Thank you to all my friends from Arlington Chinese Church for their prayers and support throughout these past seven years.

DEVELOPMENT OF A T-LOOP ASSAY TO INVESTIGATE
T-LOOP DYNAMICS AND STRUCTURE

Publication No. _____

Sin Man (Sabrina) Mak, Ph.D.

The University of Texas Southwestern Medical Center at Dallas, 2014

Supervising Professor: Jerry W. Shay, Ph.D.

ABSTRACT

An attractive target in cancer therapy development has been the study of telomeres, which are repetitive sequences at the ends of chromosomes critical in maintaining genomic stability. T-loops, formed by the 3' overhang inserting into the double strand region of the telomere, are thought to protect the ends from being recognized as double-strand breaks. An almost universal marker for cancer, telomerase, is a promising therapeutic target since its inhibition results in critically short telomeres, compromising t-loop structures. The clinical application has yet to be fully realized due to the lag phase between the times in which telomerase is inhibited and the times that telomeres become sufficiently short that the tumor undergoes apoptosis. Thus, improvements are needed including a greater understanding in t-loop

dynamics and the cooperative interaction with telomerase to provide the strategy in which the lag phase can be shortened.

Unfortunately, the study of t-loops has been challenging due to the difficulty of isolating and visualizing DNA with intact loop structures. Thus, we have developed novel methods to isolate DNA such that biochemical assays and microscopic visualizations for authentic t-loops are now possible. Digestion of proteins that stabilize t-loop and significant melting at the ends of DNA allow the 3'overhang to migrate out of the double strand region, thus unfolding t-loop and exposing the overhang. DNA isolated with typical procedures (Proteinase K at 55°C for 4 hrs, phenol/chloroform extraction) are thus linear and telomeric overhangs are susceptible to digestion by a 3'-5' exonuclease (ExoI). The "overhangs" in t-loop structures should be resistant to ExoI. If we lower the temperature of Proteinase K digestion to 4°C to reduce the amount of DNA melting that can occur, we find that the ends are in fact resistant to ExoI digestion. A consistent ~2 fold higher overhang signal in isolated t-loops compared to linear telomeres was observed to distinguish between the two samples. Heating these 4°C samples to 37°C and 55°C caused unfolding of t-loops, resulting in sensitivity of the overhangs to ExoI to the same extent as normal DNA preparations. To validate the t-loop assay, transmission electron microscopy (TEM), a method with powerful magnification and extremely high resolution, is used to visualize DNA isolated at 55°C (linear structures) and 4°C (t-loop structures). The assay was then used to investigate t-loop dynamics throughout cell cycle, and we found that t-loops remain in a folded conformation throughout S phase, confirming the hypothesis that t-loops would unfold a second time for late S/G2 C-strand fill in. We also found that an overhang size of ~30 nts is too short to maintain stabilized t-loops compared to ~90 nts in BJ cells.

In summary, we have significant evidence that we are able to prepare and analyze t-loops. Using this assay to determine t-loop structure and timing of t-loop repackage following replication and telomerase action will exceedingly add to our understanding of telomere biology. These are the key steps in setting the stage for many additional future studies, such as what factors contribute in generation of t-loops, how t-loop folding varies with telomere length, and what is the timing of t-loop folding and unfolding throughout cell cycle. All of which will provide critical information for the discovery of new improvements in anti-telomerase therapeutics.

TABLE OF CONTENTS

Title …….. i

Dedication ……..... ii

Title Page …… iii

Copyright …… iv

Acknowledgements …….. v

Abstract ……... vi

Table of Contents …… ix

List of figures …….. xii

List of Abbreviations …….. xv

CHAPTER ONE: General Introduction and Background Review ……... 1

I. An Introduction to Telomere Biology…… 1

Telomeres and T-loops …….. 1

Replicative Senescence and End Replication Problem ……. 2

Telomerase and ALT Pathway ……... 5

II. Structures of Telomere ……... 7

Shelterin Complex …… 7

3’ G-rich Overhang ……... 9

T-loops …… 13

G-Quadruplex …… 18

CHAPTER TWO: Development of a New Assay for T-loops …… 23

Introduction……... 23

Results …….. 25

Conclusions …….. 41

Materials and Methods ……. 43

CHAPTER THREE: Validation of the T-loop Assay by Electron Microscopy ……... 52

Introduction…….. 52

Results …….. 54

Conclusions …….. 69

Materials and Methods ……. 70

CHAPTER FOUR: Using the Assay to Analyze T-loop Behavior …… 72

Introduction……... 72

Results …….. 74

Conclusions …….. 79

Materials and Methods ……. 80

CHAPTER FIVE: Discussions and Future Directions ……... 82

Bibliography ……..... 91

PRIOR PUBLICATIONS

Mak, Sabrina S.; Smiraldo, Phillip G.; Chow, Tracy T.; Cornelius, Crystal; Shay, Jerry W.; Wright, Woodring E. T-loops are Refolded after Telomerase Extension and Must Unfold Again at Late S/G2 for C-strand Fill-in: Purification and Biochemical Assay for T-loops. (In preparation)

Chow, Tracy T.; Zhao, Yong; **Mak, Sabrina S.M.**; Shay, Jerry W.; Wright, Woodring E. Early and Late Steps in Telomere Overhang Processing in Normal Human Cells: The Position of the Final RNA Primer Drives Telomere Shortening. *Genes Dev.* 26(11):1167-78 (2012).

Harmon, Jamie S.; Bogdani, Marika; Parazzoli, Susan D.; **Mak, Sabrina S.M.**; Oseid, Elizabeth A.; Berghmans, Marleen; LeBoeuf, Renee C; Robertson, R. Paul. B-Cell-Specific Overexpression of Glutathione Peroxidase Preserves Intranuclear MafA and Reverses Diabetes in db/db Mice. *Endocrinology* 150(11):4855-62 (2009).

EDITING/REVISION

Chow, Tracy T.; **Mak, Sabrina S.M.**; Shay, Jerry W.; Wright, Woodring E. Brenner's Encyclopedia of Genetics, 2nd edition. Revise/update "Telomere" section from 1st edition. Submitted on May 1, 2011. Revised on Jan 31, 2012.

LIST OF FIGURES

Figure 1-1. A schematic model of t-loop structure ……

Figure 1-2. The end replication problem ……...

Figure 1-3. Two stage M1/M2 model of cellular senescence ……..

Figure 1-4. Schematic model of shelterin (telomere binding proteins) …….

Figure 1-5. Early and late steps in telomere overhang processing in normal human cells: The position of the final RNA primer drives telomere shortening……..

Figure 1-6. A two-step model for telomere replication in telomerase-positive cells ……

Figure 1-7. Visualization of mammalian t-loops via electron microscopy …….

Figure 1-8. T-loops generated *in vitro* by human TRF2……..

Figure 1-9. Proposed model in formation of t-loop by TRF1 and TRF2 ……

Figure 1-10. Schematic illustration of G-quadruplex …….

Figure 2-1. Schematic model of branch migration of a Holliday junction and t-loop ……

Figure 2-2. Branch migration oligo models used to explore the effects of time and temperature.

Figure 2-3. Branch migration studies with different $MgCl_2$, NaCl, and EtBr concentrations ….

Figure 2-4. Schematic models of t-loops in 3 vs 4 stranded structures ……

Figure 2-5. LiCl results in the least amount of Exo I inhibition (G-quardruplex formation) when compared with NaCl and KCl ……...

Figure 2-6. Coomasie blue stain: Proteinase K digestion of cells at 4°C and 55°C ……

Figure 2-7. Alu I digest genomic DNA under different LiCl concentrations at 4°C ……..

Figure 2-8. The t-loop assay with Exonuclease I ……

Figure 2-9. Exo I works at 150 mM LiCl ……

Figure 2-10. Exo I digests overhang during agarose electrophoresis …….

Figure 2-11. T-loop assay with Exo I: T-loop vs Linear Telomere DNA at varied temperatures ……..

Figure 2-12. T-loop sample shows consistent retention of overhang signal compared to signal decrease in linear telomeres ……

Figure 2-13. Increase amount of Exo I does not result in more overhang digestion in linear telomeres at 4°C ……..

Figure 2-14. Schematic illustration of oligonucleotide model design ……

Figure 3-1. Schematic illustration of the sequence of events during telomere purification …..

Figure 3-2. Control experiments determining the amount of oligos to beads for optimal capture

Figure 3-3. Telomere purification with varied biotinylated oligo lengths ……...

Figure 3-4. AMT crosslinking with different lengths of oligos ……..

Figure 3-5. Telomere DNA were successfully crosslinked ……

Figure 3-6. Plasmid and lambda DNA visualization on TEM ……..

Figure 3-7. Visualizing telomeric DNA from t-loop and linear telomere samples on TEM …

Figure 3-8. TRF analysis shows Hela cells overexpressed with hTERT has a 145 bp per PD telomere elongation rate ……..

Figure 3-9. Hela+hTERT cells were synchronized at 4 hours with telomere purification yield of 10-15% …….

Figure 3-10. EM images of t-loop and linear telomeres and their quantifications …….

Figure 4-1. Cell cycle analysis by t-loop assay shows t-loops stay folded throughout cell cycle ..

Figure 4-2. CsCl separation of replicated fractions showed t-loop conformation at 4 hours in to cell cycle …….

Figure 4-3. CsCl separation of replicated fractions showed t-loop conformation at 8 hours in to cell cycle ……

Figure 4-4. Analysis of leading vs. lagging strand overhangs in BJ cells showed higher stability of t-loops with longer overhangs …….

LIST OF ABBREVIATIONS

ALT	Alternative lengthening of telomeres
AMT	Aminomethyltrioxsalen
Bp	Basepair(s)
CsCl	Cesium chloride
D-loop	Displacement loop
Ds	Double-stranded
EM	Electron microscopy
EtBr	Ethidium bromide
Exo I	Exonuclease I
hTERT	Telomerase reverse transcriptase
hTR/hTERC	Telomerase RNA
Kb	Kilobase(s)
Kbp	Kilobase pair(s)
LiCl	Lithium chloride
M1/M2	Mortality stage 1/mortality stage 2
MEF	Mouse embryonic fibroblast
Mg	Milligrams
NHEJ	Non-homologous end joining
Nt	Nucleotides
PBL	Peripheral blood leukocytes
PI	Propidium iodine
POT1	Protection of telomeres 1

Rap1	The human ortholog of the yeast repressor/activator protein 1
SEM	Scanning electron microscopy
Ss	Single-stranded
SSB	Single-stranded binding protein
TEBP	Telomere end-binding protein
TEM	Transmission electron microscopy
TIN2	TRF2- and TRF1-interacting nuclear protein
TRF1/2	Telomere Repeat binding Factor ½
U	Units (of enzyme)
Ug	Micrograms

CHAPTER ONE

General Introduction and Background Review

An Introduction to Telomere Biology

Telomeres and T-loops

The ends of eukaryotic chromosomes are capped by a specific repetitive sequence of variable length (TTAGGG/AATCCC) called "telomeres". In human cells, they contain a double-strand 15-20 kilobase pairs region (at times less than 5 kilobase pairs in chronic disease states) (Shay and Wright, 2002) and a 3'- single-strand G-rich 12-300 bases known as the overhang region. This overhang is believed to be inserted into the double-stranded region of the telomeres forming a secondary lariat-like structure called t-loop (Shay and Wright, 2006; Zhao et al., 2009) (Fig. 1-1).

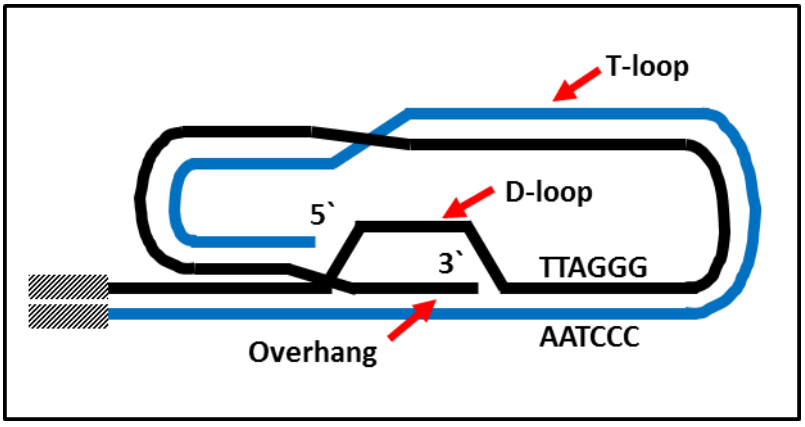

Figure 1-1. A schematic model of t-loop structure. In native mammalian telomeres, the 3'-G-rich overhang (black line) is inserted into the double-strand region, forming a large t-loop. The displaced strand formed by the invasion of the overhang forms a smaller loop called D-loop.

T-loops are thought to protect telomeric ends from being recognized as double-strand breaks, thus, avoiding the activation of DNA damage repair mechanisms that can result in degradation and loss of essential genes, such that they can be detrimental to normal cell functions (Hockemeyer et al., 2005). Studies in the past have shown the effect of radiation on chromosomes such that broken ends are prone to indiscriminate rejoining with possible segmental rearrangements. These broken ends provide substrates for NHEJ (non-homologous end joining) and possibly erosion by exonucleases. Thus, it is clear that a method of protection to mask the ends of chromosomes is necessary, whether in terms of t-loops, protein complexes, and any other possible secondary structures.

Replicative Senescence and End Replication Problem

In normal eukaryotic cells, functional telomeres are essential for continued cell proliferation, and yet telomeres progressively shorten with time such that telomere length in almost all middle-aged human tissues is approximately half that of the new born length (Shay and Wright, 2006). During normal somatic cell division, the unidirectional nature of DNA polymerase and processing events causes telomeres to lose about 50-200 base pairs with each division. This phenomenon is known as the end replication problem. The original hypothesis by Watson (1972) and Olovnikov (1973) about 40 years ago referred this as the inability to copy the 10-14 nucleotides at the end of the chromosome after the final lagging Okazaki fragment RNA primer has been removed (Chow et al., 2012). DNA is replicated by two distinct mechanisms since linear parental chromosomes consist of two DNA strands that are positioned in opposite orientation and that daughter strands can only be synthesized in the 5’ to 3’ direction (Fig. 1-2). Leading daughter strand is synthesized from the replication fork all the way to the end of the

chromosome continuously, but the lagging daughter stand is synthesized in small incremental Okazaki fragments discontinuously that start with a RNA primer. At the end of the chromosome, the last RNA primer is removed and no additional DNA synthesis can occur resulting in a 10-13 nucleotide gap. Thus, extreme ends of chromosomes cannot be fully replicated during DNA replication and result in progressively shorter telomeres (Chow et al., 2012).

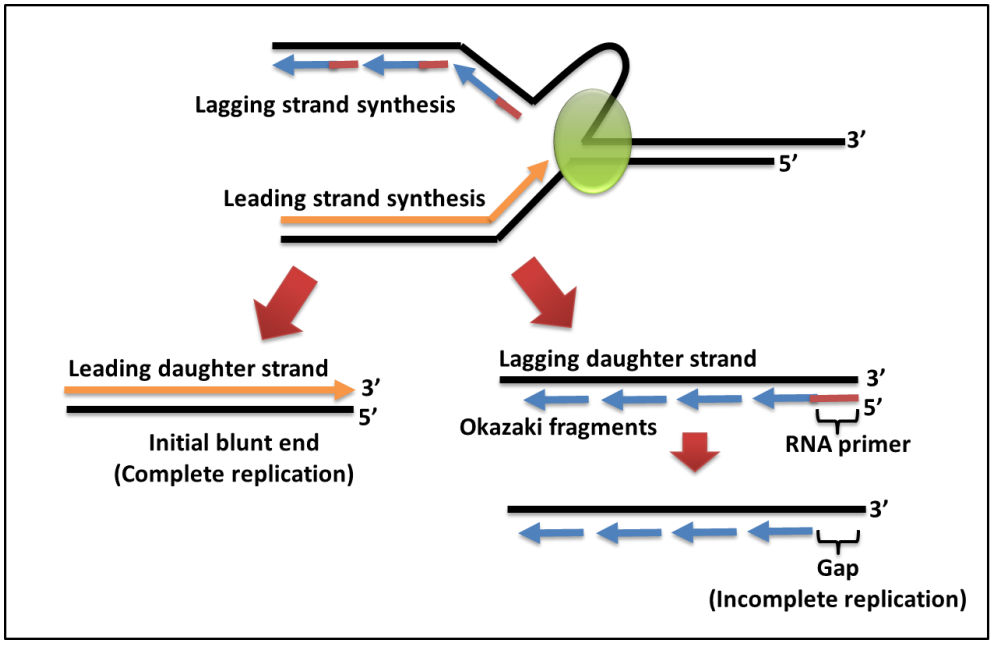

Figure 1-2. The end replication problem. In DNA replication, the leading daughter strand is synthesized all the way to the end of the chromosome and have an initial blunt end. The lagging daughter strand is synthesized by Okazaki fragments with a RNA primer, thus, leaving a gap at the end when the final RNA primer is removed after replication is completed. This results in incomplete replication yielding shorter telomeres with each cell division.

Overtime, telomere shortening will continue until it reaches a critical length that compromises t-loop structures and triggers cells to undergo replicative senescence, or known as mortality stage 1 (M1). When telomeres are so short that they can no longer form t-loops, they undergo a change of state called uncapping where telomeric ends become exposed and vulnerable to DNA damage repair mechanisms. This leads to a rapid induction of growth arrest that may involve

end-to-end fusions and fusion-bridge-breakage cycles, and the cells reach a state of mitotic catastrophe, or M2 (Shay and Wright, 2006) (Fig. 1-3). In normal cases, these cells will then undergo apoptosis and cell death thereby preventing any further essential genetic changes. This cellular response and processes can serve as a potent tumor-suppressor mechanism.

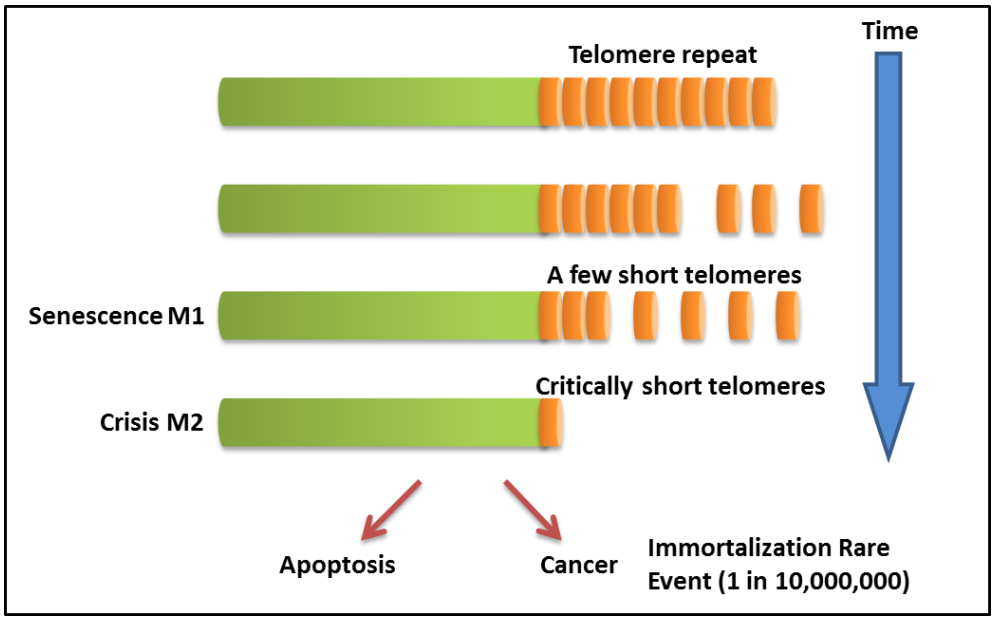

Figure 1-3. Two stage M1/M2 model of cellular senescence. M1, replicative senescence, occurs when a few short telomeres present DNA damage signals that lead to growth arrest. However, M1 may be bypassed in cells that have inactivated cell-cycle checkpoint genes where they will continue to proliferate, and telomeres further shortens until they reach a critical length such that the ends are no longer protected against end fusions. This marks the M2 stage, crisis. Normally, cells will then undergo apoptosis (cell death), but in rare cases, cells can escape M2 and transform into an immortal cell or what is better known as cancer. (Figure modified from Shay and Wright, 2006)

But in very rare cases, one in ten million chances, cells at M2 may bypass or completely ignore this cell cycle checkpoint gate, and continue to proliferate for an unlimited amount of time leading to immortality in which normal cells have transformed into cancer.

Telomerase and ALT Pathway

Due to this end replication problem and replicative senescence, most cancer and germline cells are able to overcome this proliferative limitation by the action of a ribonucleoprotein called telomerase. It functions to add about 50-60 nucleotides of TTAGGG repetitive sequence to the ends of telomeres, thereby enabling cells to overcome the detrimental effects of telomere shortening (Zhao et al., 2009). Telomerase activity can be detected in 85-95% of the most common cancers such as prostate, breast, colon, lung, and liver (Shay, 1997). Although tumor cells generally have short telomere lengths, they do not present any net loss in average telomere lengths with successive cell divisions due to telomerase activity. The human telomerase has two components, a catalytic subunit called hTERT (telomerase reverse transcriptase) and a functional subunit called hTR or hTERC (telomerase RNA). The hTR subunit is an integral RNA component that provides the 11 base pairs template that encodes for the telomeric repeats added to the chromosome, and hTERT serves as an enzyme that adds nucleotides complimentary to the hTR template thereby extending telomere length. Studies have shown that there is a direct correlation between telomerase and overcoming replicative senescence by introducing the hTERT component to telomerase-negative cells. This led to telomere length stabilization, absence of telomere shortening, and direct immortalization of cells without oncogenic transformation as long as they were cultured in the right conditions (Shay and Wright, 2002). Thus, telomerase, an almost universal marker for cancer, has become a promising therapeutic target such that its inhibition will result in telomere shortening and eventually cell death. Unfortunately, the clinical application has yet to be fully realized due to the lag phase between the time in which telomerase is inhibited and the time that telomeres become sufficiently short that the tumor undergoes apoptosis (Mokbel, 2003). Thus, improvements are needed including a

greater understanding in t-loop dynamics, overhang processing, and the cooperative interaction with telomerase to provide the strategy in which the lag phase can be shortened.

In telomerase-positive cells, significant amounts of evidence have shown that telomerase is the main contributor in providing cancer cells with cellular proliferation and immortality. On the other hand, there exist approximately 10% of human tumors that are telomerase-negative and yet have been found able to maintain their telomere lengths (Bryan et al., 1997). These cells elongate their telomeres to sustain viability by a telomerase-independent pathway called alternative lengthening of telomeres (ALT). In contrast to telomerase-positive cells that have similar average telomere lengths, ALT cells have highly heterogeneous telomere lengths, often extremely long. Although the detail process of how the ALT pathway works is limited, studies in yeast have shown that mutants lacking telomerase elongate their telomeres on a pathway that is dependent on RAD52 and other genes that are involved with homologous recombination (Basenko et al., 2010). The recombination rate in and near telomeres is greatly increased when telomeres become short, and telomeres are elongated by what is known as a "roll and spread" mechanism. In this model, a small duplex DNA circle with telomeric sequence (t-circle) is formed by homologous recombination. These t-circles are used as templates for extending at least one telomere by a rolling circle copying event. Once one long telomere is formed, the rest of the telomeres can also extend by copying its sequence.

Structures of Telomere

Shelterin Complex

In addition to t-loops, human telomeres and perhaps all mammalian telomeres are bound by a six-subunit protein complex known as shelterin. These telomere binding proteins, including TRF1, TRF2, TIN2, RAP1, TPP1, and POT1, altogether contribute in function to preserve the capping of telomeric ends (Palm and de Lange, 2008) (Fig. 1-4). In similar function as t-loops, shelterin prevent cells from recognizing their natural chromosome ends as double-strand breaks, thereby repressing DNA repair activation. Three of the shelterin protein components are responsible for the complex's specificity to the telomeres: TRF1 and 2 (telomere Repeat binding Factor 1 and 2) recognizes the TTAGGG repeats and bind to the double-strand region of the telomeres, and POT1 (protection of telomeres 1) binds to the single-strand 3'overhang and the D-loop region of the t-loop conformation (Palm and de Lange, 2008). When TRF2 is depleted in MEFs (mouse embryonic fibroblast) that are p53 deficient, telomeres join together forming long stretches of fused chromosomes. This is due to the ends being recognized as DNA breaks and activated NHEJ mechanisms (Konishi and de Lange, 2008).

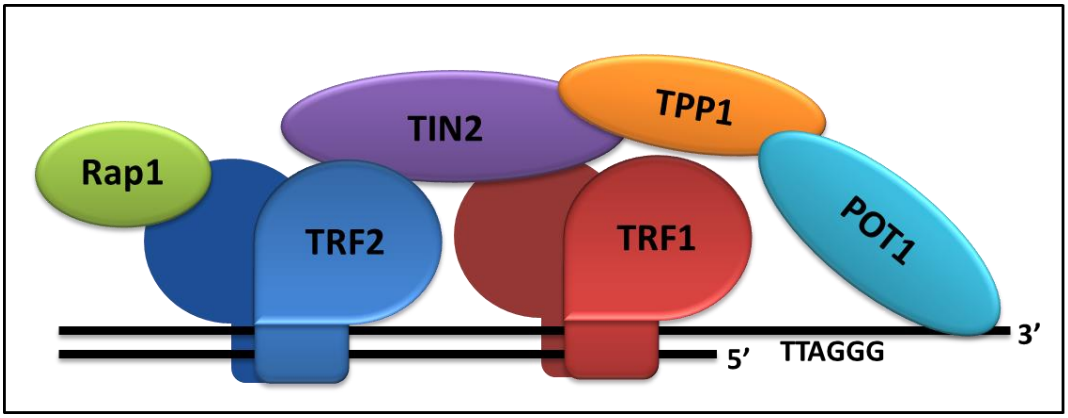

Figure 1-4. Schematic model of shelterin (telomere binding proteins). See text for details. (Figure modified from Palm and de Lange, 2008)

TRF1 and TRF2 recruits the other four components of the shelterin complex: TIN2 (TRF2- and TRF1-interacting nuclear protein), Rap1 (the human ortholog of the yeast repressor/activator protein 1), TPP1 (formerly known as TINT1, PTOP, or PIP1), and POT1.

TRF1 (TTAGGG repeat binding factor 1) and TRF2 both bind to the double stranded region of the telomeres. TRF1 has homology to the DNA-binding domain of the Myb family of transcription factors and contains only one single DNA-binding motif. It behaves as a negative regulator of telomere maintenance by inhibiting the activity of telomerase at telomeric ends. *In* vitro studies have also shown that it can function to bend DNA and promote DNA looping and strand pairing such that it can influence the overall structure of the telomeric complex in a manner that is important for telomere function (Bianchi et al., 1997). TRF2 was identified as a TRF1 homolog, and it binds to the junction of 3' G-rich overhang and promotes formation of t-loops. Three properties found *in vitro* that enhance this process is that 1) TRF2 preferentially binds to a telomere repeat if it has a G-rich overhang that is at least 6 nucleotides long, 2) multiple TRF2s can bind to the telomere region introducing positive supercoiling that promote unwinding and strand invasion, and 3) the GAR domain of TRF2 has a sequence-independent affinity for DNA junctions, such as the Holliday junction that is formed when 3'overhang invades into duplex telomeres (Palm and de Lange, 2008).

TIN2 binds to three components of shelterin, TRF1, TRF2, and TPP1, thereby forming an interacting bridge between them. TIN2 recruits TPP1 to the complex. Though its detailed function is not yet known, it definitely serves as an important intermediate between these three proteins for structural or communicating purposes. Rap1 binds to TRF2, but it has not been characterized yet other than that it serves as an essential role in the shelterin complex. TPP1 connects POT1 with TIN2, and has a domain that interacts with telomerase, though whether it

recruits or regulates telomerase activity is still unknown. POT1 binds to TPP1 and the single stranded 3' G-rich overhang (Palm and de Lange, 2008).

3' G-rich Overhang

At the ends of telomeres, there is a single-strand overhang at the 3' end on the G-rich strand of the duplex DNA. This 3' overhang is thought to loop back and insert into the double-strand region of the telomeres forming a lariat like structure known as t-loop. Thus, the overhang plays an important role in structurally masking the chromosome end from being recognized as double-stranded break and preventing end-to-end fusions, abnormal recombination, and degradation. In normal BJ human foreskin fibroblasts, the leading strand overhangs were found to be approximately 40 nucleotides (average, the shortest being only 12 nucleotides long), and the lagging strands are 115 nucleotides (almost three times longer than leading strand overhangs) (Zhao et al., 2008). In telomerase negative cells, the original hypothesis of the end replication problem by Watson and Olovnikov presented the inability of cells to copy the last 10-14 nucleotides at the end of chromosome after the final lagging Okazaki fragment RNA primer has been removed in the process of DNA replication (Chow et al., 2012). There are organisms with G-overhangs that are in that length range: about 14 nucleotides in ciliates ((Jacob et al., 2001; Klobutcher et al., 1981) and about 12-14 nucleotides in *Saccharonmyces cerevisiae* (Larrivee et al., 2004). But clearly as seen in BJ cells, normal cells in general have G-overhangs that are longer than 10-14 nucleotides. This leads to the idea that it is the reduction of C-strands that gives the final overhang size after DNA replication and represents the rate of telomere shortening in the absence of telomeric damage (Zhao et al., 2009). In cultured human telomerase-negative cells, the rate of telomere shortening is 50-100 base pairs per division, and

the average overhang size is about 60-70 nucleotides in length (a close estimate with the rate of telomere shortening) (Chow et al., 2012). But current studies have found that instead of having mature overhang size due to the degradation of C-strand, it is actually the position of the final RNA priming event of DNA replication that results in the overhang length specified. The updated model of overhang processing presents the final lagging RNA primer remained intact immediately after replication with an overhang size of about 80 nucleotides, which would be the initial overhang length that is almost mature (Fig 1-5).

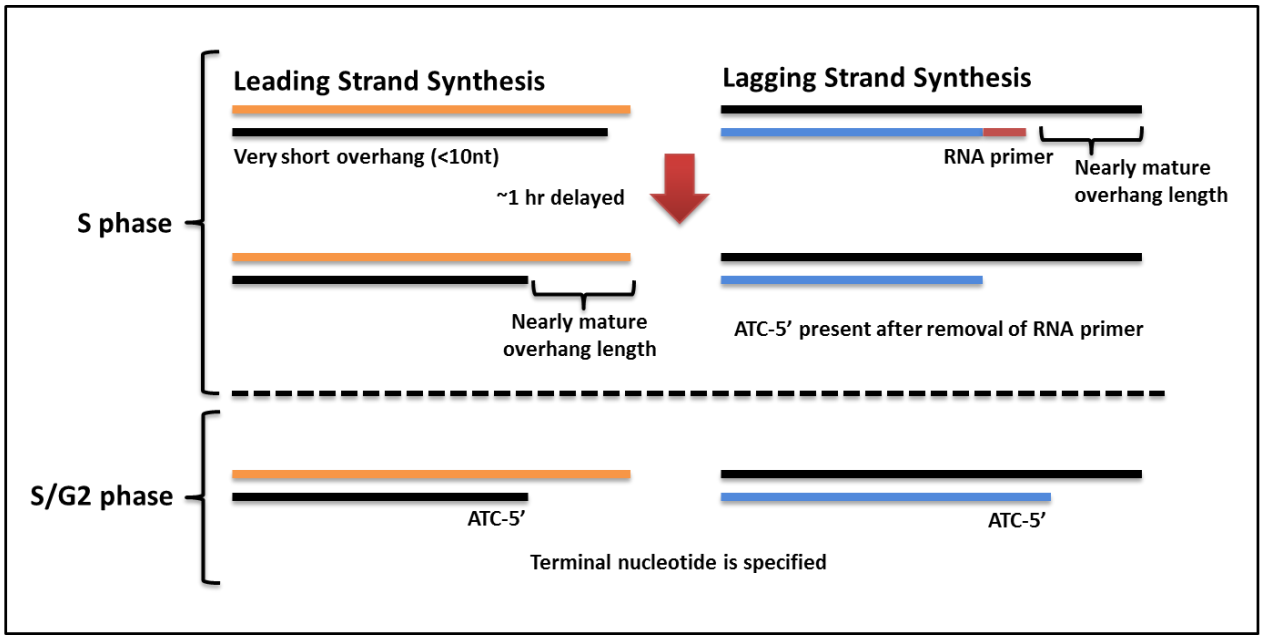

Figure 1-5. Early and late steps in telomere overhang processing in normal human cells: The position of the final RNA primer drives telomere shortening. See text for details (Figure modified from Chow et al., 2012).

This is due to the fact that conventional replication complex is unable to copy the gap between the final RNA primer position and the very end of chromosome, leaving an approximate overhang length (Chow et al., 2012). The telomeric G-strand is always generated by leading

strand synthesis, and should end in GGTTAG since 80-85% of fully processed telomeres have C-strands ending in the complementary sequence CCAATC-5'. However, approximately equal amounts of G-ends of the sequence GGTTAG, GGTTA, and GGTT were found in normal diploid cells (Sfeir et al., 2005). This represents the model that the replication apparatus simply runs off the ends and often fails to incorporate just the final one or two nucleotides at the extreme termini due to the challenges of making fully blunt-ended products, resulting in an initial overhang of 0, 1, or 2 nucleotides. Within about an hour of replication, leading daughters will acquire an almost mature overhang size by any transient resection and fill-in at S/G2 phase of the cell cycle (Chow et al., 2012) (Fig. 1-5).

In telomerase-positive cancer cells or germ line cells, telomeres do not get increasingly short with each cell division. Instead, they overcome the end-replication problem by elongating their telomeres with the action of telomerase. Telomerase, a ribonucleoprotein with reverse transcriptase activity, adds telomeric repeats to the 3' G-overhang thereby extending its length (Zhao et al., 2009). This could result in an excessively long overhang, thus complementary C-strand fill-in synthesis occurs to extend the C-strand such that the overhang size is normalized. Thus, in contrast to normal telomerase-negative cells, telomerase-positive cells do not exhibit differences in leading and lagging overhang lengths but both are of approximately the same size. Studies have shown that this telomere extension occurs in a two-step process such that the G-strand extension by telomerase and the C-strand fill-in are uncoupled (Zhao et al., 2009) (Fig. 1-6). In *Euplotes*, the newly synthesized G-strands are heterogeneous in length ranging around 95-100 nucleotides long, whereas most of the C-strands are exactly 84 nucleotides in length (Price, 1997). This suggests that the C-strand fill-in is a more tightly regulated step. In addition, 80% of the C-strands end in CCAATC-5' in human cells, more specific than the G-terminal

nucleotide (Sfeir et al., 2005). Human telomeres replicate throughout S phase, and chromosomes replicate asynchronously throughout. *In situ* cytological studies have demonstrated that hTERT and hTR only associate with a few telomere molecules at any particular time during S-phase (Jady et al., 2006; Tomlinson et al., 2006). This leads to the prediction that telomerase is rapidly recruited to the telomeres after telomere replication.

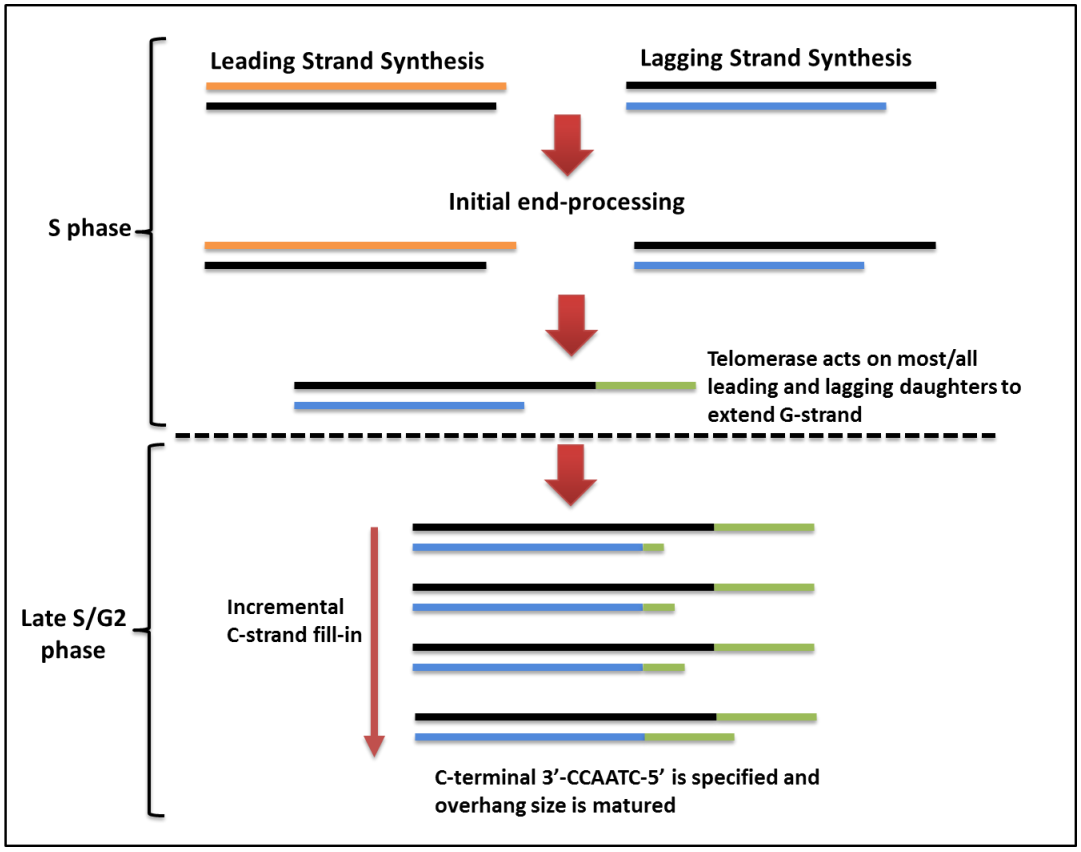

Figure 1-6. A two-step model for telomere replication in telomerase-positive cells. See text for details. (Figure modified from Zhao et al., 2009)

Evidence has shown that telomerase is able to elongate telomeres within 30 minutes of telomere replication, and that 70%-100% of the ends in Hela and H1299 cells were extended during each cell cycle suggesting that there is no preferential recruitment of telomerase to shorter telomeres under maintenance conditions (Zhao et al., 2009). In Hela cells, the overhang lengths of leading

and lagging strands shortly after replication are about 35 nucleotides and 50 nucleotides, respectively. Telomerase adds approximately 50 nucleotides to 70% of both strands for telomere length maintenance purposes to overcome senescence (Zhao et al., 2009). Although telomere replication and elongation by telomerase occurs in S phase, C-strand fill-in has been shown to occur as a second step in late S/G2 phase (Fig. 1-6). There is preliminary evidence that show it is an incremental C-strand fill-in versus what would be expected as the conventional lagging-strand synthesis machinery, such that an RNA primer is extended, added to the end of C-strand, and rapidly convert to double-stranded DNA. But the detailed mechanisms of this incremental process have yet to be discovered (Zhao et al., 2009).

T-loops

The telomeric ends of chromosomes must be protected from being recognized as double-stranded breaks or any other DNA lesions to prevent activation of unnecessary DNA repair mechanisms that can result in end-to-end fusions, abnormal recombination, and degradation, all of which are detrimental to normal cellular functions. The molecular mechanism of such capping functions of the ends has been proposed to 1) having proteins bound to the 3' telomeric end in the double-stranded and/or single-stranded region and 2) the single-stranded 3' G-overhang transformed into a specific DNA secondary structure (Griffith et al., 1999). Both cases will serve the purpose of blocking any DNA damage recognition/activation processes. Two of the six proteins in the shelterin complex bind to the double-stranded region of the telomeres, TRF1 and TRF2. Without TRF2, the cells presents immediate activation of ATM/p53-dependent DNA damage checkpoint pathway, resulting in end –to-end fusions and subsequently cell cycle arrest and apoptosis (Karlseder et al., 1999). The duplex telomeric repeats were found to be

intact, but the single-stranded 3’ G-overhangs were lost upon inhibition of TRF2 (Makarov et al., 1997). This provides the evidence that there is a direct link between presence of 3’ G-overhang and protection of the ends. Thus, this led to the idea that TRF2, in an unknown mechanism, works with the 3’ single-stranded tail to prevent inappropriate activation of DNA repair proteins at natural chromosome ends (Griffith et al., 1999). The final outcome of these ideas and experiments was the hypothesis that TRF2 facilitates the formation of a lariat, lasso like structure called t-loops.

T-loops are formed by the 3' single-stranded G-overhang inserted into the double-stranded region of the telomeres (intramolecular) in a way that displaces the G-strand at the insertion region creating another structure called D-loop (displacement loop) (Fig. 1-1). The Griffith laboratory was the first and only group that was able to isolate and view these large duplex loops by electron microscopy (Fig. 1-7).

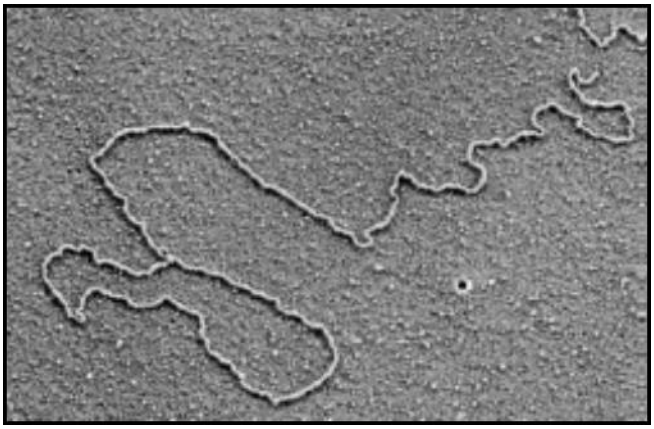

Figure 1-7. Visualization of mammalian t-loops via electron microscopy. Telomeric DNA from mouse liver cells was isolated by size fractionation following psoralen/UV treatment of nuclei, deproteinization, and restriction cleavage (Griffith et al., 1999).

In vitro studies with duplex telomere sequence ending in a single-stranded overhang model showed that adding TRF2 alone produced 17-20% lasso-like molecules (t-loops), given that only 35-40% of the model substrate actually had a long 3'TTAGGG repeat overhangs. In addition, TRF2 was found at the loop-tail junction of all t-loops that were formed by these DNA models (Fig. 1-8), suggesting that TRF2 may play a crucial role in facilitating the strand invasion of the 3' overhang into the double-stranded region of the telomeres (Griffith et al., 1999).

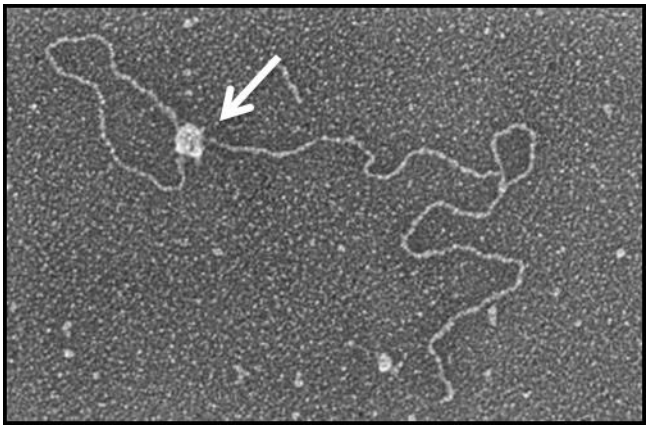

Figure 1-8. T-loops generated *in vitro* by human TRF2. Telomeric DNA model containing 3kb of unique sequence followed by ~2kb of repeating TTAGGG with a 150-200 nucleotides 3' G-strand overhang was incubated with human TRF2 protein (Griffith et al., 1999). Arrow points to the loop-tail junction in which TRF2 was bound.

With these *in vitro* studies, additional clues as to the characteristics of t-loops are revealed. Although the conclusions to these studies may be different *in vivo*, there is such limited information in this field that any inference drawn from *in vitro* studies are valuable. Using the same type of duplex telomere with an overhang model, they found that at least one single-stranded TTAGGG repeat adjacent to the telomeric duplex is required for efficient t-loop formation. Interestingly, if the single-stranded tail began with TTAGGG repeat sequence but end with a non-telomeric sequence, only a modest reduction of t-loops were found. On the other

hand, if the single-strand/double-strand junction is non-telomeric sequence but the tail end is telomeric sequence, t-loop formation is abolished (Stansel et al., 2001). If the telomeric DNA model has a 3' overhang of C-rich sequence instead of the normal G-rich sequence, TRF2 was unable to form t-loops as well even if it was oriented in such a way that base pairing can be achieved with the double-stranded region. Although the steps in forming a t-loop and the proteins involved are still unknown, there are possible speculations and model as to how t-loops are formed *in vivo*. The current model for t-loop formation is that first TRF1 was inferred to induce a shallow bend in duplex TTAGGG repeats (Bianchi et al., 1997) and able to achieve intratelomeric base pairing (Griffith et al., 1998); second, TRF2 is able to promote strand invasion of the 3' overhang into the double stranded region (Griffith et al., 1999) (Fig. 1-9).

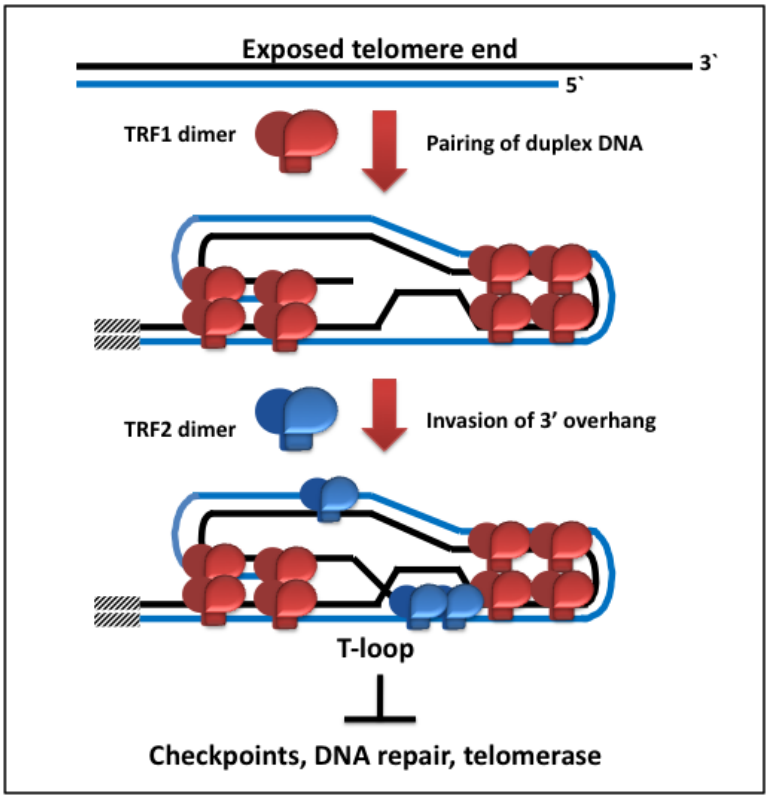

Figure 1-9. Proposed model in formation of t-loop by TRF1 and TRF2. Schematic drawing depicting possible mode of t-loop formation based on *in vitro* biochemical activities of TRF1 and TRF2. T-loops are proposed to mask telomere ends from cellular activities that can act on DNA ends at an inappropriate time (Figure modified from Griffith et al., 1999).

T-loops were also found in *in vivo* models such as Hela cells, mouse liver (long telomeres), and normal human peripheral blood leukocytes (PBL) (short telomeres). The isolated DNA was cross-linked with psoralen, a chemical that intercalate into duplex DNA and preferentially cross-link T residues of opposite strands upon UV irradiation, purified on a column by size and imaged by electron microscopy. The results were that 15-40% of t-loops were found in Hela cells, 15-20% in mouse liver, and 15% in human PBL (Griffith et al., 1999). Less than 1/1000 molecules were found to have double loops (loop at both ends of DNA), suggesting that t-loops were not a result of sticky ends forming loops by chance during purification or EM procedures. Even in the absence of psoralen cross-linking, 2-5% of the DNA isolated from Hela cells were found to be in t-loops. Genomic DNA randomly sheared into 5-20 kilobase (kb) fragments and cross-linked gave only 0.25% t-loops, highly suggesting that t-loops are only specific to telomeric sequenced DNA (Griffith et al., 1999). Furthermore, there is some correlation of t-loop sizes with telomere lengths. In a clone of Hela cells that has long telomeres (range from 15-40 kb), although the contour lengths of t-loops found varied from 3 to 25 kb, but two-thirds of them laid between 12 and 18 kilobase. In samples with shorter telomeres (another Hela clone and human PBL), they gave mean t-loop lengths that are shorter—10 kb for Hela clone and 8 kb for PBL (Griffith et al., 1999). This correlation between telomere length and t-loop sizes gives additional evidence that the t-loops seen arose from telomeric DNA instead of genomic DNA.

To provide evidence that t-loops are formed by strand invasion of the 3’ overhang into the double-stranded region of the telomeres, the displacement loop (D-loop) was investigated *in vivo*. Looking at the structure of a t-loop, a single-stranded segment of DNA is predicted to be present at the t-loop junction (the loop-tail junction) forming a D-loop (Fig. 1-1). Thus, to prove this model, *E. coli* single-stranded binding protein (SSB) was added to a sample of t-loop

prepared for EM analysis. SSB was found to localize at the loop junction in 35% of t-loops isolated from human and mouse cells, suggesting that t-loops are formed by strand invasion-mediated telomere looping. The amounts of SSB at loop junction varied between a single SSB and a group of proteins, indicating that there is a considerable amount of variability in the size of the single-stranded region of t-loops due to the range of sizes 3' G-overhang can have (Cesare et al., 2008).

Apart from Hela cells, mouse liver cells, and human PBLs, many other higher eukaryotes including *Pisum sativum*, a type of plant commonly known as garden pea (Cesare et al., 2003), and smaller species including *Trypanosoma brucei*, a kinetoplastid protozoan with abundant telomeres due to the presence of many mini-chromosomes (Munoz-Jordan et al., 2001), have also been investigated by the Griffith laboratory to show that t-loops are present across species and evolutionary distance. It suggests that t-loops were evolved from a common ancestor of mammals and plants, but its architectural properties have been maintained as telomeric sequences and lengths diverged across species.

G-Quadruplex

In addition to forming t-loops with the 3' single-stranded G-overhang at the ends of telomeres, another secondary structure (though even more controversial than t-loops) was proposed as the medium in regulation of telomerase, end processing, and any other process that have steps involving linear telomeres for action. Chromosomes are capped at both ends with tandem repeats TTAGGG of telomeric DNA. This special repetitive sequence brought about a very special base pairing called cyclic Hoogsteen hydrogen bonding, where four guanines associate with each other by forming two hydrogen bonds with its neighbor. These four

guanines are known as the G-quartets, and they can stack on top of each other to form a quadruple-helical structure called G-quadruplex (Rhodes and Giraldo, 1995) (Fig. 1-10). Four TTAGGG repeats can fold into a G-quadruplex, a bulky DNA conformation compared with linear DNA that gives rise to the potential in blocking telomerase action in telomere elongation (Tang et al., 2008). Thus, G-quadruplex has been proposed as the negative regulator of telomerase *in vivo*, making it a potential target for cancer therapy since cancer cells are able to overcome replicative senescence by the action telomerase.

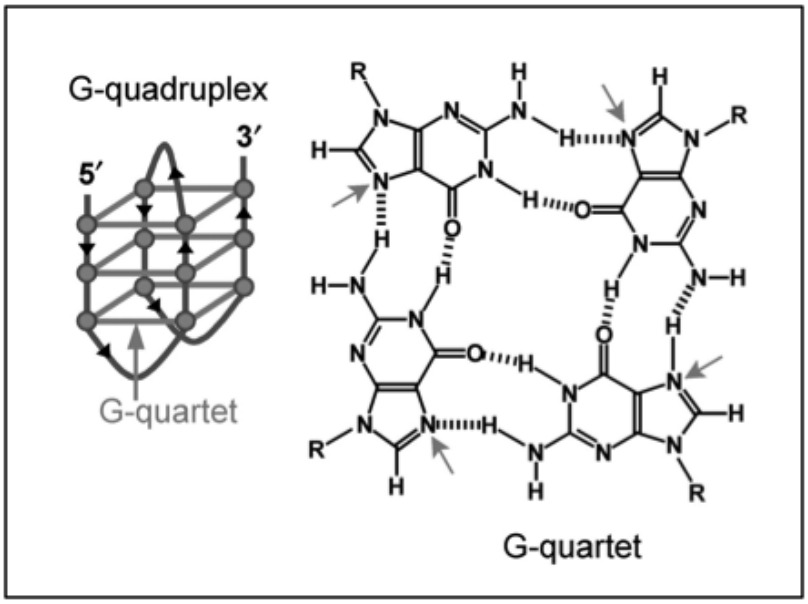

Figure 1-10. Schematic illustration of G-quadruplex. Four TTAGGG repeats can fold back to form G-quadruplex structure that is held together by three stacked G-quartets. Dashed lines indicate the location where Hoogsteen hydrogen bonding occurs. This secondary structure can serve as blockage to any processes involving the telomeric ends, such as telomerase action (Figure from Tang et al., 2007).

Though there are extensive studies on G-quadruplex *in vitro*, the *in vivo* evidence has been scarce. The only *in vivo* occurrence of telomeric G-quadruplex was found in ciliates. There are two telomere-binding proteins in ciliates that regulate and promote G-quadruplex

formation: telomere end-binding protein (TEBP) alpha and TEBPbeta. Silencing these genes showed that they cooperate to form G-quadruplex, TEBPalpha being responsible in attachment to telomere in the nucleus and recruiting TEBPbeta to these locations (Paeschke et al., 2010). *In vivo* telomeric RNA structures were also examined by generating G-rich transcripts with plasmid and RNA polymerases *in vitro*. This G-rich transcript exhibited spectral signatures of parallel G-quadruplex formation in presence of salt, and visualizations by EM showed tracts of condensed RNA compact rods and round balls (Fig. 1-11). These chains of beads can even further folds on itself to form higher compact structures (Randall and Griffith, 2009).

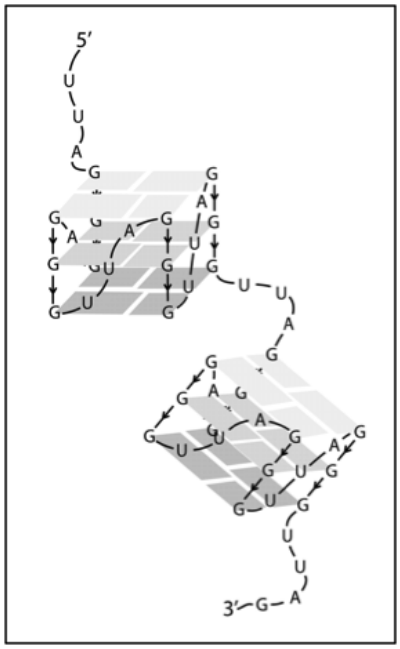

Figure 1-11. Model of folding G-rich RNA transcript into a string of beads. The G-rich RNA transcript is shown to fold into a string of RNA beads, with each bead consisting of a parallel G-quadruplex formed by three G-quartets joined by a UUA linker. (Figure from Randall and Griffith, 2009)

The formation of these DNA four-stranded secondary structures *in vitro* derived from oligonucleotides of telomeric G-strands has been very well established. It was found that the

formations of these higher orders of structures depend highly on monovalent salt concentrations such as Na^+ and K^+. Depending on the number of G-tracts in a strand, different types of G-quadruplex structures can be formed, parallel quadruplexes are formed by association of four strands containing G-tracts, and antiparallel quadruplexes arise from dimerization of two strands containing two G-tracts (or from intramolecular folding of one strand containing four G-tracts) (Rhodes and Giraldo, 1995). The G quartets are planar, connected to the backbone by glycosidic bonds in *anti*-conformation, and allowing uniform stacking of these planes and four grooves of equal sizes. Na^+ and K^+ ions are located between consecutive G-quartets thereby driving the formation of G-quadruplex (Rhodes and Giraldo, 1995). The stability of these complexes are very high such that in comparison with the open kinetics of regular Watson and Crick base-pairing being in the order of a few milliseconds, G-quadruplex of three G-quartets exhibit open kinetics of minutes and those of four G-quartets in matter of months (Rhodes and Giraldo, 1995). This highly stable property seem to create a challenge for convenient kinetics required by normal cellular functions such as DNA replication (replication fork proceeding all the way to the ends of telomeres), telomerase action (elongating 3' G-overhangs by adding additional telomere repeats), and even ALT activation (telomere strand exchange necessary for template extension) (Tang et al., 2008). But several proteins in human cells that are capable of unfolding telomere G-quadruplex *in vitro* were found. The hPOT1 protein in human cells bind to the single-stranded telomere overhangs is able to disrupt G-quadruplexes and allowed for telomerase extension (Zaug et al., 2005). Other proteins that have been shown to bind to G-quadruplexes are QUAD, a protein isolated from rabbit hepatocyte chromatin, transcription factor MyoD and alpha-thrombin, and rat liver proteins uqTBP25 and qTBP42 (Simonsson, 2001). Two clear evidence of proteins that actually promote G-quadruplex formations are telomere-binding protein from

Oxytricha and Rap1p, the major DNA-binding protein of *S. cerevisiae* telomeres (Rhodes and Giraldo, 1995).

In conclusion, G-quadruplexes has the potential to inhibit telomerase action, possibly normal DNA replication, and ALT pathway in telomerase-negative cells. Thus, it may appear to be a very attractive target for cancer therapy since it has potential in blocking multiple pathways such that cells will undergo severe DNA aberrations and result in cell death via a much quicker fashion than e.g. anti-telomerase therapy. But whether G-quadruplexes exists *in vivo* is still the main question and controversy in the field of telomere biology. Nevertheless, the formation and regulation of secondary structures such as t-loops and G-quadruplexes are important information in our understanding of telomeres. Evidence have supported the fact that they may play a key role in telomere function and normal capping in the ends of chromosomes, but the *in vivo* evidence are limited for t-loops and even less for G-quadruplexes due to multiple experimental challenges.

CHAPTER TWO

Development of a New Assay for T-loops

Introduction

The ends of eukaryotic chromosomes contain tandem arrays of hexameric sequence TTAGGG called telomeres. Adult human telomeres range in size with an average of 5-9 kbp. One of the essential functions of telomeres is protect the ends from being recognized as double-stranded breaks and prevent chromosome end-to-end fusions and degradation, thereby stabilizing genomic integrity (Shay and Wright, 2002). At the very terminal end of telomeres is a 3' single-stranded G-rich overhang that ranges in size from about 12 to 300 nt in length (Chow et al., 2012; Makarov et al., 1997). This 3' G-overhang is able to strand invade into the preceding double-stranded region of the telomere, forming a lariat-like structure called t-loop with a D-loop at the loop-tail junction (Stansel et al., 2001). T-loops have been found in *Oxytricha fallax* (Murti and Prescott, 1999), *Trypanosoma brucei* (Munoz-Jordan et al., 2001), *Pisum sativum* (Cesare et al., 2003), Hela cells, mouse liver cells, and normal human PBLs (Griffith et al., 1999), with electron microscopic images as the major supporting evidence for their existence. This demonstrates the fact that t-loops are highly likely to be a universal architectural structure for telomeres that have a defined sequence.

In somatic cells, normal telomeres lose about 50-200 bps per cell division due to the fact that DNA replication machineries such as DNA polymerase and other processing events are unidirectional (Zhao et al., 2009), and the inability of the cells to replicate the gap between the

last priming event and the very end terminus of telomeres (Chow et al., 2012). This phenomenon is known as the end-replication problem. Over time, the telomeres can get critically short such that replicative senescence and apoptosis are triggered (Smogorzewska and de Lange, 2004). Cancer cells, however, have the ability to overcome replicative senescence by the action of a ribonucleoprotein called telomerase, and it is the enzyme responsible for elongating telomeres by adding TTAGGG repeats to the 3' ends of chromosomes (Shay and Wright, 2002). During normal cell cycle progression, lagging strand overhangs are already at their nearly mature sizes immediately following replication, while the leading strand required an hour before developing a full overhang (lagging strands have a full overhang but require an hour before the RNA primer is removed, which doesn't change the size of the overhang very much)(Chow et al., 2012). T-loops would presumably have to be unfolded for the first hour following replication in order for this processing to occur. However, in cancer cells that are telomerase-positive, telomerase extends the G-strand soon after replication, creating initial overhang sizes that are long during S phase. The incremental C-strand fill-in that must occur in order to achieve a final mature overhang size, on the other hand, have been shown to take place at late S/G2 phase (Zhao et al., 2009). The time between when telomeres are replicated and elongated and the time C-strand fill-in occurs raises the question whether t-loops are unfolded when telomeres replicate throughout S phase, refolded soon after telomere extension, unfold again at late S/G2 for C-strand fill-in, and finally refold again once overhang sizes are matured, or whether t-loops stay unfolded throughout S-phase until late S/G2 and only reform after C-strand fill-in is completed. Any information about t-loops other than the fact that they exists is limited due to difficulty in developing an efficient biochemical assay that could test for their

presence in various cellular conditions. Thus, the only currently available important evidence for t-loops is shown by EM imaging.

EM imaging is a highly sophisticated and challenging method to study about t-loops since it requires massive amount of DNA (e.g. 3 milligrams (mg) or 300 million Hela cells). The main difficulty in studying t-loops is the ability to isolate them in authentic t-loop conformation. After deproteinization during common DNA isolation procedures, what is left to stabilize the t-loop structure are the hydrogen bonds between the complementary 3' G-overhang and the strand invasion region of double-stranded telomeres. The melting of DNA when expose to higher temperatures for increasing amounts of time will result in complete unfolding of t-loops by branch migration. Based on what is understood about branch migration, we developed a biochemical assay that only requires about 5 micrograms (ug) of DNA per sample and utilizes common gel electrophoresis and native in-gel hybridization of a C-rich probe to confirm presence of t-loops.

Results

Branch migration is where competing DNA strands are capable of moving back and forth in a stepwise fashion, breaking and reforming the hydrogen bonds between complementary base pairs, so that the branch point moves. This has mainly been studied in terms of the movement of the Holliday junction (Allers and Lichten, 2000) (Fig. 2-1 A), but the t-loop forms a somewhat similar structure (Fig. 2-1 B). The rate of branch migration is known to increase 10 fold with every 10°C increase in temperature (Panyutin and Hsieh, 1994). Our hypothesis is that if t-loops are unfolded by branch migration at higher temperatures (a requirement for optimal Proteinase K activity that is commonly used for deproteinization in DNA isolation procedures), then t-loops

should be stabilized and preserved at lower temperatures. Thus, the goal is to keep all procedures in isolating and assaying for t-loops at as low a temperature as the enzymes could function.

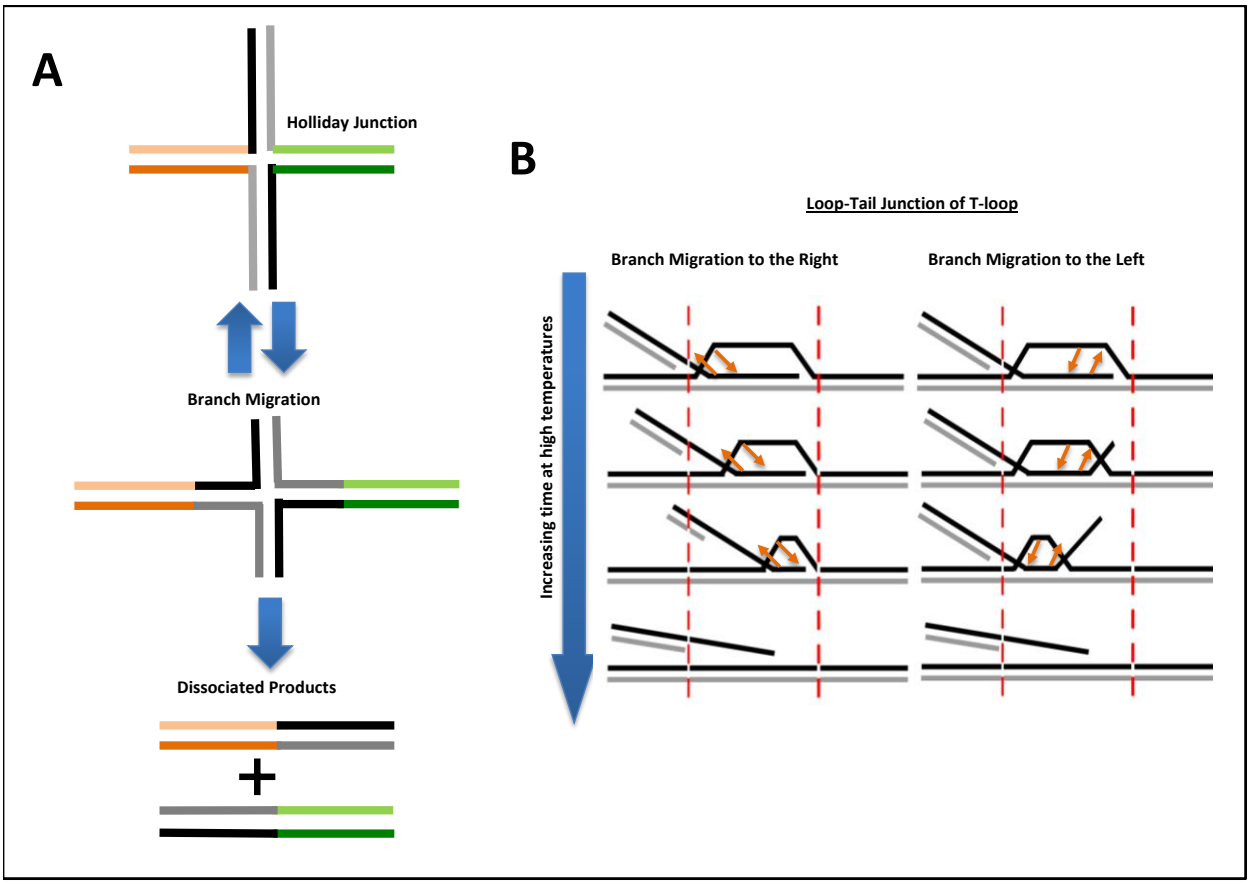

Figure 2-1. Schematic model of branch migration of a Holliday junction and t-loop. (A) Two homologous duplexes with heterologous tails (orange and green) form a four-stranded structure and will undergo spontaneous branch migration such that the complementary strands will move and dissociate into two double-stranded products. **(B)** A close-up schematic drawing of the loop-tail junction of a t-loop such that with increasing time at high temperature, the 3' G-overhang will melt away from the double stranded region until complete branch migration of the overhang, unfolding t-loops.

Before we tested authentic t-loops from cells, the amount of branch migration was explored using oligonucleotide model systems in order to both establish what to expect with human t-loops and to optimize conditions to minimize branch migration. The way we designed the models was to have two annealed left and right halves to form a four-stranded branch

migration structure (Fig. 2-2 A), and at the center of the complex is a Holliday junction that would be mobile at higher temperatures. Thus, at a given high enough temperature and allotted time, the Holliday junction slides/moves back and forth until complete branch migration of the complex occurs, yielding the two branch migrated products. For a first attempt to see the effects of temperature and length of incubation, we chose a structure formed by 30 nts of annealed arms (Fig. 2-2 B).

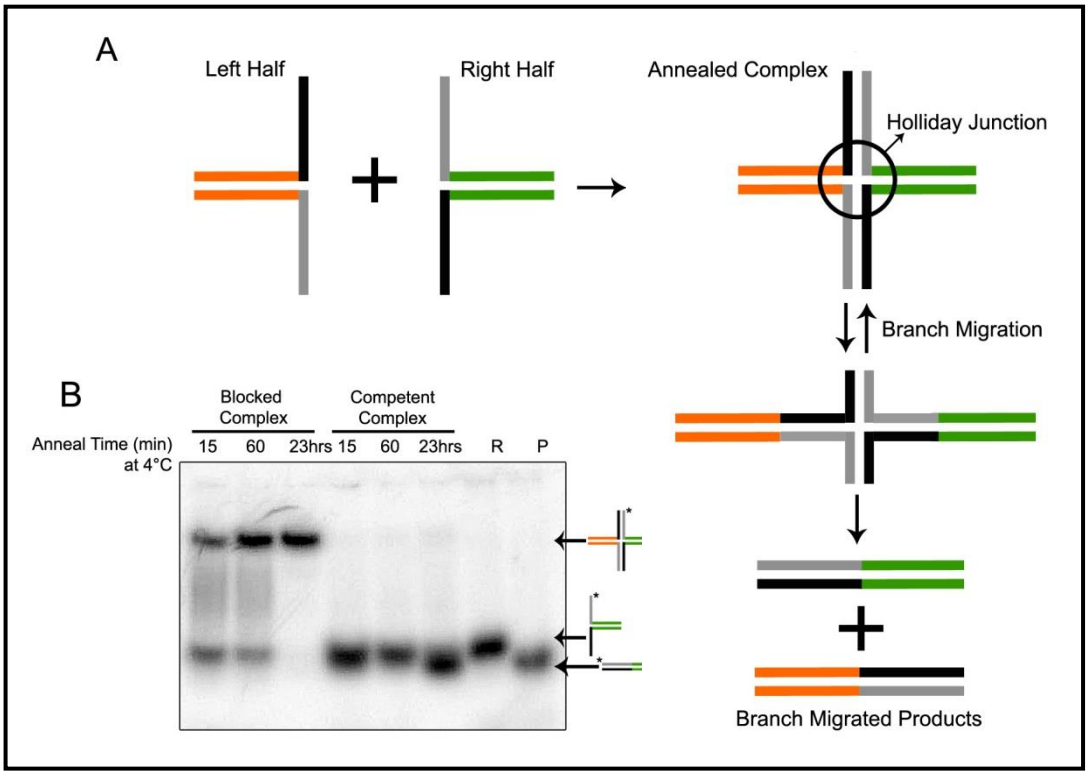

Figure 2-2. Branch migration oligo models used to explore the effects of time and temperature. (A) Annealed left and right halves are combined to form a four-stranded complex that has a center called Holliday junction. When branch migration occurs at higher temperatures or prolonged length of time, the oligos will slide back and forth until complete branch migration of the oligos occur yielding two branch migration products. **(B)** A complex with annealed arms 30 nts in length was designed first to see whether 4°C would be sufficient to stabilize the complex. Blocked complex, four stranded structures that do not contain complementary tails and will not undergo spontaneous branch migration, was used as control to confirm presence of the four-stranded product and the location it will run on a gel. The branch migration competent complex resulted in just the double-stranded products even in the shortest time of incubation (15 mins).

Branch migration incompetent (blocked) complexes, four stranded structures that do not contain complementary tails and will not undergo spontaneous branch migration, were made as a control to see rate of annealing to form the four-stranded complex and the location in which it will run in the gel. With the blocked complex, four-stranded products are beginning to form at 4°C within 15 mins. All of unblocked complexes had branch migrated to double-stranded products at all time points of incubation. Thus, this shows that a 30 nt annealed oligo complex is not stabilized even at temperature as low as 4°C and as short a time as 15 mins.

The conditions in which branch migration can be minimized were explored with the combined efforts of a post doc (Phillip Smiraldo) and technician (Troy Hutchens) in our lab,. Since the 30 nt complex was not stabilized, a new oligo model system was designed with annealed arms that are 150 nts in length. They tested the affects of adding different concentrations of $MgCl_2$ and NaCl, both of with enhance DNA interactions, and incubated the oligos at 37°C for 2 hrs (Fig. 2-3 A and B). Ethidium bromide (EtBr), a DNA binding dye, was also explored as another crucial factor in minimizing branch migration (Fig. 2-3 C). Both Mg^{2+} and ethidium bromide are thought to function by increasing base stacking of ds DNA across the Holliday junction. The conclusion of their results was that 50 mM of $MgCl_2$ alone, or 50 mM NaCl in presence of 25 mM of $MgCl_2$, or 5 ug/mL of EtBr was enough to stabilize the 150 nt complex. When the combination of salts, 50 mM $MgCl_2$, 50 mM of NaCl, and 5 ug/mL of EtBr were incubated with the same 30 nt complex that could not be stabilized in previous experiment, we found that the 30 nt complex can now be stabilized even at prolonged incubation time point (23 hrs) at 4°C (Fig 2-3 D).

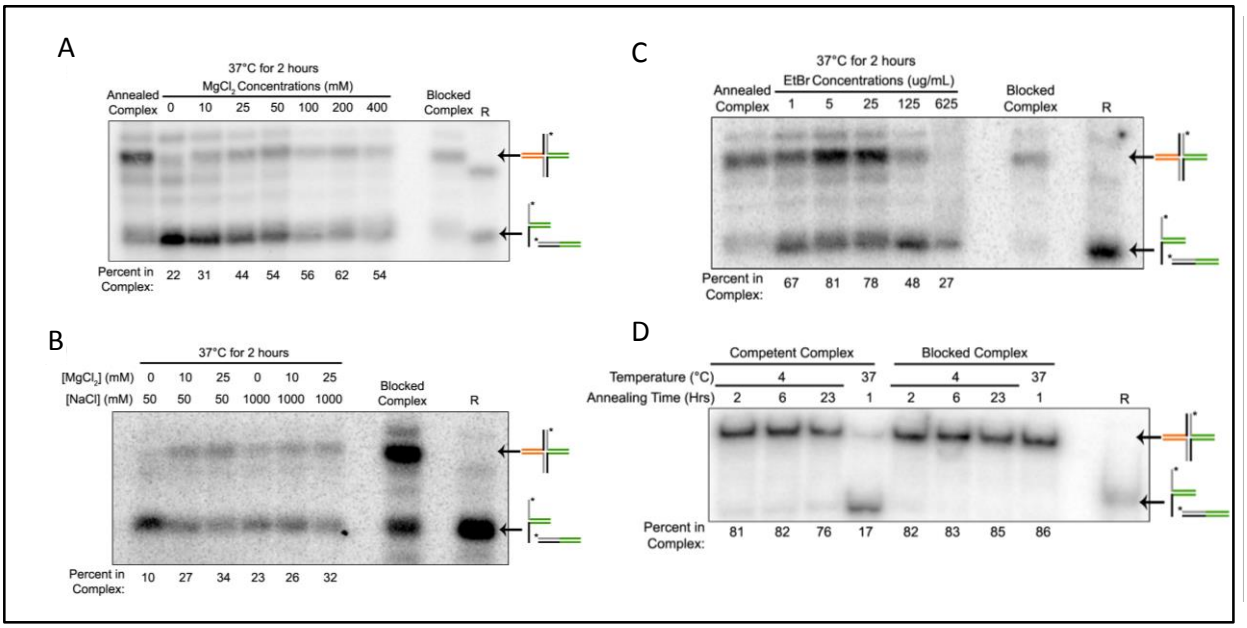

Figure 2-3. Branch migration studies with different $MgCl_2$, NaCl, and EtBr concentrations. **(A)** Varied concentrations of $MgCl_2$ were incubated with a 150 nt annealed oligo complex at 37°C for 2 hours. 50 mM of $MgCl_2$ was able to yield a high enough percentage in complex (minimize branch migration). **(B)** Varied concentrations of NaCl were incubated with $MgCl_2$ with the same complex at same conditions to show that 50 mM of NaCl was sufficient to yield the highest percentage in complex in presence of 25 mM of $MgCl_2$. **(C)** Varied concentrations of ethidium bromide (EtBr) were incubated with the same complex and same conditions to show that only 5 ug/mL of the dye is necessary to minimize branch migration and give the highest percentage in complex. **(D)** With all the collected information from (A-C), the same 30 nt complex from Fig 2-2 B was incubated at 4 and 37°C for 2, 6, and 23 hrs in presence of 50 mM $MgCl_2$, 50 mM NaCl, and 5 ug/mL of EtBr. The 30 nt competent complex were stabilized at all time points at 4°C, thereby confirming the effects of salt and DNA binding dye in minimizing branch migration. (Quantitation was done by our lab technician, Troy Hutchens, and some of the calculated percentages may be inaccurate, but the visual image is enough to draw estimated trends and conclusions.)

The oligonucleotide model studies thus far refers to a four-stranded structure, but the typical illustration of t-loop structure shows a model in which only the 3' G-overhang invades into the ds telomeric region (Fig. 2-4). If authentic t-loops are formed by such conditions, then it will not behave as a four-stranded, but as a three-stranded structure. But if the 5' C-strand also invades into the ds telomeric region, being complementary to the D-loop, then t-loop would exist as a four-stranded structure. Whether or not Mg^{2+} and EtBr will stabilize 3-stranded structures

needs to be explored. If the mechanism of their action is, in fact, stabilizing base stacking in ds DNA as in four-stranded structures, then they will not stabilize 3-stranded structures.

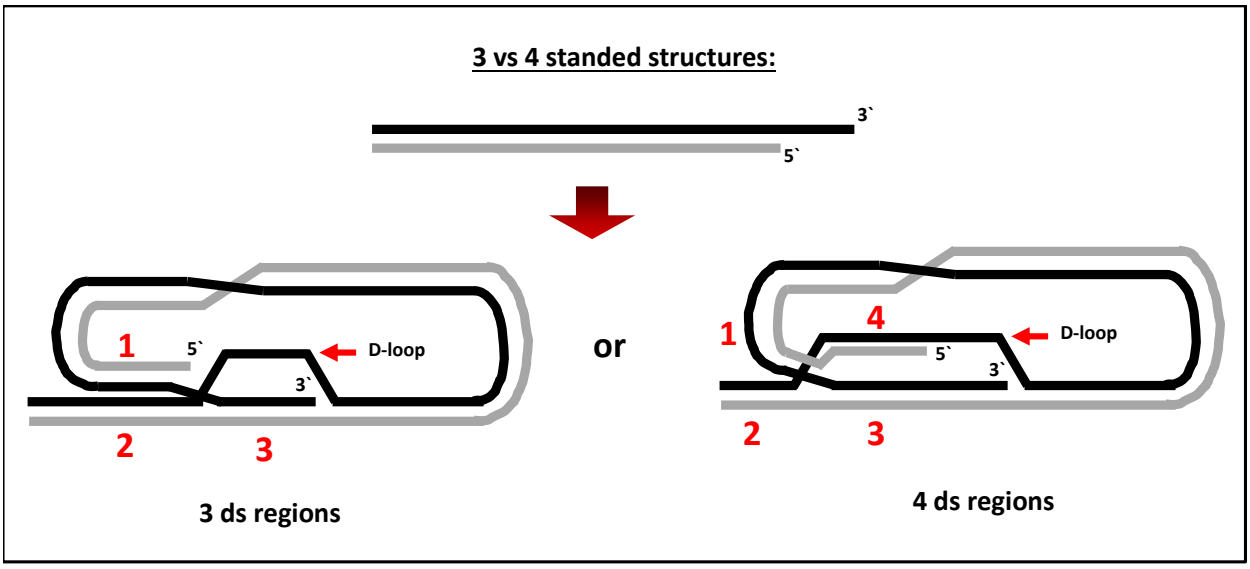

Figure 2-4. Schematic models of t-loops in 3 vs 4 stranded structures. The left model illustrates the typical representation of t-loops, where only the 3' G-overhang invades the ds region of telomeres resulting in a three-stranded structue. But hypothetically, the right model can also exist where the 5' C strand also invades and binds to the D-loop resulting in a four-stranded structure. The authentic nature of which structure t-loop conformation makes is still unknown and will be explored further via three-stranded oligonucleotide models.

This should allow us to then determine if both C- and G-strands invade during t-loop formation (forming a 4-stranded structure), or if only the G-strand invades (as is typically illustrated, forming a 3-stranded structure). Thus, the study with branch migration oligonucleotide models enabled us to determine the conditions in which branch migration can be minimized and allow for the incorporation of the salts for our t-loop assay that will maximize the amount of stabilized t-loops in the sample.

Another modification was made for the purposes of the actual t-loop assay where we substituted all buffers that contain NaCl to LiCl. We found that NaCl promotes formation of G-

quadruplex at the 3' single-stranded end and therefore inhibits digestion by Exo I, the main enzyme used as the basis of our assay (described later in the text). Single-stranded oligo of 50 nts in length were incubated in presence of 200 mM LiCl, NaCl, and KCl at different temperatures 4-37°C (Fig 2-5), where K+ have the highest G-quadruplex stabilization affect, followed by Na+, and the least with Li+ (Simonsson, 2001).

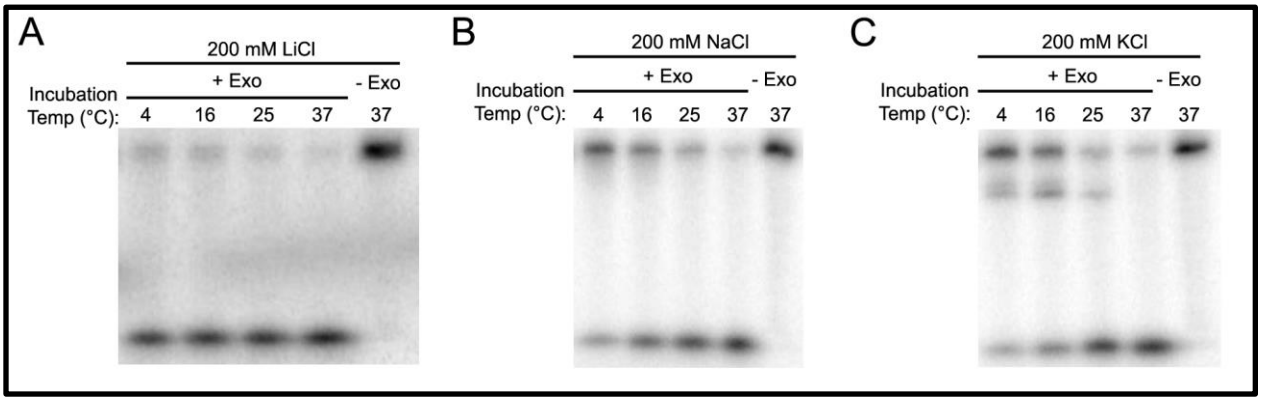

Figure 2-5. LiCl results in the least amount of Exo I inhibition (G-quardruplex formation) when compared with NaCl and KCl. (A) 200 mM LiCl was incubated with a single-stranded oligo at 4, 16, 25, and 37°C in presence of Exo. (-)Exo was added as a negative control to see where the full size (undigested) oligo run on the gel. Almost all oligos were successfully digested by Exo I at all temperatures in presence of LiCl. **(B)** In presence of NaCl, however, an increase in the amount of undigested oligos was seen at 4, 16, and 25°C. **(C)** In presence of KCl, a greater amount of undigested oligos was observed with appearance of a second higher molecular weight band.

Digestion of the single-stranded oligos by Exo I was observed at all temperatures in presence of LiCl. But in presence of NaCl, an increase in undigested oligos appeared at 4, 16, and 25°C. Lastly, in presence of KCl, a second higher molecular weight band appeared to show that digestion of the single-stranded oligo actually stopped after a few nucleotides were digested, a possible location where G-quadruplex were formed. Thus, this confirms that LiCl substitution is required in all the buffers that would be used in the t-loop assay to minimize formation of G-quadruplex.

For our t-loop assay, the first thing we tested was to see whether the Proteinase K we use to deproteinize DNA after cell lysis is functional at 4°C compared with the common 55°C digestion, and to determine the amount of time necessary for reasonable digestion. Hela cells were harvested and lysed at 4°C, and 2 mg/mL of Proteinase K was added to cell pellets incubating at 4°C for 1, 2, and 4 hours. We also examined protein digestion in the presence of two different concentrations of lithium chloride (LiCl), 100 mM and 600 mM. Salts, such as LiCl, were added at higher concentrations to promote stability of t-loops since higher concentrations of salt has been shown to promote DNA binding affinity where the 3' G-overhang may have higher chances of not branch migrating out of the double-stranded telomeric region. Coomassie blue staining showed that majority of the proteins were digested at both 4 and 55°C with one of the bands being Proteinase K itself (Fig. 2-6).

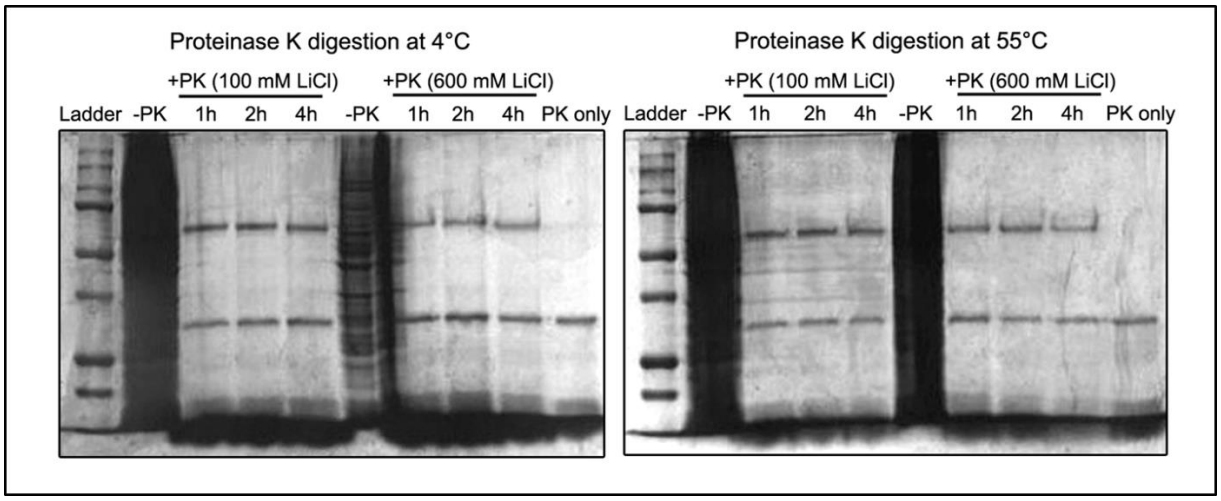

Figure 2-6. Coomasie blue stain: Proteinase K digestion of cells at 4°C and 55°C. Hela cells were harvested/lysed and 2 mg/mL of Proteinase K were added to each sample digested at 1, 2, and 4 hours in presence of 100 mM LiCl (lanes 3-5) and 600 mM LiCl (lane 7-9) at **(A)** 4°C and **(B)** 55°C. Cell lysates without Proteinase K (lane 2, 6) and Proteinase K without any cell lysates controls were loaded as well. The digestion at both temperatures and LiCl concentrations were comparable.

Genomic DNA harvested after Proteinase K digestion has a very high viscosity, such that loading the sample in a gel would be impossible (where the DNA doesn't stay in the well because it sticks to the pipette tip). Thus, DNA harvested under such crude conditions (no column clean up and all steps carried out at 4°C) will need to be digested with a restriction enzyme in order to lower the viscosity. We chose to use a blunt-ended 4 base cutter, Alu I, and it can digest genomic DNA into smaller pieces in order to lower the viscosity. We tested whether Alu I is able to digest genomic DNA at 4°C and at varied concentrations of LiCl to see what would be the highest concentration of salt that would be able to function just as efficiently (normal conditions is 50 mM NaCl). 5 U of Alu I was added to 2.5 ug of genomic DNA from Hela cells under varied concentrations of LiCl for 1 hour at 4°C and visualized under UV light after gel electrophoresis stained with Gel Red. DNA was well digested at 50, 75, and 150 mM of LiCl, while Alu I digestion activity is gradually lowered with increasing concentrations of LiCl above 150 mM (Fig. 2-7). Thus we have set the restriction enzyme digestion of genomic DNA at 150 mM LiCl for the t-loop assay.

We've developed an assay for t-loops using an enzyme called Exonuclease I (Exo I), which is a 3'→5' single-stranded DNA exonucleases. In the case of linear telomeres, the 3' G-overhang is exposed at the end and susceptible to Exo I digestion. In t-loops, however, the 3' G-overhang is safely strand-invaded into the double-stranded region, and it is protected from the digestion by Exo I. The two samples are run on a native agarose gel and probe with a radioactive P-32 C-rich probe that could bind only to the 3' G-overhang under native conditions, or to the G-strand in the D-loop region of a t-loop. After Exo I digestion, t-loops should retain a strong signal, while there would be a weak to no signal in the absence of the 3' G-overhang for linear telomeres (Fig. 2-8).

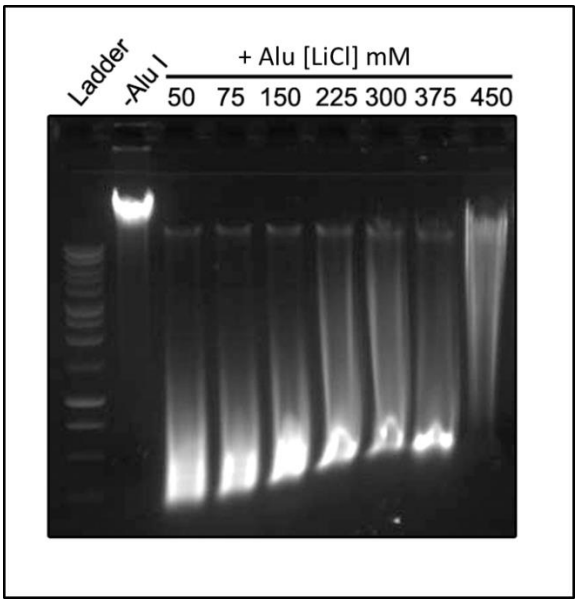

Figure 2-7. Alu I digest genomic DNA under different LiCl concentrations at 4°C. DNA was isolated from Hela cells and 5 U of Alu I was added to 2.5 ug of genomic DNA per sample in presence of 50, 75, 150, 225, 300, 375, and 450 mM of LiCl at 4°C for 1 hour. Genomic DNA digestion was efficient at 50-150 mM LiCl (lanes 3-5), but start to decrease from 225-450 mM LiCl (lanes 6-9). DNA without any Alu I incubations was loaded as negative control (lane 2).

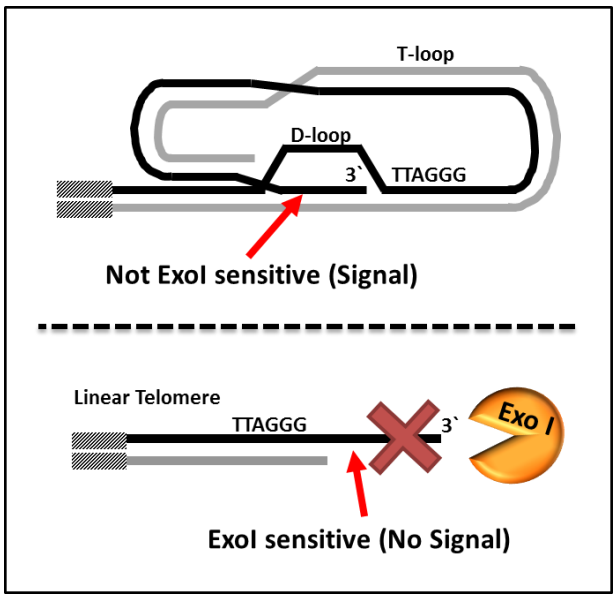

Figure 2-8. The t-loop assay with Exonuclease I. See text for details.

Before we tested t-loop sample from cells, we examined whether Exo I works at different LiCl concentration (similar to the Alu I experiment). The normal optimal buffer for Exo I only contains 50 mM NaCl (New England Biolabs), and since we know that Alu I only works up to 150 mM LiCl, we wanted to make sure Exo I digests overhang sufficiently at higher LiCl concentrations as well.

A single stranded oligo was used to test the efficiency of Exo I such that if there was no digestion, the oligo would remain at the same length as (-)Exo I control. If there were digestion, a shorter oligo than the negative control would be observed. The experiment showed that Exo I was able to digest the oligo very efficiently up to 150 mM LiCl and sufficiently up to 750 mM LiCl where you start to see a slightly darker band at original size of the oligo and some retention of oligos at the origin of the gel (Fig 2-9). Since Exo I digestion would be a step in our assay after Alu I digestion, we will use the same concentration of 150 mM LiCl for both reactions.

With the all the conditions optimized and tested, we next try to isolate t-loops at 4°C and test whether Exo I is able to show a difference in overhang signal compared to linear telomeres isolated at 55°C.

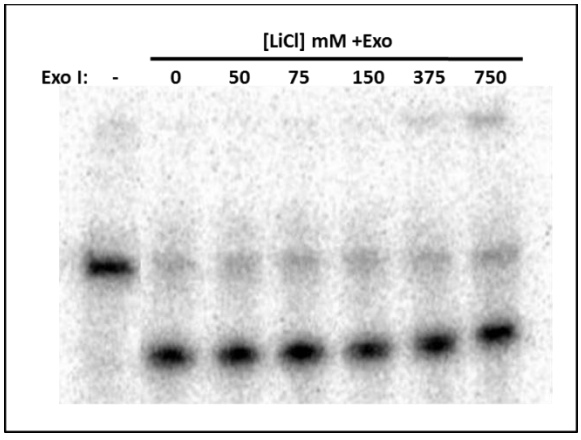

Figure 2-9. Exo I works at 150 mM LiCl. A single-stranded oligo was used to test the ability of Exo I to digest overhangs at different LiCl concentrations at 37°C for 1 hour. A smaller size band than the (-) Exo I control appeared at all concentrations tested and only with slightly darker band at the original oligo size at 375 and 750 mM LiCl.

The first attempt at our t-loop assay with samples from cells did not result in what was expected. The t-loop sample isolated at 4°C resulted in decrease overhang signal in presence of Exo I at 4°C for 1 hr (Fig. 2-10), showing almost no difference with linear telomere sample. We suspected that Exo I might still be active in the gel loading buffer, and might then be able to act at room temperature during the loading of the gel. We thus tested the addition of 50 mM of EDTA in triplicates immediately after Exo I digestion but prior to agarose gel electrophoresis to stop the reaction (where EDTA sequesters all the available Mg+ in the buffer necessary for the enzyme to function). The three additional lanes after t-loop and linear telomere lanes show a great increase in overhang signal in presence of EDTA (Fig. 2-10).

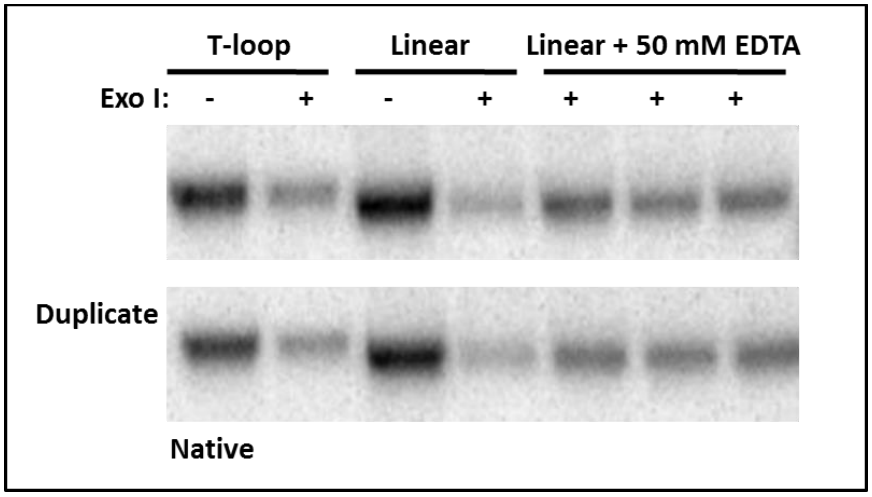

Figure 2-10. Exo I digests overhang during agarose electrophoresis. 5 ug of H1299 DNA isolated at 4°C (t-loop) and 55°C (linear) were Exo I digested at 4°C for 1 hr and ran on an agarose gel and probed for telomeres under native conditions to observe the overhang signal in each sample. A decrease in signal was observed in both t-loop and linear telomere sample. But if 50 mM of EDTA was added after immediately after digestion to stop the reaction, a much higher overhang signal was observed for the linear telomeres, suggesting that Exo I gave digested more overhangs during the process of electrophoresis.

Thus, this observation tells us that Exo I is able to digest more overhangs during room temperature agarose gel electrophoresis resulting in error prone results. Any increase in

temperature with prolonged amount of time may cause t-loop to unfold via branch migration. It is very critical that we keep all steps prior to final readout at 4°C. Thus, the last modification we made to our t-loop assay was to add 50 mM EDTA immediately after Exo I digestion so any overhang digestion should stop at that point in time.

The optimal temperature at which Exo I functions at is 37°C for 1 hour. Thus, the next thing we tested for is whether Exo I is able to digest 3' overhangs at 4°. DNA was isolated under normal conditions (Proteinase K digestion at 55°C) from Hela cells such that majority of the telomeres would be in the linear conformation. 20 units (U) of Exo I was added per 5 ug of DNA (estimated 10 ug of DNA per 10 million cells for cancer cells) and incubated at 4, 16, and 25°C for 1 hour. The native gel showed that 52% of overhang signals were left with incubation at 4°C in presence of Exo I; 22% at 16°C; and 13% at 25°C (Fig. 2-11).

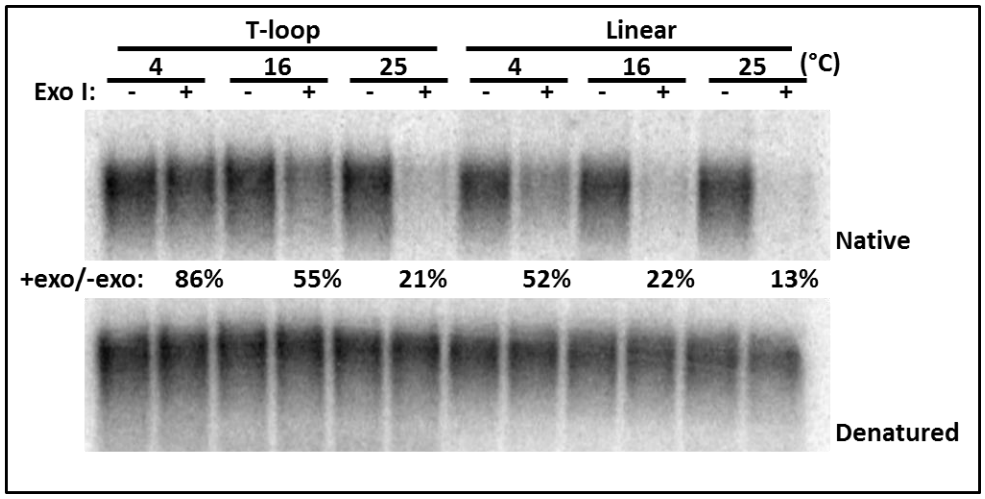

Figure 2-11. T-loop assay with Exo I: T-loop vs Linear Telomere DNA at varied temperatures. DNA was harvested from Hela cells in t-loop and linear telomeres conditions. After Proteinase K and Alu I digestion at 4°C, Exo I was added and incubated at 4, 16, and 25°C for 1 hour. The +exo/-exo ratio is representative of overhang (or D-loop) signal. Native gel was denatured to normalize native signals to total amount of telomeric DNA in the samples. T-loop samples consistently showed a greater amount of native signal than linear telomere samples at all temperatures, suggesting stabilization of t-loops in DNA isolated under t-loop conditions.

Although the digestion at 4°C is not as efficient as 25°C, we may still be able to detect a difference between t-loop and linear telomere samples. The same experimental conditions were conducted with DNA that was isolated under t-loop preservation condition (Proteinase K digestion at 4°C). 86% or D-loop signals were left at 4°C; 55% at 16°C; and 21% at 25°C (Fig. 2-11). T-loop samples consistently showed a greater remaining signal after Exo I digestion than linear telomere samples (difference of 34%, 33%, and 8% respectively). This strongly suggests that DNA isolated under t-loop conditions (Proteinase K digestion at 4°C) preserve t-loops, and that under linear conditions (Proteinase K digestion at 55°C) many t-loops unfold. The residual amount of signal left over in the linear telomeric sample at 4°C attributes to the fact telomeric overhang range in sizes such that there would be distributed percentages from short to long overhangs. Hela cells have average overhang lengths of 80 nts (Zhao et al., 2008), thus many overhangs are longer and more resistant to temperature effects of branch migration resulting in a high stability of t-loops. But the signal decreases with increase in temperature, thus demonstrating the fact that more t-loops are being unfolded due to higher rates of branch migration in presence of Exo I. Experiments were done where t-loop samples were incubated overnight at 16 and 25°C in absence of Exo I followed by 1 hr digestion with Exo I the next day. Results showed that none of the overhang signals in t-loop samples were decreased, suggesting that increasing the temperature alone over prolonged periods of time is not sufficient to unfold t-loops (data not shown). Rather, what we think is happening is that during the 1 hr incubation with Exo I at higher temperatures than 4°C, branch migration occurs such that the 3' G-overhang slides back and forth which possibly causes the very end of the overhang to melt away from the ds telomeric region. Thus, this allows Exo I to access the 3' end, begin digestion, and rapidly

unfolding t-loops. This hypothesis explains why the overhang signals from t-loop samples only decrease in presence of Exo I.

After confirming that t-loops are only highly preserved at 4°C and that any increase in temperature even during the 1 hr of Exo I digestion would enhance unfolding of t-loops, we next verify that this is a repeatable assay in multiple cell lines in triplicates. Results showed that there is a consistent retention of overhang signal under native conditions in presence of Exo for t-loop samples in triplicates, ranging from 70-76% (H1299) and 78-82% (Hela) (Fig. 2-12).

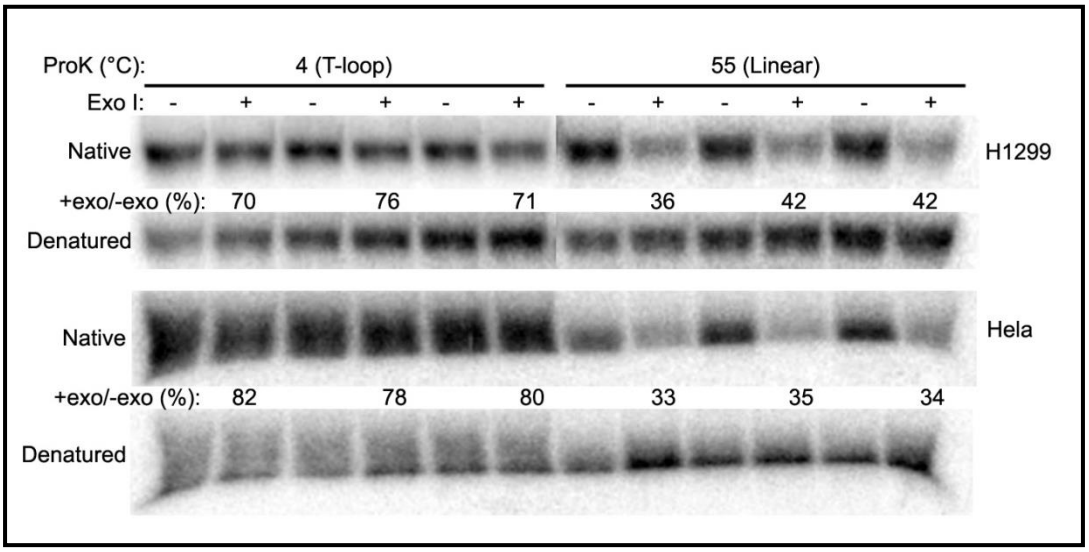

Figure 2-12. T-loop sample shows consistent retention of overhang signal compared to signal decrease in linear telomeres. Triplicates of t-loop vs. linear samples shows consistent higher overhang signal in t-loop than linear. DNA was harvested from H1299 and Hela cells under t-loop (ProK at 4°C) or linear conditions (ProK at 55°C). 20 U of Exo I was added to 5 ug of DNA to digest overhangs. A consistent retention of signal in (+)Exo lanes was observed in t-loop samples, and a consistent decrease in signal was observed in linear telomeric samples for both cell lines. T-loop assay can successfully distinguish between t-loops and linear telomeres.

In the case of linear telomeres, overhang signal decreased in presence of Exo I, ranging from 36-42% (H1299) and 33-35% (Hela). This shows an almost two fold difference consistently across two cell lines in overhang signal, or D-loop signal in t-loops, between t-loop and linear telomere

samples, suggesting presence and stabilization of t-loops at lower temperatures. Thus, this provides the evidence that we now have discovered a way to assay for t-loop presence with minimal of 2.5 to 5 ug of DNA using biochemical techniques with consistent and repeatable results.

Since Exo I digestion at 4°C seem to only yield a ~two fold difference between t-loop and linear sample, we wanted to know whether adding additional enzyme would allow for increase in the amount of overhang digestion at the same temperature (resulting in greater overhang signal difference between t-loop and linear sample). 5 ug of DNA isolated from H1299 cells was incubated with 0, 5, 10, 20, 30, and 40 U of Exo I after Alu I digestion of genomic DNA at 4°C for 1 hour. Southern blotting shows that the amount overhang remaining in the sample (~30%) does not change with notable degree in 20, 30, and 40 U of Exo I (Fig. 2-13).

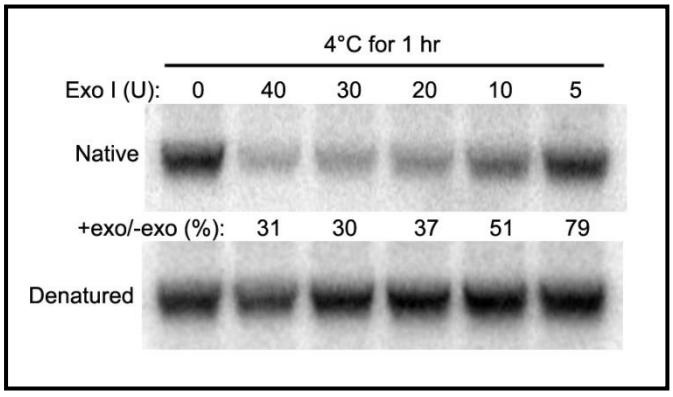

Figure 2-13. Increase amount of Exo I does not result in more overhang digestion in linear telomeres at 4°C. The amount of Exo I to use for the t-loop assay plateaus after 20 U per 5 ug of DNA. DNA from H1299 cells was isolated with same method as B. 5 ug of DNA were digested with different amounts of Exo I to see if a greater decrease in signal can be observed with higher amounts of enzyme. There was no significant decrease in overhang signal at enzyme concentrations higher than 20 U.

The samples with equal to or less than 10 U of Exo I shows a dramatic increase in the amount of overhang signal. Thus, adding additional Exo I higher than 20 U does not increase the amount of overhang digestion.

Conclusions

At the ends of telomere is a ss 3' overhang that strand invades into the ds region resulting in a lariat, loop-like structure called t-loop, which is a secondary structure that is crucial in protecting the ends of chromosomes being recognized as ds breaks and preventing inappropriate DNA damage repair machineries. Yet, very little is known about t-loops since the only method that have been used to prove their existence is done by transmission electron microscopy, a highly difficult method that require large amounts of starting DNA material and special expertise in the EM field. Thus, we have developed a novel t-loop assay based on biochemical approaches such that intact t-loops can be isolated and analyzed.

We have used oligo model system to determine the conditions in which intact t-loops can be isolated based on the theory of branch migration, where ds DNA slides back and forth until one strand completely displaces another strand of DNA. Modifying temperature, different salt concentrations, and DNA binding dyes, the conditions that are best for isolating maximum amount of t-loops (minimizing branch migration) are: keeping samples at 4°C, 25 mM $MgCl_2$, 50 mM NaCl, and 5 ug/mL of EtBr. However, we substituted NaCl with LiCl due the fact that Na^+ highly promotes formation of G-quadruplex at the end of ss 3' overhang (need reference here) such that it inhibits Exo I digestion (supplementary data). We have also found that the maximum concentration of LiCl that Proteinase K is still sufficiently functional at 4°C is 600 mM, and that restriction enzyme (Alu I) is can still digest genomic DNA sufficiently at is 150

mM. Thus, the buffer used for cell lysis and Proteinase K digestion contains 600 mM LiCl, 100 mM Tris, and 100 mM EDTA (Quick Prep Buffer). The buffer used for Alu I and Exo I digestion contains 150 mM LiCl, 10 mM Tris, 25 mM $MgCl_2$, and 1 mM DTT. All of which are conditions that we optimized for in order to isolate intact t-loops without the need of psoralen crosslinking.

The basis of our t-loop assay uses a 3→5' ss Exonuclease (Exo I) to distinguish between t-loops and linear telomeres. In t-loops, the 3' overhang is protected from Exo I digestion via strand invasion into the ds region of the telomeres. In linear telomeres, the 3' overhang is exposed and allow for Exo I digestion. Thus, using a radioactive P32- telomere specific probe for the C-rich strand using Southern blotting under native conditions, t-loops will retain the overhang/D-loop signal in even in presence of Exo I, and linear telomeres will show a decrease in overhang signal due to digestion by Exo I. We have shown that an almost two fold difference in overhang signal was achieved in comparing t-loop (Pro K digestion at 4°C) vs. linear telomere (Pro K digestion at 55°C) samples. Attempts to increase the difference between t-loop and linear telomere samples were made, but increasing enzyme concentration does not yield a higher digestion above background at 4°C and increasing temperature of Exo I digestion results in spontaneous t-loop unfolding due to increase in branch migration in presence of Exo I. But the consistency and high reproducibility of experiments with various cell lines for t-loop samples yielding an almost 2 fold higher overhang signal than linear telomere samples provide enough evidence to distinguish between the two samples.

Materials and Methods

Oligo Model System Design for Branch Migration Assay

Generation of the 30 nts Oligo Branch Migration Complex (Also Linkers for the Extended 155 nts Oligos)

DNA oligonucleotides were purchased from Integrated DNA Technologies, Inc (IDT). Oligonucleotide QA – KpnEco (5`-phospho-CGCTGTGAATTCTGTACTCCAGCTTGTGCCTCACCTCGACCATGGTATGA-3`) was annealed to Q`B – KpnEco (5`-CATATATGGAGTTCCGCGTTGGCACAAGCTGGAGTACAGAATTCACAGCGGTAC-3`) and the product is herein referred to as QA/Q`B. Oligonucleotide A`Q` - KpnEco (5`-TCATACCATGGTCGAGGTGAGGCACAAGCTGGAGTACAGAATTCACAGCGGTAC-3` was annealed to B`Q – KpnEco (5`-phospho-CGCTGTGAATTCTGTACTCCAGCTTGTGCCAACGCGGAACTCCATATATG-3`) and the product is herein referred to as A`Q`/B'Q. Oligonucleotide XA – KpnEco (5`- phospho-CCTGATGAATTCATGCGCTGACAACTGAGGTCACCTCGACCATGGTATGA-3`) was annealed to X`B – KpnEco (5`-CATATATGGAGTTCCGCGTTCCTCAGTTGTCAGCGCATGAATTCATCAGGCATG-3`) and the product is herein referred to as XA/X`B (this is the branch migration incompetent "blocked" complex). Underlined portions of the above sequences indicate the complimentary sequences for the oligonucleotide pair (See Fig 2-14). For each respective annealing pair, tubes containing 5 µM of each oligonucleotide, 10 mM Tris pH 8.0, and 5 mM EDTA (final volume of 200 µL) were placed into water bath containing approximately 3.5 L of water, which was heated

to 80°C and allowed to cool to room temperature. Tubes containing the annealed linkers were stored frozen at -20°C.

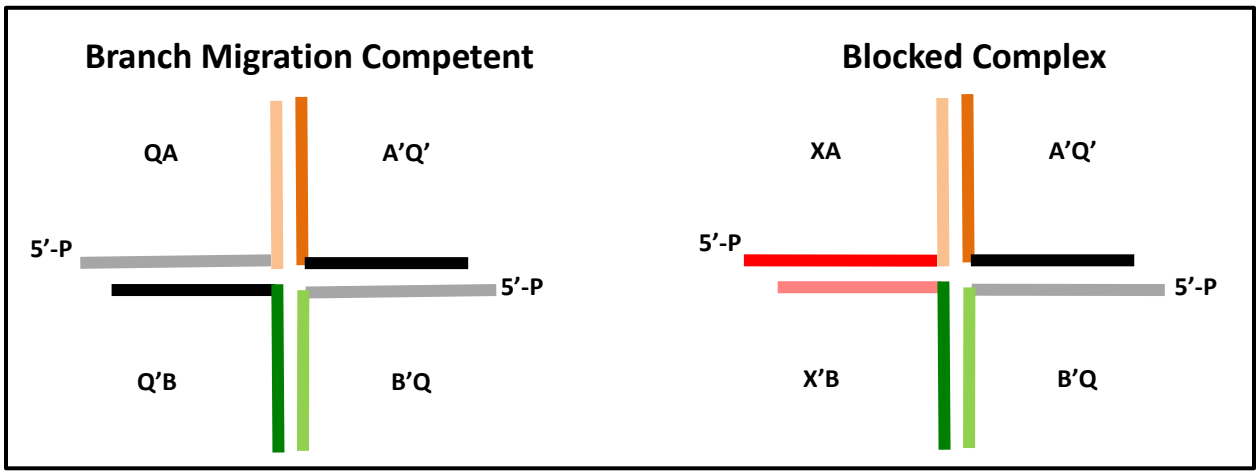

Figure 2-14. Schematic illustration of oligonucleotide model design. (See text for details.)

Generation of the 155 nts Oligos (Random and Telomeric Sequences Extension Arms)

DNA oligonucleotides were purchased from IDT. The extension arm containing 100 bp of telomeric sequence was PCR amplified using the SK primer (5`-CGCTCTAGAACTAGTGGATC – 3`), the T7 primer (5` -GTAATACGACTCACTATAGGGC – 3`), and the template BM Telo 100mer (5` -AGAACTAGTGGATCACCC[TAACCC]$_{16}$GGTACCGCCCTATAGTGAGT – 3`) (Promega GoTaq Kit). KpnI restriction enzyme site is underlined. PCR conditions were 95°C 2 min, (95°C 1 min, 56°C 1 min, 72°C 1 min) 30 cycles, 72°C 5 min. The extension arm containing 100 bp of random sequence was PCR amplified using the SK primer (5`-CGCTCTAGAACTAGTGGATC – 3`), the T7 primer (5` -GTAATACGACTCACTATAGGGC – 3`), and the template BM Random 100mer (5` -AGAACTAGTGGATCCACTGTAGGTATCTCAGTTCGGTGTAGGTCGTTCGCTCCAAGC TGTGCAGTGTACACGAATAGTCGTTCAGCACGACAGCTACGCATTATCCAGTAACTG

GGTACCGCCCTATAGTGAGT – 3`) (Promega GoTaq Kit). KpnI restriction enzyme site is underlined. PCR conditions were 95°C 2 min, (95°C 1 min, 56°C 1 min, 72°C 1 min) 30 cycles, 72°C 5 min.

The extension arm containing approximately 250 bp of telomeric sequence was PCR amplified using the SK primer (5`-CGCTCTAGAACTAGTGGATC – 3`), the T7 primer (5` -GTAATACGACTCACTATAGGGC – 3`), and the template plasmid Rep1 (Promega GoTaq Kit). PCR conditions were 95°C 2 min, (95°C 1 min, 64°C 1 min, 72°C 1 min) 30 cycles, 72°C 5 min.

Following PCR amplification, all amplified products were phenol:chloroform extracted, ethanol precipitated, re-suspended in 10 mM Tris pH 8.0, and digested with KpnI (Promega) at 37°C for 3 hours. The restriction enzyme-digested products were separated by agarose gel electrophoresis and the appropriate fragments were purified by placing the agarose gel pieces into dialysis tubing followed by electrophoresis dialysis. Recoveries were assumed to be 100%. The actual DNA concentrations were not determined due to the potential interference from ethidium bromide bound to the recovered DNA (all subsequent steps were performed with relative values). The tubes containing the KpnI-digested products were stored frozen at -20°C.

Radioactive End Labeling of the A`Q`/B`Q Purified Ligation Products

The branch migration complexes containing the A`Q`/B`Q linker (right half of the branch migration complex) were radioactively end-labeled by mixing 10 µL of A`Q`/B`Q purified ligation product with 10x T4 polynucleotide kinase reaction buffer (1x final concentration, New England Biolabs (NEB)), 2 µL of T4 polynucleotide kinase (NEB), and 5 µL of gamma-^{32}P ATP in a final volume of 25 µL. Reactions were incubated at 37°C for 1 hour. The remaining

unincorporated gamma-^{32}P ATP was removed by centrifuging the sample(s) through a G-25 sephadex column. The recovered product was stored frozen at -20°C. The relative concentration of the radioactively-labeled A`Q`/B`Q purified ligation products to the QA/Q`B (or XA/X`B) ligation products was estimated to be 2:5.

Generation of Left and Right Halves of the Branch Migration Complexes

The left and right halves of the branch migration complexes were individually prepared by mixing the appropriate PCR-amplified-KpnI-digested DNA fragment, QA/Q`B, A`Q`/B`Q, or XA/X`B, ligation buffer (final concentration of 1x, Promega), 6 µL of $MgCl_2$, 30 µL of ligase (? Units, Promega) in a final volume of 240 µL. Reactions were incubated at room temperature for 2.5 hours and the products were separated by agarose gel electrophoresis, and the appropriate fragments were purified by placing the agarose gel pieces into dialysis tubing followed by electrophoresis dialysis. A portion of each recovered product was separated by agarose gel electrophoresis, and the concentrations of the recovered products (ie, left and right halves) were estimated and diluted, as appropriate, to be approximately equal. The tubes containing the purified ligation products were stored frozen at -20°C.

Annealing the Left and Right Halves to form Branch Migration Complexes

One part (volume) radioactively-labeled A`Q`/B`Q purified ligation product (for example, 1 µL) was mixed with three parts (volume) QA/Q`B (or XA/X`B) ligation product (for example, 3 µL) in 1x TNM buffer (10 mM Tris, 0.1 mM EDTA, 50 mM NaCl, 10mM $MgCl_2$) and incubated at 37°C for 1 hour. The relative concentration of the radioactively-labeled A`Q`/B`Q purified

ligation products to the QA/Q`B (or XA/X`B) ligation products was estimated to be approximately 1:9.

Following the 1 hour incubation, a portion of the reaction was removed, diluted approximately 20-fold in ice-cold Stop Buffer (10 mM Tris, 0.1mM EDTA, 10 mM $MgCl_2$, 10% glycerol, 1ug/mL EtBr), and stored frozen at -20°C. This sample was collected for every experiment and served as a baseline for the amount of branch migration complexes that had formed.

Branch Migration Assay

To assess branch migration at 37°C vs. time, the remaining portion of the annealing reaction was diluted approximately 20-fold in 10 mM Tris, 10 mM $MgCl_2$, 50 mM NaCl, 0.1 mM EDTA and incubated at the higher temperature. At specific time points (for example, 15, 30, 45, 60, 90, 120, and 180 minutes) following the initiation of incubation, a sample was removed at each time point, diluted approximately 3-fold in ice cold Stop Buffer, and stored frozen.

To assess branch migration vs. $MgCl_2$ concentrations, the remaining portion of the annealing reaction was diluted approximately 20-fold into tubes containing 10 mM Tris, 10-400 mM $MgCl_2$, 50 mM NaCl, and 0.1 mM EDTA. An additional sample was diluted approximately 20-fold into a tube containing 10 mM Tris, 50 mM NaCl, 10 mM $MgCl_2$, and 100 mM EDTA (this results in a 0 mM $MgCl_2$ sample). All samples were incubated at 37°C for 2 hours. Following the incubation, each sample was diluted approximately 3-fold in ice cold Stop Buffer, and stored frozen.

To compare the ability of NaCl to prevent branch migration rates compared to $MgCl_2$ the remaining portion of the annealed reaction was diluted approximately 20-fold into tubes containing 10 mM Tris, 50 mM or 1 M NaCl, and 10 mM $MgCl_2$, 25 mM $MgCl_2$, or 100 mM EDTA (0 mM $MgCl_2$). All samples were incubated at 37°C for 2 hours. Following the incubation, each sample was diluted approximately 3-fold in ice cold Stop Buffer, and stored frozen.

To determine if ethidium bromide can prevent branch migration in the absence of $MgCl_2$, the remaining portion of the annealed reaction was diluted approximately 20-fold into tubes containing 10 mM Tris, 10 mM $MgCl_2$, 50 mM NaCl, 100 mM EDTA, and 1-625 µg/mL ethidium bromide. All samples were incubated at 37°C for 2 hours. Following the incubation, each sample was diluted approximately 3-fold in ice cold Stop Buffer, and stored frozen.
All samples were separated on a 1.2% agarose gel by electrophoresis. The gels were then placed onto a nylon membrane, dried at 60°C for approximately 2 hours, and exposed to a PhosphorImager screen overnight. Images from the phosphorimager screens were obtained using the Typhoon Trio Imager. For assessing branch migration for each sample, the amount of radioactive signal for the 4-way branch migration complex was normalized to the total radioactivity of the lane (ImageQuant software). The normalized value for the baseline sample was set at 1 (or 100%) and represents the maximum amount of 4-way complex that could be achieved for each experiment. The normalized value for each experimental sample was compared back to the baseline sample to obtain a percent 4-way complex remaining after incubation at the respective storage conditions.

Cell Culture

Hela cervical carcinoma, H1299 lung adenocarcinoma, and Hela overexpressed with hTERT cells were cultured at 37°C in 5% CO_2 in medium containing 10% cosmic calf serum (HyClone). BJ foreskin fibroblasts E6/E7 were cultured with same conditions but in 20% cosmic calf serum.

T-loop Assays

Proteinase K Digestion of Proteins at 4 vs 55°C at 100 and 600 mM LiCl

Hela cells were harvested and lysed with Quick Prep Buffer (100 mM/600 mM LiCl, 100 mM EDTA, and 10 mM Tris pH 7.5 (made with LiOH instead of NaOH)) and 25% Triton X-100. 2 mg/mL of Proteinase K (Ambion) was added to the cell lysate and incubated at either 4 or 55°C for 1, 2, or 4 hrs. The reaction was stopped with 2 mM phenylmethylsulfonyl fluoride (PMSF) protease inhibitor (Sigma-Aldrich) and loaded onto a polyacrylamide gel after denaturation and addition of dye. The gel was then Coomassie blue stained for protein content in each sample.

Alu I Restriction Enzyme Genomic DNA Digestion at Various LiCl Concentrations

H1299 cells were harvested and isolated DNA via Qiagen Blood and Cell Culture Midi Kit. DNA were quantified by NanoDrop DNA Spectrophotometer (Thermo Scientific). 20 U of Alu I was added to 2.5 ug of DNA in presence of 10 mM Tris pH 7.5, 10 mM $MgCl_2$, 1 mM DTT, and various concentrations of LiCl—50, 75, 150, 225, 300, 375, and 450 mM. The reaction mixture was then incubated at 4°C for 1 hour. The enzyme activity was accessed by agarose electrophoresis followed by UV visualization of DNA.

Final complete T-loop Assay with Exonuclease I

Hela cells were harvested and resuspended with Quick Prep Buffer (100 mM LiCl for linear telomeric sample and 600 mM LiCl for t-loop sample) at 30 ul per million cells, followed by cell lysis with 1% Triton X-100. 2 mg/mL of Proteinase K (Invitrogen, catalog #AM2548) was added to deproteinize the samples at 4°C (t-loop)/55°C (linear telomeres), and the reaction was stopped with 2 mM PMSF (Sigma-Aldrich, catalog # P7626-5G). 150 mM of Tris pH 8.9 was added to buffer the pH change with each Mg being uptake by EDTA. Sequentially, 125 mM of $MgCl_2$ was added to neutralize the 100 mM EDTA in Quick Prep Buffer. 3 U Alu I per ug of DNA was added to digest genomic DNA and lower viscosity of the samples. Since the sample was highly viscous before Alu I digestion, an estimation in the amount of DNA was done such that there should be ~10 ug of DNA per 1 million cancer cells or 6 ug per million normal diploid human cells. 0.7 U of RNase A (Qiagen) per ug of DNA was also added to digest RNA. The reaction mixture was then agarose dialyzed for 1 hr at 4°C (a method in which liquid sample is rocked over a surface area of 1% agarose containing the final desired buffer for the purpose of buffer exchange, 8 mL of agarose per well in a 6-well cell culture dish for sample volumes less than 1 mL). After dialysis, the sample is collected back into a tube and aliquoted for necessary experimental variations. 20 U of Exonuclease I (NEB) was added to 5 ug of DNA to digest overhang at 4°C, and the reaction is stopped by adding 50 mM EDTA (EMD Millipore, catalog # 60-00-4). The samples were then analyzed by 0.8% agarose gel electrophoresis and Southern blotting with P32-labeled probe with sequence $[(AATCCC)_4]$ under native conditions. We used a special high-activity probe containing nine P-32 dCTP per 18 bp probe to detect the small signal from the D-loop or 3' overhang (John Wiley & Sons, 2003). The gel was visualized with a PhoshporImager Screen on a Typhoon Trio Imager, and the amount of overhang signal was

quantified by the ImageQuant software. A denatured signal was obtained by denaturing the gel and re-probing again to determine the total amount of telomeres in each lane. This signal was used to normalize the native signal such that the amount of DNA loaded was taken into account for the quantification procedures.

CHAPTER THREE

Validation of the T-loop Assay by Electron Microscopy

Introduction

T-loop is a secondary structure formed by repetitive sequences (TTAGGG) at the ends of chromosome called telomeres where the 3' overhang inserts into the ds region (Fig. 1-1) (Shay and Wright, 2006; Zhao et al., 2009). This conformation serves as protection from inappropriate DNA damage repair that can result in cellular dysfunctions (Hockemeyer et al., 2005). The first and only group thus far that has been able to visualize t-loops by TEM is Dr. Jack Griffith's Laboratory (UNC, Chapel Hill, NC) (Fig. 1-7). They discovered that 15-40% of their DNA samples were in t-loop conformation in Hela cells, 15-20% in mouse liver, and 15% in human peripheral blood lymphocytes (PBLs) (Griffith et al., 1999). They were also able to determine a correlation between telomere length and sizes of t-loops. Two-thirds of the t-loops they observed had contour lengths of 12-18 kb (the total distribution laid between 3 and 25 kb) in a clone of Hela cells with long telomeres (range from 15-40 kb)(Griffith et al., 1999). Yet, in another clone of Hela cells and human PBLs that have shorter telomeres, the average contour lengths of t-loops were 10 and 8 kb, respectively(Griffith et al., 1999). This essentially summarizes everything we know about t-loops *in vivo* since the technicality of doing EM imaging limits the amount of molecular/biochemical experiments that can be easily done. Thus, this gives the rationale as to why the development of a biochemical t-loop assay is of such high importance.

In order to provide strong evidence that we are isolating and enriching for actual, authentic t-loops biochemically from cells, the second important part of this thesis project was to achieve the EM imaging technique on t-loops from DNA isolation samples. Many attempts with other imaging techniques were made such as light microscopy and scanning electron microscopy (SEM). While we attempted to spread control plasmid DNA on the mounting slide, there were many technical problems, and we were unable to clearly distinguish linear vs. circular plasmids due to resolution limitations in these techniques. Thus, transmission electron microscopy (TEM) has proven to be the "gold standard" because it provides very high spatial resolution, allowing analysis of features at an atomic scale-range of few nanometers.

The art of visualizing DNA by EM was first achieved successfully by Kleinschmidt and Zahn in 1959 (Kleinschmidt and Zahn, 1959), hence the technique was known as the Kleinschmidt method. It achieves evenly spreading of nucleic acids by taking advantage of its negative charge and forming a complex with a basic protein monolayer film, usually cytochrome *c*, which holds DNA in a 2-D conformation (Kleinschmidt and Zahn, 1959). However, current methods from the Griffith laboratory do not require the protein film, but instead, cytochrome *c* is added to the DNA sample that has been pH adjusted by ammonium acetate and placed on a piece of parafilm. Then DNA-protein complex can be picked up by a copper grid that has been coated with parlodion, a hydrophobic translucent substance that will adhere to the cytochrome *c*. Using this method, we were able to visualize DNA in the range of a few nanograms on TEM.

Another important procedure that is critical for visualizing t-loops on EM is the crosslinking of DNA during DNA isolation procedures. As depicted in Fig. 1-1, t-loops are believed to only be held together by the hydrogen bonds between the complementary sequences of the 3' G-overhang and a part of the ds region of the telomere after deproteinization. *In vivo*, t-

loops are said to be held together by parts of the shelterin complex, TRF1 and TRF2 dimers. TRF1 was inferred to induce a bend in the TTAGGG repeats thereby promoting intratelomeric base pairing (Griffith et al., 1998), and TRF2 promotes strand invasion by the ss 3' G-overhang into the ds region of the telomere (Griffith et al., 1999). Thus, once deproteinization is completed by Proteinase K, t-loops can be subjected to branch migration where the 3' G-overhang slides back and forth and completely unfolds with time depending on the size of the overhang inserted. The Griffith laboratory follows a procedure where a chemical class called psoralen is added to nuclei after outer cell membrane is lysed. Psoralen and its derivatives can covalently crosslink pyrimidines on opposite strands of DNA duplex when activated by ultraviolet light of long wavelength (320 to 380 nm) (Hanson, 1979). It is permeable to both outer cellular and nuclear membranes, thus if necessary, the crosslinking reaction can take place in live cells (Hanson, 1979). The specific derivative their lab uses is 4' aminomethyltrioxsalen (AMT). Therefore, if the 3' G overhang is covalently crosslinked to the ds region of the telomeres, then t-loops can be permanently stabilized over the prolonged length of time for the procedures of telomere purification and EM preparations.

All of these procedures including purifying telomeres after isolating t-loops via the t-loop assay method, crosslinking DNA, preparing samples for EM, and imaging with TEM must be explored and optimized in order to provide strong evidence to validate the biochemical purification assay.

Results

After the establishment of the biochemical t-loop assay, we next sought to validate our assay by visualizing t-loops and linear telomeres from our biochemical isolations via t-loop assay

method by transmission electron microscopy (TEM). Since one cannot distinguish between genomic vs. telomeric DNA on an EM image, a method in which we can isolate enriched telomeres from a genomic DNA mixture was established. Our telomere purification method utilizes a ss-biotinylated telomere sequence specific probe to "capture" the telomeres which then could be pulled down by streptavidin-coated magnetic beads. The sequence of this method is illustrated in Fig. 3-1.

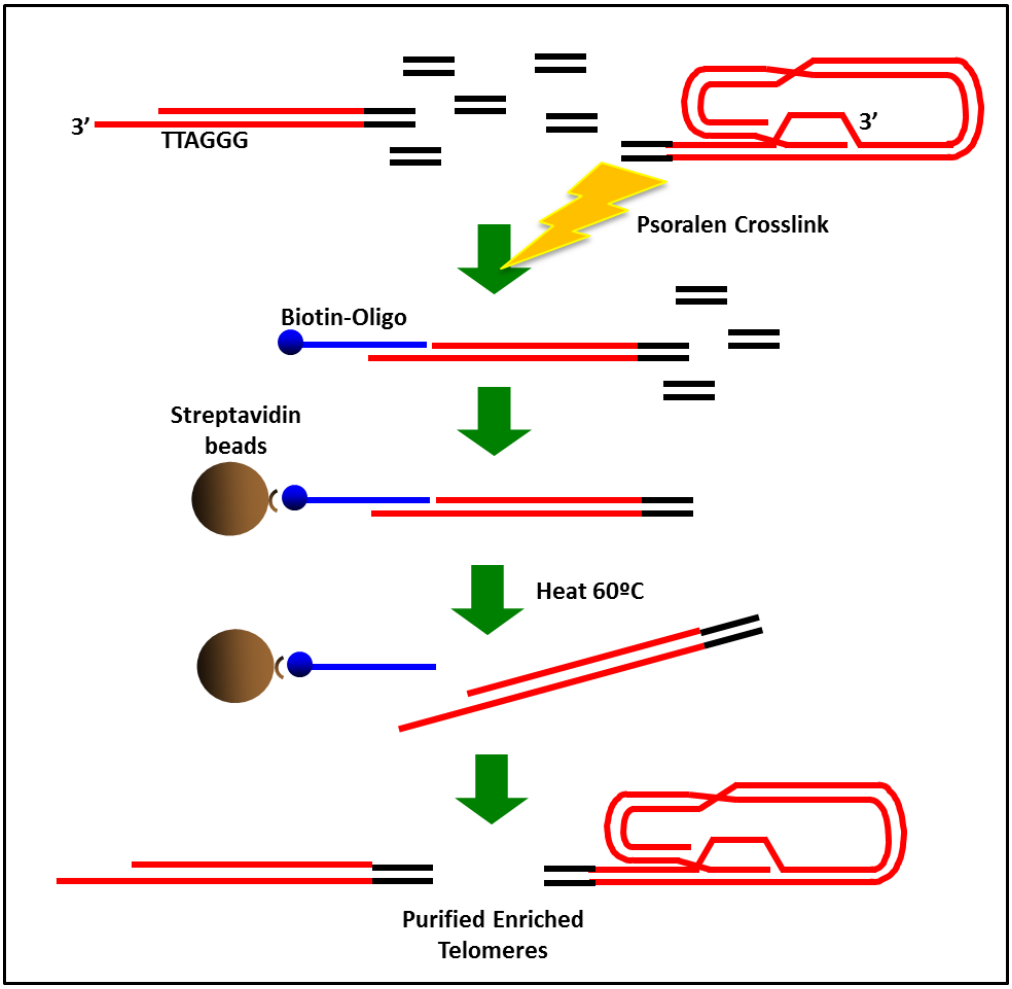

Figure 3-1. Schematic illustration of the sequence of events during telomere purification. Genomic DNA isolated from cells is first digested with restriction enzymes leaving only telomeric DNA intact. Then the DNA sample is psoralen crosslinked. A biotinylated oligo containing telomere specific sequences complementary to the 3' G overhang or the D-loop is annealed to the telomere. The complex can then be pulled down by magnetic streptavidin beads and released pure telomeres by heat.

Control experiments with different amount of beads and concentrations of biotinylated oligos were tested to determine the optimal conditions for maximum yield. First, a set amount of kinased biotinylated oligos with eight C-rich repeats (B-L-6RE-CTR8) was incubated with different volumes of beads at 4°C overnight. Amount of oligos captured was calculated according to the radioactive signal in the beads. Ten microliter of beads was required for good recovery of 25 pmol of oligos (Fig. 3-2 A), which would be approximately 1 ul of beads for every 3 pmol of oligos (a ratio of 1:3).

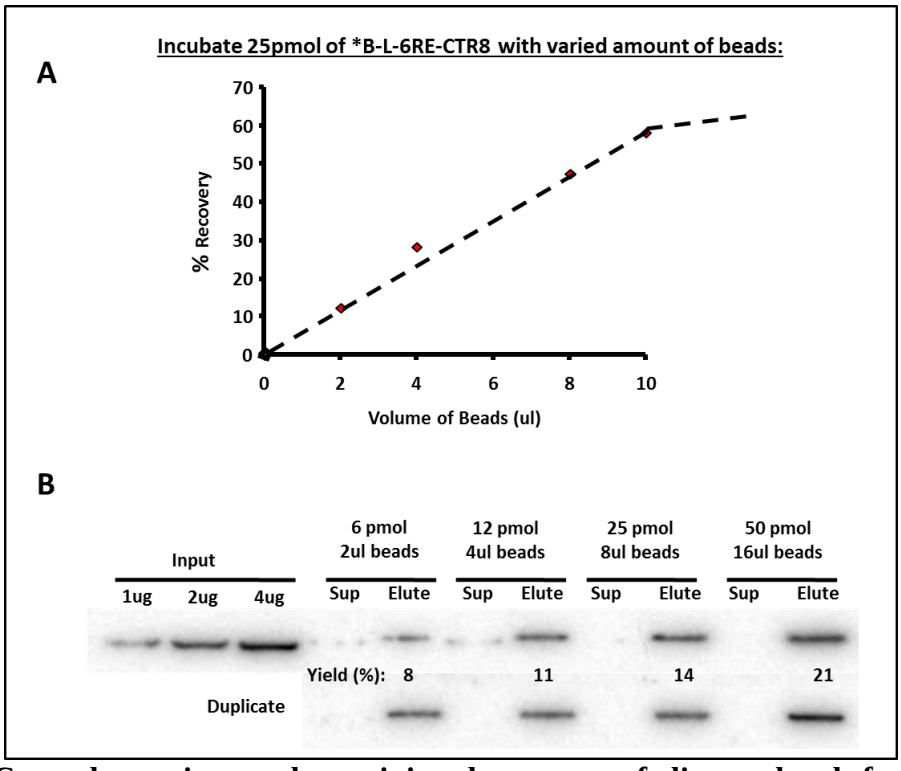

Figure 3-2. Control experiments determining the amount of oligos to beads for optimal capture. (A) 25 pmol of radioactively kinased oligo B-L-6RE-CTR8 was incubated with 2, 4, 6, 8, and 10 ul of beads at 4°C overnight. % Recovery was calculated by the amount of radioactive signal in the beads vs. supernatant. 10 ul of beads was found to yield ~60% recovery of 25 pmol of oligos, yielding a ratio of 1ul beads to 3 pmol of oligos. **(B)** Different amount of oligos to beads were incubated at 4°C overnight with 100 ug of H1299 DNA (Qiagen Kit prepped). Supernatants and eluted samples were then loaded onto a slot blot and probed with C-rich probe to calculate the amount of telomeres in the samples. Input DNA was loaded as controls so that calculation of yield is possible. 50 pmol of oligos incubated with 16 ul of beads per mL of sample resulted in a decent yield of 21%.

Next, using this known ratio, a variety of concentrations of oligos and beads in a set volume of binding buffer and 100 ug of DNA sample were incubated at 4°C overnight to determine which combination would result in highest yield of telomeric DNA. 50 pmol oligos incubated with 16 ul of beads in 1 mL of binding buffer resulted in a high yield of 21% telomeric DNA (Fig. 3-2 B). Thus, a reasonable concentration of oligos to beads in a specific volume of sample and buffer for telomere purification was determined (50 pmol/mL B-L-6RE-CTR8; 16 ul beads/mL of sample).

Other than just using a biotinylated oligo that consists of eight C-rich telomeric repeats to capture telomeres, another control experiment was to use oligos of different C-rich repeats with only a short linker (the original oligo sequence that was used to develop this method in the Shay/Wright laboratory) to determine which oligo would give a maximum yield. Originally, we designed the oligo (B-L-6RE-CTR8) with a longer linker that contains 21 nts of sequences that are cut sites of six restriction enzymes for the possibility of releasing final eluted telomeres by a restriction enzyme. This method resulted in inefficient release of the telomeres from the beads where a large amount of residual telomeric DNA were still attached (only ~50% of the total yield were eluted with Alu I digestion at 4°C, data not shown). In addition, this elution method required multiple subsequent steps to clean up the DNA sample (commercial restriction enzymes contain large amounts of BSA that covers the entire EM grid, blocking any real telomeric DNA from attachment, data not shown). These two caveats turned our direction back to the original oligo design for telomere purification (developed by the Shay/Wright laboratory). A series of lengths of C-rich repeats were tested to determine the amount of telomeres being pull down from 100 ug of DNA (prepared by Qiagen kit). The oligos were incubated overnight at room temperature to anneal to the telomeres, followed by incubating with streptavidin coated beads overnight at 4°C. Using input DNA to calculate yield, BL-CTR2 and BL-CTR3 resulted in the

highest yield, 35 and 33% respectively (Fig. 3-3). A significant yield decrease was observed just by doubling the C-rich sequence in length. Surprisingly, the BL-6RE-CTR8 also resulted in the same high yield as the shorter oligos. A possible explanation would be that a longer linker, 21 nts, allows for more flexibility around the beads in a way that the long stretches of telomeres can twist around the beads relieving any steric hindrance present. The oligos with a shorter linker but the same length of C-rich repeats have less flexibility since the linker only contains 4 nts, making it more susceptible to torsional drag stress of the kilobases of telomeres. Thus, all three oligos, BL-CTR2, BL-CTR3, and BL-6RE-CTR8, are good candidates for optimal telomere purification.

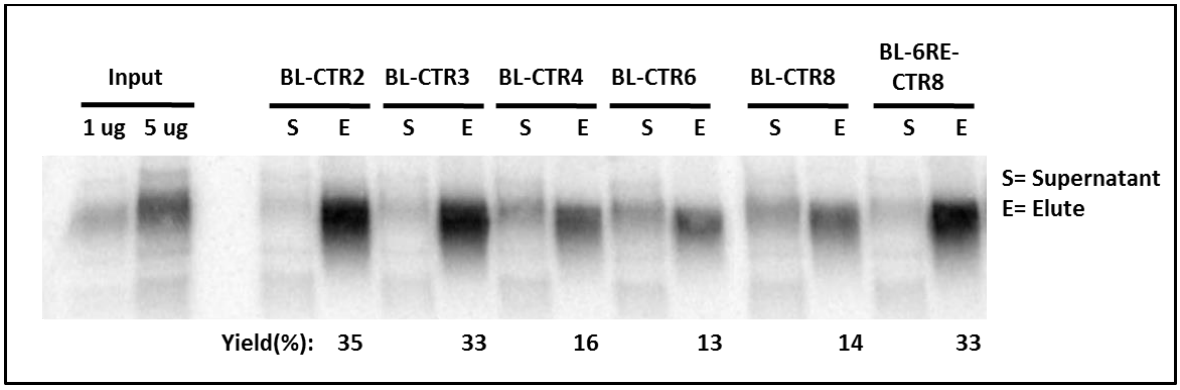

Figure 3-3. Telomere purification with varied biotinylated oligo lengths. 50 pmol/mL of each oligos were used to pull down 100 ug of DNA from Hela cells at room temperature. BL-CTR2, BL-CTR3, and BL-6RE-CTR8 all resulted in high yields of 35 and 33 % respectively. The yield decreases with BL-CTR4, BL-CTR6, and BL-CTR8 by half the amount.

After the telomere purification method had been optimized, we next explored the parameters of psoralen crosslinking. Although the Griffith laboratory provided the protocol with specific dosages necessary for optimal crosslinking (about one crosslink per 100 base pairs is best for t-loop stabilization and not crosslinking so much that the DNA tangles into a ball), the conditions were explored to ensure correct psoralen crosslinking was achieved. Ds oligos with

telomeric sequences in length 100, 200, and 400 bps were incubated with increasing concentrations of AMT (30-500 ug/mL) and UV crosslinked with long wavelength (365 λ). Samples were run on a denaturing agarose gel, dried, and probed (C-rich). Oligos that were not crosslinked ran as a lower molecular weight ss DNA, and oligos that were successfully crosslinked ran higher in the gel as duplex DNA. At higher concentrations of AMT, oligos of all lengths were successfully crosslinked (Fig. 3-4 A), whereas some of the lower concentrations in the 100 bp oligo did not run as duplex DNA.

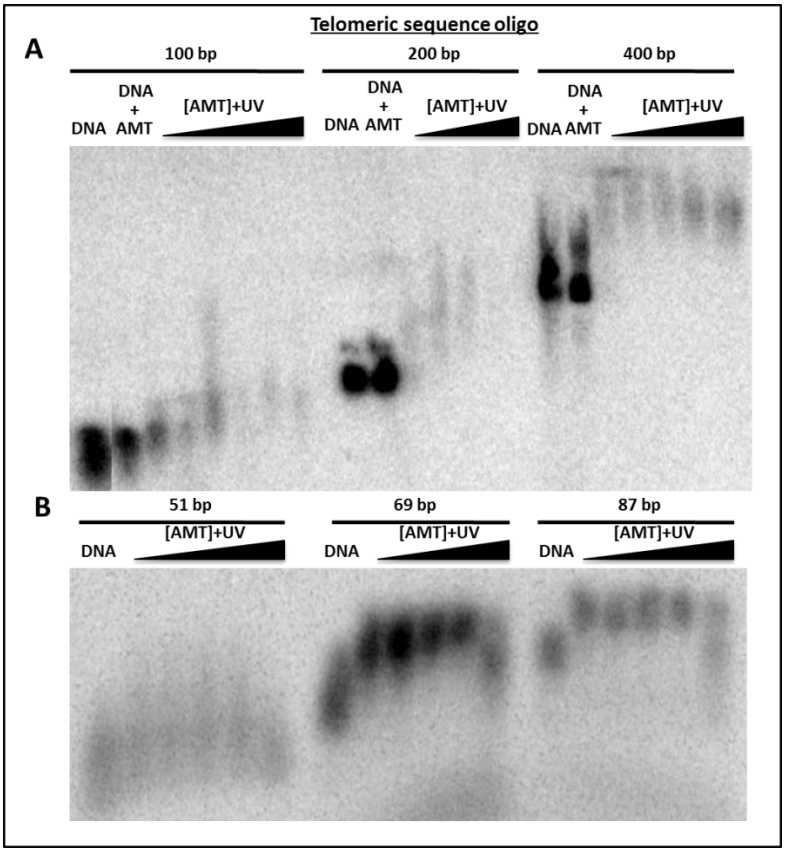

Figure 3-4. AMT crosslinking with different lengths of oligos. (A) Ds oligos with telomeric sequences of 100, 200, and 400 bp were UV crosslinked with increasing concentrations of AMT (30-500 ug/mL). DNA samples were run on a 2% alkaline agarose gel to distinguish between ss DNA (run faster) and ds DNA (run slower). DNA and DNA with AMT but no UV were added as negative controls. The 200 and 400 bp oligo were successfully crosslinked with all concentrations of AMT, while the lower concentrations of AMT did not crosslink the 100 bp oligo. **(B)** Similar experiment was done as (A) but with shorter lengths of oligos, 51, 69, and 87 bps. 500 ug/mL AMT clearly denatures the DNA. Both 69 and 87 bp oligos were crosslinked

successfully at all concentrations of AMT (except 500 ug/mL). But the results with 51 bp oligo seem to be inconclusive since there is no a big difference in gel shift for ss vs. ds DNA. The suggested 250 ug/mL of AMT according to the experimental procedures from the Griffith laboratory resulted in good crosslinking in all three oligos. Since the results for 100 bp were not conclusive as the bands were not crisp but a bit fuzzy, we conducted another similar experiment with shorter oligos, 51, 69, and 87 bps. Results clearly showed that both 69 and 87 bp oligos were successfully crosslinked at all concentrations of AMT (Fig. 3-4 B) with the exception of the highest concentration 500 ug/mL AMT where DNA appeared to have been denatured. The result for the 51 bp oligo was inconclusive as the different gel mobility between ss and ds DNA was not large enough to distinguish. Since suggestions from the Griffith laboratory was at least 1 crosslink per 100 bps of DNA, the 87 bp oligo clearly justifies that criteria at the same recommended concentration of AMT 250ug/mL.

Next, we took normal Hela cells and harvested DNA under t-loop vs. linear telomere conditions. After treating with Proteinase K, 250 ug/mL AMT was added to the samples and UV crosslinked with long wavelength. Then the samples were treated with restriction enzyme Alu I and subjected to native agarose electrophoresis. Native signals represent either the 3' G overhang in linear telomeres or the D-loop in t-loops. Denatured signal represents total amount of telomeric DNA in the samples. Thus, if DNA was successfully crosslinked, there should be a decrease in signal in (+) AMT lanes since DNA should stay as duplexes. Both t-loop and linear samples showed a significant decrease in signal for (+) AMT compared with (-) AMT in the denatured gel (Fig. 3-5). This suggested that the telomeric DNA stayed double-stranded and blocked any additional C-rich probe from binding other than what was in the native gel. This provided robust evidence that AMT crosslinking was successful.

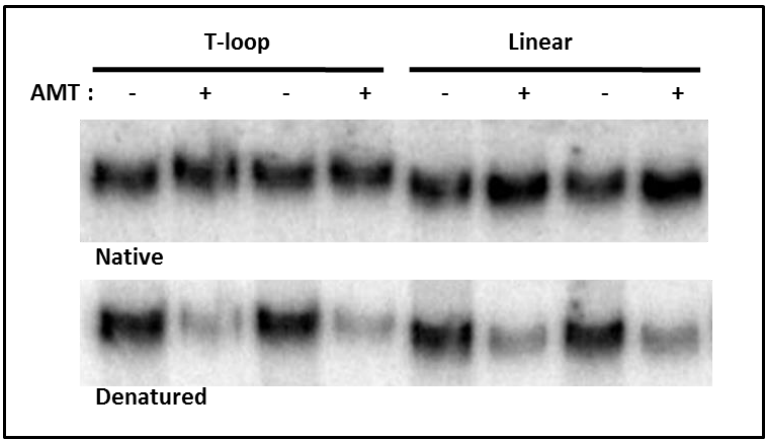

Figure 3-5. Telomere DNA were successfully crosslinked. DNA was harvested from Hela cells under t-loop and linear telomere conditions (4 vs. 55°C). After deproteinization by Proteinase K, 250 ug/mL AMT was added to the samples and UV crosslinked with long wavelength for 30 mins on ice. Then the samples were treated with Alu I, and 5 ug of DNA were ran on agarose gel. Native signals indicate where the C-rich probe is binding to the 3' G overhang in linear telomeres or the D-loop in t-loops. Denatured gel should represent total amount of telomeres in the sample unless the DNA was crosslinked and stays as native signal. A significant decrease in signal was seen in the denatured gel for (+) AMT, suggesting that telomeric DNA was successfully crosslinked.

With no previous experience in EM and no expertise on campus in visualizing nucleic acids on EM, I went to the Griffith lab at University of North Carolina to learn the technique. The first control I've accomplished to look at first was 11 kb plasmid. The plasmid DNA was spread using the Kleinschmidt method with cytochrome *c*. Copper grids used as sample platform was coated with the Griffith laboratory's own supply of parlodion. To give the sample contrast and be able to see contour lines on the TEM, the copper grid spread with DNA must be shadowed with a metal wire containing platinum: palladium followed by carbon, a critical additional step that strengthens the parlodion coating so that it will not burn a hole in the sample when the high power electron beam goes through the grid. The cytochrome *c* bound to the plasmid molecules allowed the DNA to look thicker and distinguishable above background compared to what was previously tried on my own according to other published EM protocols (Fig. 3-6 A, B). The main goal of doing these control experiments was to ensure that DNA does

not get into a tangled mess on the grid, and the contour outline of the DNA can be clearly seen above background as a thick line. The second EM challenge Dr. Griffith had me do was to spread lambda DNA, which are long DNA molecules that can be easily tangled if the Kleinschmidt method was not done correctly. Following the same protocol, lambda DNA was spread as single stretches of lines across the EM grid (Fig. 3-6 C). These controls were repeated multiple times at our own campus to ensure that the EM technique was repeatable before any attempt to visualize real DNA sample from telomere purification.

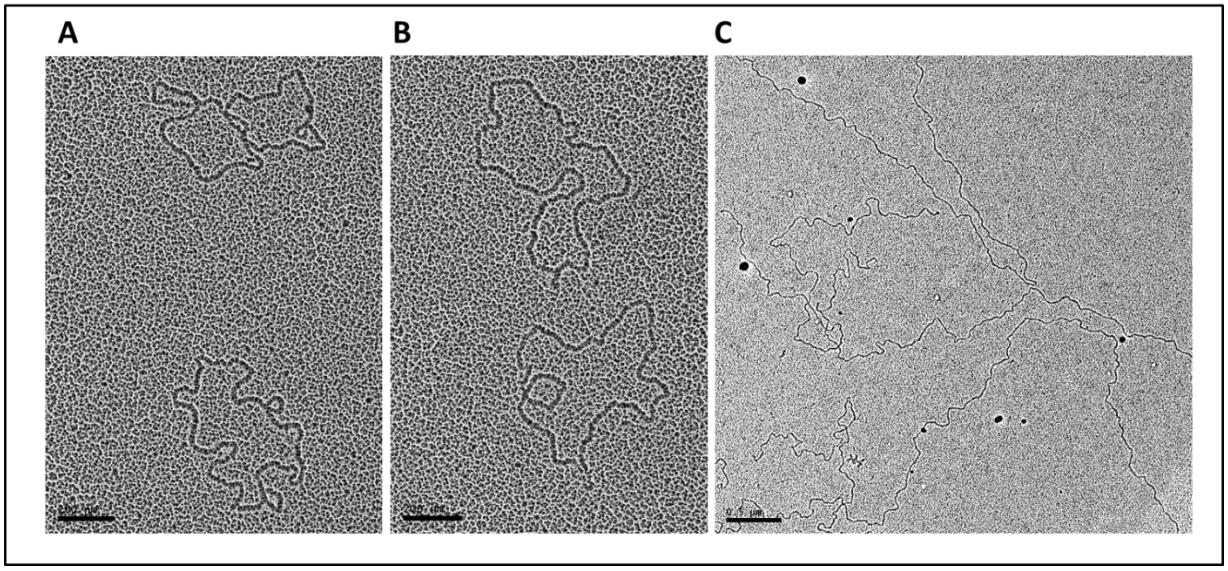

Figure 3-6. Plasmid and lambda DNA visualization on TEM. (A and B) Circular 11 kb plasmids spread on EM copper grids by the Kleinschmidt method with cytochrome *c*. No tangles were seen and only with occasional twist/overlapping of the DNA were seen. **(C)** Lambda DNA prepared the same way and visualized on TEM. Long stretches of DNA was observed with no tangles.

With the EM techniques solidified, we next tried to visualize the DNA isolated from t-loop and linear telomere purifications. 100 million Hela cells were harvested to start the process with 1 mg of DNA. The purification process alone will lose 80-90% of the starting material. Since telomeres are only approximately 1/6000 of genomic DNA, a 20% recovery from 1 mg of

DNA will only result in 33 ng of telomeres. Following the EM sample preparation protocol from plasmid control experiments, my first attempt to visualize t-loop and linear telomere sample on the TEM from actual telomere purification resulted in a high background of unknown globular structures (Fig. 3-7 A). The way that we isolate t-loops is actually a crude DNA isolation where no affinity columns or protein precipitations were done to clean up the sample.

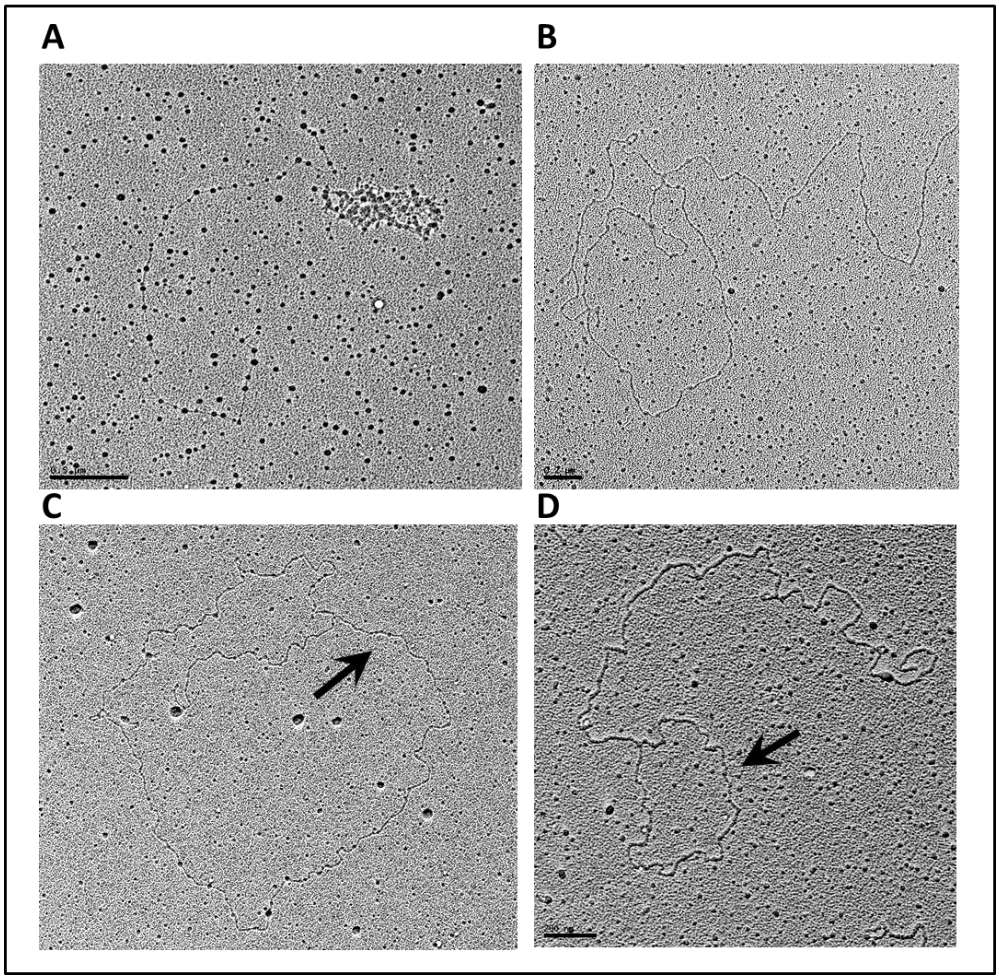

Figure 3-7. Visualizing telomeric DNA from t-loop and linear telomere samples on TEM. **(A)** Unknown globular structures were spread all over the grid, masking any DNA present in the sample. **(B)** After one G25 column clean-up, a long stretch of DNA molecule can be seen. But the background is still higher than what was seen in the plasmid control samples. **(C & D)** After two G25 column clean-up, DNA molecules can easily be identified with a significantly lower background. Two good candidates of t-loop structure were found in our t-loop isolation sample (Proteinase K at 4°C).

Thus, any small molecules of proteins that were left undigested from the 4°C Proteinase K digestion and other cellular lipid molecules will be picked up by the cytochrome *c* onto the EM grid and masked any DNA that was present in the sample. Visualizing the size of these globular structures, we suspected that they are most likely very small and can be removed by a G25 column. Thus, after the final elution of telomeres from beads at the end of telomere purification, sample was loaded onto a G25 column to remove any small contaminants, leaving long stretches of telomeres intact in the flow through. After one G25 column clean-up, actual DNA molecules can be visualized although scarce in quantity since there was still some background in the sample (Fig. 3-7 B). Thus, we cleaned up the eluted samples from telomere purification with total of two G25 columns, and this resulted in DNA molecules easily being identified on the grid by TEM. Two good candidates of t-loop structures were found in the t-loop sample (Proteinase K at 4°C to stabilize t-loops) (Fig. 3-7 C&D). In order to provide strong, convincing evidence that authentic t-loops exist in our t-loop preps, we needed to have enough DNA molecules to be scored and quantified as percentages over all the DNA molecules seen on the grid. With normal Hela cells, we were unable to find sufficient amount of t-loops present for quantification.

One possible explanation for the lack of t-loops seen is that since the average overhang size of normal Hela cells are only about 80 nts long on average (Zhao et al., 2008). We showed by oligo crosslinking experiments that we may not be able to crosslink DNA with lengths less than or equal to 51 bps (Fig. 3-4 B). Thus the bulk of the t-loops may not have been successfully crosslinked and many could become unfolded during the duration of telomere purification, confirmation of telomeres in the final elution, and sample preparations for EM. We next attempted to overcome this problem by using cells that would exhibit longer average overhang

lengths than normal Hela cells. Previously in our lab, A549 cells that overexpressed hTERT, the human catalytic subunit of telomerase, resulted in an increased overhang size by several hundred nts during S phase when synchronized before returning to the original size in unsynchronized cells (Zhao et al., 2009). Thus, to keep the same cell line background as all my previous experiments, we chose to use Hela cells overexpressing with hTERT for EM. The cell line has a telomere elongation rate of 145 bp per PD from as young as PD 28.5 to as old as PD 93.4 (Fig. 3-8). A colleague in our lab, Dr. Guido Stadler, has kindly provided this cell line.

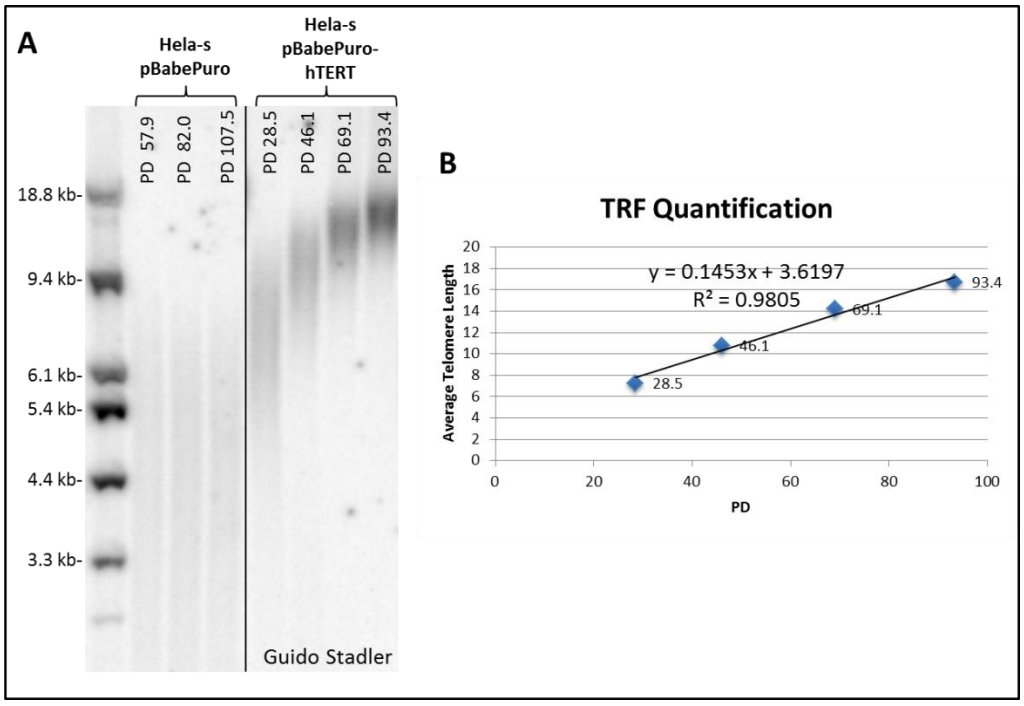

Figure 3-8. TRF analysis shows Hela cells overexpressed with hTERT has a 145 bp per PD telomere elongation rate. (A) TRF analysis of HeLa cells with hTERT overexpression. Left 3 lanes showing control empty vector, thus shorter telomeres. Right 4 lanes shows the hTERT overexpression vector, thus increasing telomere size with increasing PDs. **(B)** Linear plot of the average telomere length analysis of the HeLa+hTERT overexpression cells. The slope is the rate of telomere elongation which is about 145 bp/PD.

The fast telomere elongation rate prove that the overexpression of hTERT is still functional during these PDs and provided us with the convenience of leaving these cells in culture for longer periods of time (expand enough cells for one EM experiment). Since unsychronized Hela+hTERT cells would have similar overhang lengths as normal Hela cells, we want to harvest only synchronized cells that have progressed to the middle of S phase (when telomerase have already elongated ends of telomeres, but before C-strand fill-in to normal overhang size). To have approximately 100 million cells (1 mg of DNA) as starting material for each of the t-loop and linear telomere conditions, 25 plates (15cm) of 8 million cells each would have to be synchronized at 4 hours into cell cycle (middle of S phase) to achieve both enough starting material and more crosslinked t-loops. Experiments were done previously to ensure that the majority of the t-loops are in folded conformation at 4 hours into S phase (data shown and discussed in Chapter 4). Propidium iodine (PI) staining and FACs analysis were used to analyze cell cycle progression and ensure that the majority of the cells are synchronized at 4 hours (Fig. 3-9 A).

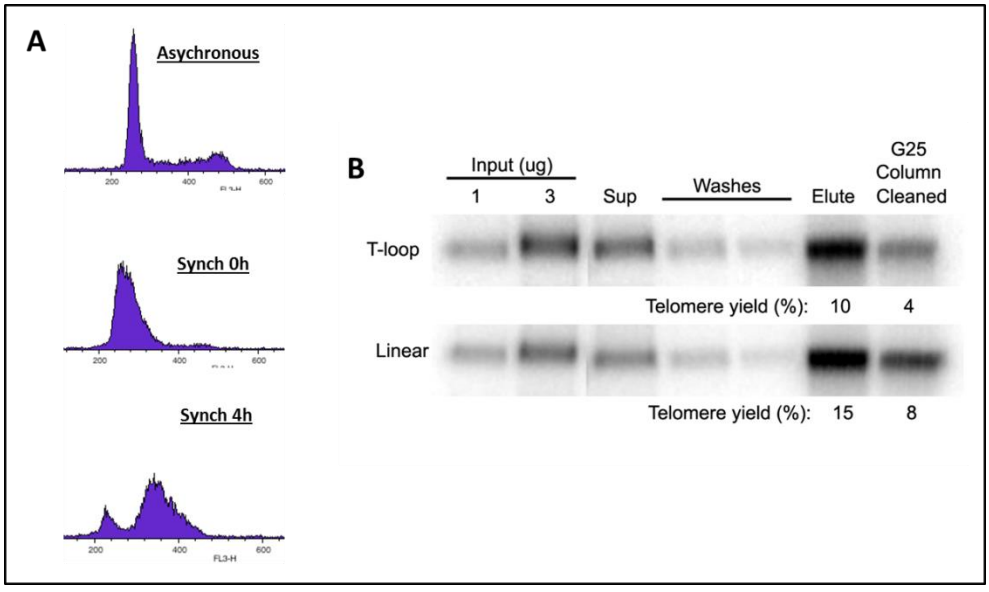

Figure 3-9. Hela+hTERT cells were synchronized at 4 hours with telomere purification yield of 10-15%. (A) 100 million cells were synchronized with a single 2mM thymidine block

for 18 hrs. 0.5 million cells were PI stained and analyzed by FACs to confirm cell cycle progression synchronously. Asynchronous sample was included as control. **(B)** After t-loop and linear telomere DNA isolation, both samples were subjected to telomere purification resulting in final yield of 10-15% as calculated by Southern blotting under denatured conditions (measures total telomeric DNA). After two G25 column clean-ups, however, the yield dropped to 4-8% (an amount that still should provide enough telomeric DNA molecules to be seen on EM).

Then DNA was isolated from these cells under t-loop (Proteinase K at 4°C) and linear telomere (Proteinase K at 55°C) conditions, followed by telomere purification with biotinylated oligo with eight C-rich repeats (BL-6RE-CTR8). The final elution achieved decent yields of 10% (t-loop sample) and 15% (linear telomere sample) (Fig. 3-9 B). These yields decreased to 4 and 8%, respectively, after two G25 column clean-ups were done. But with the high resolution and specificity of visualizing nucleic acids on TEM, these yield provided us with more than enough material to quantify.

Both t-loop and linear telomere samples were prepared for EM by adding cytochrome *c* and rotary shadowed with platinum: palladium followed by carbon coating. 200 DNA molecules were counted for each of the t-loop and linear telomere conditions in one experiment. 13% of the DNA molecules scored in the t-loop prepped sample were in actual t-loop conformation, and 37% were in linear conformation (while the rest were tangled and inconclusive) (Fig. 3-10 Table 1). 76% of the DNA molecules scored in the linear telomere prepped sample were in linear conformation while only 2% were in t-loop conformation. In another independent experiment, 400 DNA molecules were counted and scored. 16% of the DNA molecules in t-loop prepped sample were in actual t-loop conformation, and 78% were in linear conformation (Fig 3-10 Table 1). In this confirmation experiment, only 1% of the DNA molecules seen in linear telomere prepped sample were in t-loop conformation, and 95% of them were in linear conformation. The scoring process was done under unbiased conditions where random numbers (200 and 400 for

each of the experiments) were assigned to each image taken on the TEM. The next experiment day, each image was scored as t-loop, linear, or N/A (tangled/inconclusive) without knowing which sample preparation the image was taken from.

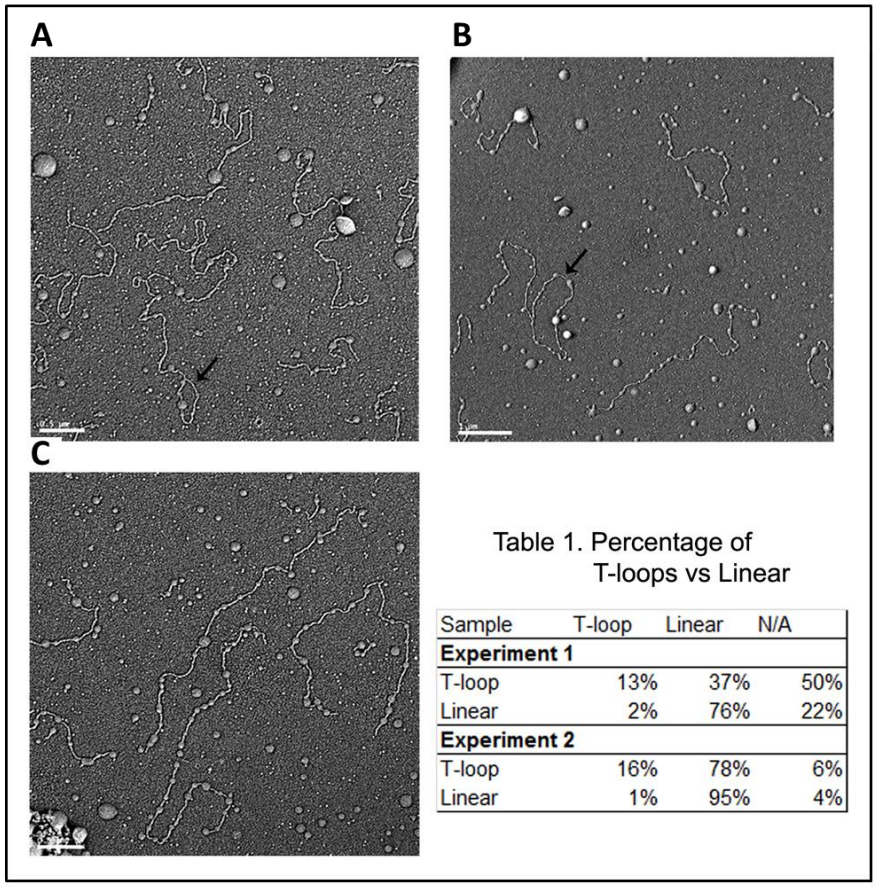

Table 1. Percentage of T-loops vs Linear

Sample	T-loop	Linear	N/A
Experiment 1			
T-loop	13%	37%	50%
Linear	2%	76%	22%
Experiment 2			
T-loop	16%	78%	6%
Linear	1%	95%	4%

Figure 3-10. EM images of t-loop and linear telomeres and their quantifications. (A&B) Two example images of t-loops seen in the t-loop prepped sample (denoted by black arrows). **(C)** An example image of multiple linear telomeres seen in the linear telomere prepped sample. **(D)** Unbiased scoring of 200 DNA molecules in experiment 1 and 400 DNA molecules in experiment 2. Both of which showed a significant difference in the amount of t-loops between t-loop prepped and linear telomere prepped samples.

The final scoring, after uncovering random number to sample assignment, was organized into their designated sample origin (t-loop prepped or linear telomere prepped) and percentages calculated (Fig. 3-10 Table 1). Fig. 3-10 A & B are two examples of t-loop images, and Fig. 3-

10 C is an example of a linear telomere image. Both sets of data from experiment 1 and 2 have provided us with strong evidence that we are indeed isolating authentic t-loops in our t-loop prepped samples using the t-loop assay method.

Conclusions

To validate our t-loop assay that we were indeed isolating intact t-loops, both t-loop and linear telomere samples were visualized by EM. Since EM provides very high resolution images to all substances in a given sample, we purified and enriched for telomeric DNA using our method of telomere purification via streptavidin beads and biotinylated oligo that contains complementary sequences to the 3' overhang. Psoralen-crosslinking was done after Proteinase K digestion such that any t-loops present would be stabilized for the duration of subsequent procedures. A typical telomere purification done at 4°C resulted in average telomere yields of 10-15%. Although the yields were lowered to 4-8% after G-25 column clean-up (a critical step done to remove any leftover globular impurities present in the sample), we were still able to visualize large amounts of DNA strands/molecules using the procedures developed by the Griffith Laboratory (as described in experimental procedures). In two independent experiments, 13 and 16% t-loops were seen in t-loop sample and only 2 and 1% of t-loops were observed in linear telomere samples. This provided very strong evidence that what we isolated for our t-loop assay was enriched with t-loops. The percentage of t-loops scored was lower than what the Griffith laboratory can typically achieve. One explanation for this is that we psoralen crosslink after cell lysis (including nuclei) whereas the Griffith laboratory crosslinks nuclei (where nuclear envelopes are intact and nuclear proteins are present to stabilize t-loops). With our methods, the stability of t-loops is entirely dependent on DNA-DNA interactions that can differ by

temperatures and salt concentrations after deproteinization. In conclusion, these results demonstrated that the biochemical t-loop enrichment is indeed capable of partially purifying intact telomere ends in the secondary structure of a t-loop.

Materials and Methods

Cell Culture

Hela cervical carcinoma, H1299 lung adenocarcinoma, and Hela overexpressed with hTERT cells were cultured at 37°C in 5% CO_2 in medium containing 10% cosmic calf serum (HyClone). BJ foreskin fibroblasts E6/E7 were cultured with same conditions but in 20% cosmic calf serum.

Hela+hTERT Cell Synchronization

Exponentially growing Hela+hTERT cells were seeded and allowed to settle for 4 hrs before being synchronized with 2 mM thymidine (Sigma-Aldrich, catalog #T9250-25G) for 18 hrs. The cells were then washed with pre-warmed PBS three times and released into fresh medium for 4 hrs. Both samples of 0 hr and 4 hr release were collected and analyzed by FACs after propidium iodine (PI) staining to confirm cell cycle arrest and progression.

Telomere Purification

DNA was harvested from cells in similar method as in t-loop assay with the addition of a psoralen crosslinking step that is done after Proteinase K digestion. 250 ug/mL 4'-aminomethyltrioxsalen (AMT) (Sigma-Aldrich, catalog#A4330-5MG) was added to the sample and UV treated at 365 nm wavelength. 2 U Alu I was added per ug of DNA at 4°C for 3 hrs (changing agarose dialysis plate at 1.5 hr) to digest genomic DNA and reduce viscosity of the

samples. After t-loop or linear telomeric samples were collected back in a tube, bead binding buffer (1XSSC and 0.1% Triton X-100) was added with 0.2 mg/mL of Proteinase K at 4°C for 30 mins to remove Alu I. 2 mM of PMSF was added again to stop Proteinase K reaction. 50 pmol/mL of a biotinylated oligo with sequence—(5'- biotin – GATCAAGCTTGAGTCGGTACC$(CCCTAA)_8$ -3') called BL-6RE-CTR8 was added at 4°C and incubated overnight to bind to the 3' overhang of the telomeres (or the D-loop for t-loops). 16 uL of streptavidin coated beads, Dynabeads MyOne C1 (Invitrogen), was then added to capture the biotinylated oligo-telomere complex at 4°C incubated overnight on a 3 RPM mechanical rotating wheel. The samples were washed with 1X SSC and 0.1% Triton X-100 with the Dynabeads magnet (Invitrogen) one time, 0.2X SSC one time, and 10 mM LiCl, 1 mM Tris pH 7.5, 1 mM EDTA one time. The final elution of telomeres were done by heating the sample to 60°C for 10 mins twice in the last wash buffer (mix the sample in between). The purified telomeres were washed twice with illustra microspin G25 columns (GE Healthcare Life Sciences) to remove contaminants that will interfere with EM analysis. 1:10 of the samples were run on 0.8% agarose gel and probe with C-rich probe after being denatured for calculation of total telomere recovery using the ImageQuant software.

Electron Microscopy

The purified telomere samples from previous step were mixed with ammonium acetate (pH 7.9) to a final concentration of 0.25 M. 4 ug/mL of cytochrome C (with courtesy from Dr. Jack Griffith Laboratory) was added to the mixture and allowed to sit on parafilm for 90 s. The droplet variation of the Kleinschmidt method was then used for surface-spreading DNA as described (Griffith et al., 1999) (See Experimental Procedures—Electron Microscopy). Samples

were visualized by FEI Technai G2 Spirit Biotwin transmission electron microscope, and the images for publication were contrast adjusted using Adobe Photoshop. At least 400 DNA molecules were counted for each t-loop and linear telomeric samples where random numbers were assigned such that an unbiased scoring of t-loop vs. linear can be achieved.

CHAPTER FOUR

Using the assay to analyze t-loop behavior

Introduction

A 3' single-stranded overhang is located at the very end of the G-rich strand of telomeres that must be protected from being recognized as DNA damage due to being exposed as a free DNA end. There are a few mechanism of protection that has been proposed: First, end protection can be due to forming a secondary structure called t-loops (where the 3' overhang inserts into the ds region of telomeres by strand invasion) (Griffith et al., 1999). Second, the overhangs can form G-quadruplexes (where the four guanines from the triple G's in telomere sequences associate with each other by a very special base pairing called cyclic Hoogsteen hydrogen bonding). The result is the stacking of these to form the quadruple-helical structure called G-quadruplex (Rhodes and Giraldo, 1995). Third, the overhang can be protected by having proteins (possibly part of the shelterin complex) bound to the 3' end (Gottschling and Zakian, 1986; Horvath et al., 1998). The strongest evidence thus far with DNA images *in vivo* is by the way of t-loops even though there are other evidences for binding of POT1 to single-strand overhang. Regardless of the exact mechanism of end capping function, these protective complexes must be resolved in order for DNA replication and telomere elongation by telomerase to proceed (Gilson and Geli, 2007).

Telomerase-positive human cells do not exhibit differences in leading and lagging overhang lengths (both are of approximately the same size). Studies have shown that this telomere extension occurs in a two-step process such that the G-strand extension by telomerase

and the C-strand fill-in are uncoupled (Zhao et al., 2009). In *Euplotes*, the newly synthesized G-strands are heterogeneous in length ranging around 95-100 nucleotides long, whereas most of the C-strands are exactly 84 nucleotides in length (Price, 1997). This suggests that the C-strand fill-in is a more tightly regulated step. In addition, 80% of the C-strands end in CCAATC-5' in human cells, more specific than the G-terminal nucleotide (Sfeir et al., 2005). Human telomeres replicate asynchronously throughout S phase. Telomerase is able to elongate telomeres within 30 minutes of telomere replication, and that 70%-100% of the ends in Hela and H1299 cells are extended during each cell cycle suggesting that there is no preferential recruitment of telomerase to shorter telomeres under maintenance conditions (Zhao et al., 2009). In Hela cells, the overhang lengths of leading and lagging strands, shortly after replication, are about 35 nucleotides and 50 nucleotides, respectively. Telomerase adds approximately 50 nucleotides to 70% of both strands for telomere length maintenance purposes to overcome senescence (Zhao et al., 2009). Although telomere replication and elongation by telomerase occurs in S phase, C-strand fill-in has been shown to occur as a second step in late S/G2 phase. There is preliminary evidence that show it is an incremental C-strand fill-in versus what would be expected as the conventional lagging-strand synthesis machinery, such that an RNA primer is extended, added to the end of C-strand, and rapidly converted to double-stranded DNA. But the detailed mechanisms of this incremental process have yet to be discovered (Zhao et al., 2009). In addition, RAD51 and RAD52, proteins responsible for homologous recombination, are present at telomeres during late S/G2 phase, and these very same proteins are found to promote t-loop formation *in vitro* (Verdun and Karlseder, 2006). This provides evidence that t-loops may be refolded at late S/G2 phase.

Thus, t-loops must be resolved/unfolded for telomere replication and elongation to occur during S phase, and yet, C-strand fill-in in telomerase positive cells is delayed until late S/G2 phase. This led us to ask whether t-loops remain unfolded after telomere replication/elongation until C-strand fill-in is completed, or if they refold soon after replication/elongation and unfold a second time for C-strand fill-in to occur. This question is now approachable by our much more efficient method of t-loop assay vs. EM imaging.

Another approach we can now take with our newly developed t-loop assay is to determine if the size of 3' overhang can affect the stability of t-loops. The average overhang lengths of BJ cells are ~100 nts long (Zhao et al., 2008), but when leading and lagging strands are separated via CsCl gradients, leading strand overhangs were found to have an average ~100-120 nts in length and lagging strand overhangs are ~30-40 nts (a difference of almost 3 fold between leading and lagging overhangs) (Zhao et al., 2008). In our previous oligo models of 30 nts in length, we observed that it is very difficult to keep branch migration to a minimal level unless kept under very stringent salt and DNA dye binding conditions. Thus, this aspect can now be explored with our t-loop assay.

Results

The question we want to answer with the new assay is whether t-loops remain unfolded during the time in which telomere extension is completed by telomerase and C-strand fill-in during late S/G2 phase, or if t-loops are refolded soon after replication and telomere extension is completed and unfold again for late S/G2 C-strand fill-in. To investigate this question, we synchronized Hela-hTERT cells at G1 phase and release them at different time points of the cell cycle (0, 4, 6, 8, 10, and 12 hrs). FACs analysis was done to ensure the cells were at the given

point of cell cycle (Fig. 4-1 A). DNA was isolated with the same method as described in development of t-loop assay section and analyzed via Southern blotting. The amount of t-loops present throughout the cell cycle in the t-loop sample does not seem to change by a significant amount, ranging ~70-78% with a slight drop at 10-hr time point 62% (Fig. 4-1 B).

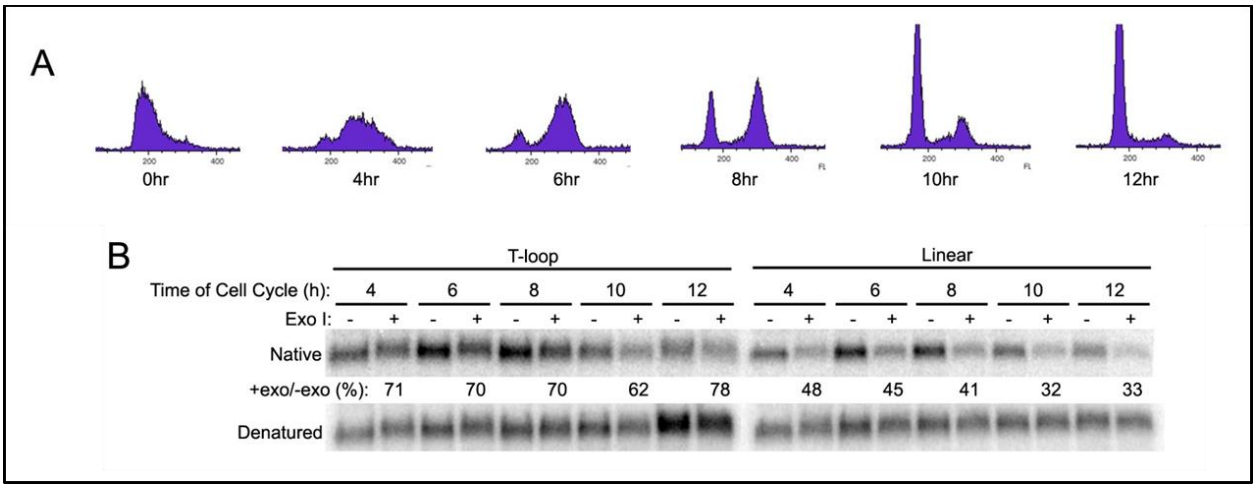

Figure 4-1. Cell cycle analysis by t-loop assay shows t-loops stay folded throughout cell cycle. (A) Hela+hTERT cells were synchronized with double-thymidine block and released into cell cycle for 12 hrs. FACs analysis show appropriate progression of cell cycle. **(B)** DNA was harvested according to the t-loop assay method (t-loop vs. linear telomeres) from each of the cell cycle time points and native overhang signal was compared after normalization of total telomere in denatured gel. The signals from both t-loop and linear samples did not show any significant changes throughout cell cycle, suggesting that t-loops are mostly intact.

There was a slightly lower percentage of overhang signals with the 10- and 12-hr sample in the linear telomere prep (Proteinase K at 55°C) as the overhang size should be matured at those time points by C-rich fill-in at late S/G2 phase. Shorter overhangs yield less stable t-loops and result in lower overhang signal by the t-loop assay. We further analyzed two single time points during cell cycle (4- and 8- hr) to focus only on replicated DNA so that our results were not obscured by unreplicated DNA. At the 4-hr time point, Hela+hTERT cells were harvested and lysed/digested according to the t-loop assay protocol. FACs analysis was done to ensure cells were properly

synchronized and released (Fig. 4-2 A). Cesium chloride (CsCl) gradients were used to separate replicated (leading and lagging peaks pooled) from unreplicated DNA (Fig. 4-2 B). Then the two pools of fractions were precipitated and ran on a gel for Southern blotting. At the 4-hr time point, a strong overhang signal (D-loop) in the presence of Exo I was observed suggesting t-loops were in the folded conformation (Fig. 4-2 C).

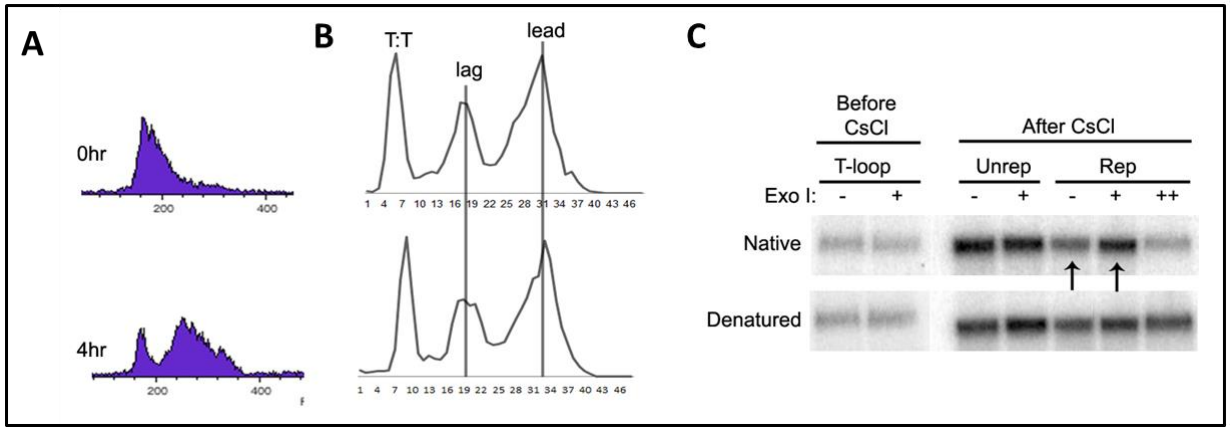

Figure 4-2. CsCl separation of replicated fractions showed t-loop conformation at 4 hours in to cell cycle. (A) Hela+hTERT cells were synchronized via double-thymidine block and released into cell cycle for 4 hrs. FACs analysis showed appropriate cell cycle arrest at 0 hr and progression into 4 hrs. **(B)** CsCl gradient was used to separate replicated telomeres (leading and lagging strands pooled) from unreplicated telomeres. **(C)** DNA was reprecipitated from pooled leading and lagging strand fractions (Rep) and ran on a native/denatured gel to show retention of overhang signal in presence of Exo I, suggesting t-loops were present at 4 hrs into cell cycle (indicated by black arrows). The (++) Exo lane was done as a control to show that the signal in (+) Exo lane was real by a second Exo I digest after CsCl gradient and re-precipitation.

Similar analysis was done at the 8-hr time point with FACs analysis and CsCl gradient separation of replicated vs. unreplicated DNA (Fig. 4-3 A&B). After leading and lagging fractions were pooled, reprecipitated DNA was run on a gel to observe native overhang signals. The replicated (+) Exo I lane showed retention of overhang signal, suggesting that t-loops were in the folded conformation (Fig. 4-3 C). This suggested that, of the two time points we chose to analyze (middle and end of S phase, 4- and 8-hr respectively), there wasn't a time in which a

large portion of telomeres converted into the unfolded state. From these experiments, the conclusion drawn is that t-loops are present throughout the cell cycle under normal conditions. Although it is possible that individual telomeres may be in unfolded/folded state asynchronously with other telomeres, such observations are beyond the limits of our t-loop assay.

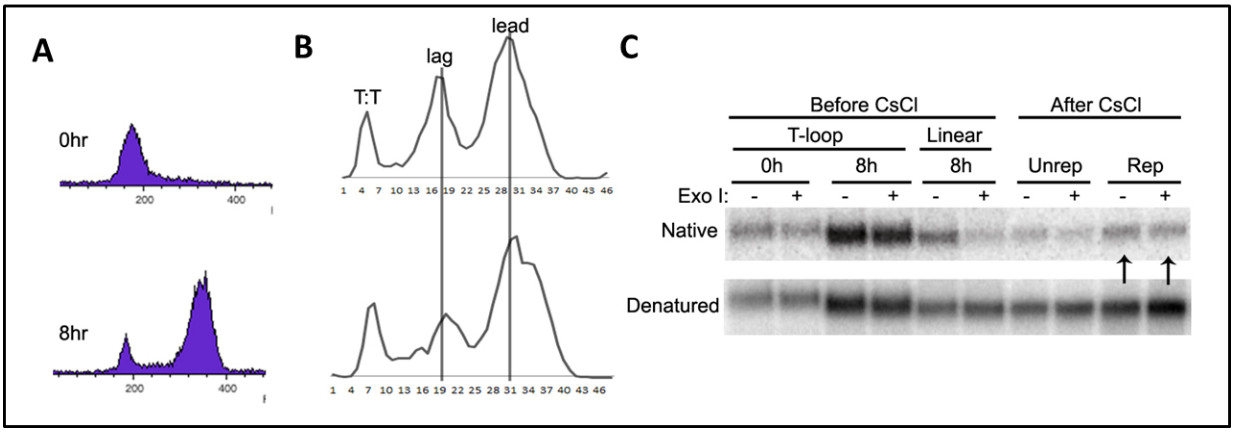

Figure 4-3. CsCl separation of replicated fractions showed t-loop conformation at 8 hours in to cell cycle. (A) Hela+hTERT cells were synchronized via double-thymidine block and released into cell cycle for 8 hrs. FACs analysis showed appropriate cell cycle arrest at 0 hr and progression into 8 hrs. **(B)** CsCl gradient was used to separate replicated telomeres (leading and lagging strands pooled) from unreplicated telomeres. **(C)** DNA was re-precipitated from pooled leading and lagging strand fractions (Rep) and ran on a native/denatured gel to show retention of overhang signal in presence of Exo I, suggesting t-loops were present at 8 hrs into cell cycle (indicated by black arrows). Linear telomeres before CsCl gradient separation were digested from same 8-hr sample to show that Exo I digestion works efficiently, and that the retention of signal does not define a nonfunctional Exo I digestion.

Another application of our assay was to determine whether there is a correlation between overhang sizes and the stability of t-loops formed. The average overhang lengths of BJ cells are ~100 nts long (Zhao et al., 2008). After CsCl gradient separation of leading and lagging strands, leading strand overhangs were found to have an average ~100-120 nts while lagging strand overhangs were ~30-40 nts (almost 3 fold difference) (Zhao et al., 2008). In our previous oligo models of 30 nts in length, we observed that it is very difficult to keep branch migration to a

minimal level unless the oligonucleotides were kept under very stringent salt and DNA dye binding conditions. Thus, in order to determine whether stability of t-loops is dependent on the lengths of the 3' overhangs without the help of shelterin proteins, we chose the BJ foreskin fibroblast model to test our hypothesis.

BJ cells were labeled with IdU for 48 hours and harvested/lysed under t-loop (Proteinase K at 4°C) or linear telomeres (Proteinase K at 55°C) conditions. Exo I was added to digest any exposed overhang present in the t-loop assay samples followed by separation of the leading and lagging strands via CsCl gradients (Fig. 4-4 A).

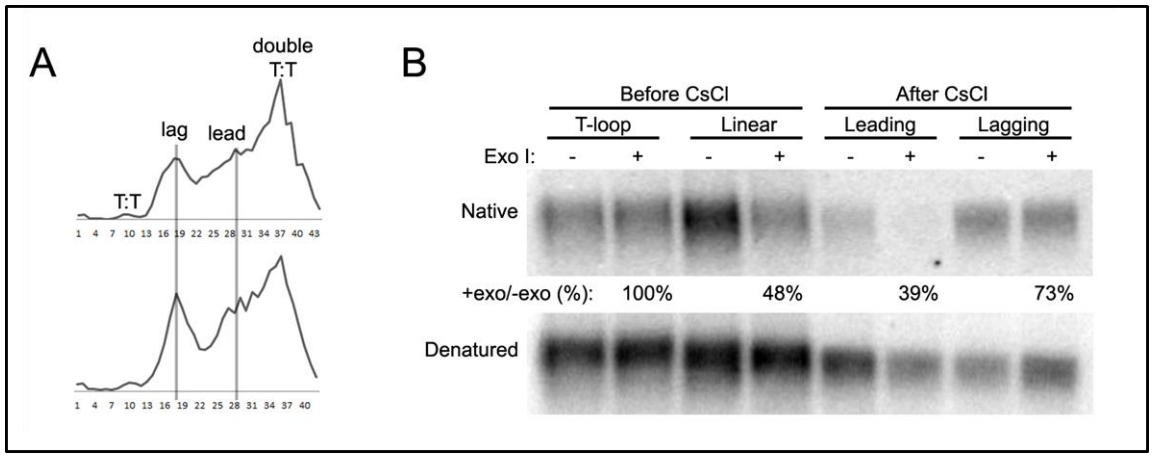

Figure 4-4. Analysis of leading vs. lagging strand overhangs in BJ cells showed higher stability of t-loops with longer overhangs. (A) BJ E6/E7 cells were labeled with IdU for 48 hrs and harvested under t-loop and linear telomere conditions. CsCl gradient as used to separate leading and lagging strands from unreplicated and double-thymidine incorporated DNA. **(B)** Fractions from leading and lagging fractions were pooled. Re-precipitated DNA was run on a gel to compare native overhang signals to confirm t-loop presence/absence. After CsCl, leading strand clearly shows a decrease in overhang signal, suggesting only 39% were in t-loop conformation. Lagging strand resulted in a higher overhang signal 73%, an almost 2-fold increase, suggesting that t-loops are more stabilized with longer overhangs.

The leading and lagging strand fractions were pooled and re-precipitated and subjected to Southern blotting for overhang signal. T-loop versus linear telomere samples before separation

by CsCl gradients were added as a control to show that Exo I was working efficiently (T-loop: 100% overhang/D-loop signal; Linear: 48% overhang signal) (Fig. 4-4 B). After CsCl gradient separation, the leading strand showed a decrease in overhang signal 39% whereas the lagging strand gave retention of signal 73%. As expected, the amount of overhang signal in lagging strands was clearly higher than that of leading strands. This provides strong evidence to support the statement that t-loops formed by shorter 3' overhangs (~30-40 nts) are less stable in absence of protein protection than longer overhangs (~100-120 nts). This also adds support that our newly developed t-loop assay is indeed examining the presence/absence of authentic t-loops in isolated DNA from cells.

Conclusions

After validation of the t-loop assay, we conclude that we are indeed isolating authentic t-loops and that the analysis of t-loop presence/absence throughout cell cycle has been accomplished. The question of whether t-loops remain unfolded after telomere replication/telomerase extension before C-strand fill-in at late S/G2 phase to achieve mature overhang size versus if they refold soon after replication is completed and unfold again later for the rest of end-processing events was a central question in the telomere and DNA replication field. Analyzing overhang signal by the t-loop assay at different time points of the cell cycle showed that there was no significant total amount of net change in t-loops throughout S phase. This demonstrates that there was no single prolonged period of time in which the majority of t-loops remain unfolded under normal cell cycle progression. This result confirms the idea that t-loops plays an important role in protecting ends of telomeres from being recognized as DNA double-strand breaks, even during S phase. If t-loops were to remain unfolded for prolonged

periods of time, one can imagine that it would require more processes and protein binding factors to inhibit the ends from being recognized as DNA damage and activation and recruitment of subsequent repair machineries. In principal, it would be much simpler if t-loops were to remain folded in the protected state, unless unfolding becomes necessary for replication and end-processing to occur (which is likely to be only a matter of a few seconds).

Another further experiment we completed was to analyze t-loop characteristics with BJ foreskin fibroblast cells. BJ cells are known to have leading strand overhangs (~30-40 nts) that are almost three times shorter than lagging strand overhangs (~90-120 nts). From our previous experiments using an oligo model system, we found that it is much more difficult to keep a 30-bp complex from branch migration compared to a 155-bp complex. Thus, we hypothesized that leading strand overhangs should result in t-loops that are much less stable compared to lagging strand overhangs. Our prediction is that we would observe a decrease in the amount of t-loops in leading strands using our t-loop assay compared to lagging strands. After separation of leading and lagging strands via CsCl gradients, our data convincingly show that there is a large difference in overhang signal between leading (39%) and lagging (73%) strands. This further provides evidence that our t-loop assay is able to distinguish between t-loops and linear telomeres

Materials and Methods

Cell Culture and Synchronization

See Materials and Methods in chapter 3

T-loop Assay

See Materials and Methods in chapter 2

CsCl Gradient to Separate Replicated Leading and Lagging Telomeric DNA

For the cell cycle analysis experiment, Hela-hTERT cells were synchronized with double-thymidine block (2 mM thymidine for 19 hrs, washed with PBS three times, release in to fresh medium for 9 hrs, and 2 mM thymidine again for 17 hrs). Then the cells were washed with PBS three times again and release into fresh medium containing 0.1 mM of iododeoxyuridine (IdU) for 4 and 8 hours. DNA was isolated from cells with same method in t-loop assay to obtain t-loop and linear telomeric samples. 20 U of Exo I was added per 5 ug of DNA to digest any overhang present in the sample. 50 mM of EDTA was added to stop the reaction. Phenol: chloroform extraction was performed to remove Exo I and any protein contaminants still present in the sample followed by ethanol precipitation and incubation at 37°C in 10 mM Tris (pH 7.5) overnight. CsCl gradient separation was performed exactly as described (Chow et al., 2012) (See Materials and Methods section—CsCl separation of leading and lagging telomeric daughters). After pooling the replicated fractions and desalting via agarose dialysis followed by DNA precipitation, DNA from unreplicated and replicated fractions were run on a 0.8% agarose gel and probed with C-rich probe under native conditions to access the amount of t-loops present in each samples. Denatured signals were also measured again to normalize native signal for accurate quantification by the ImageQuant software. The same method was used in BJ E6/E7 cells to analyze t-loop presence/absence in leading and lagging strands with the exception that no synchronization was done and 0.1 mM of IdU was added for 48 hrs to allow as much labeling of the replicated DNA as possible.

CHAPTER FIVE

Discussions and Future Directions

Telomeres are important in keeping the fidelity of cellular growth progression during different stages of cell cycle such as during DNA replication, especially in the case of telomerase-positive cancer cells where the ability to continue to proliferate depends on the cells ability to elongate telomeres thereby maintaining homeostasis. One of the major caveats in developing anti-telomerase therapy is the lag phase in which one has to wait until a cancer cell's telomeres become critically short enough to trigger cellular crisis and consequently cell death. A potential telomere target for cancer associated therapies is a structure located at the ends of telomeres called the t-loop. T-loops are structures that are essential for protecting the ends of chromosomes from being recognized as double-stranded breaks, therefore inhibiting inappropriate activation of DNA damage repair machineries. One of our theories is that if we can inhibit t-loop formation in cancer cells in addition to anti-telomerase treatment, then can we eliminate the described lag phase and quicken cell death? Unfortunately, almost nothing is known about t-loops due to the difficulty of developing assays to investigate its true structure and dynamics throughout the cell cycle. Here we have successfully developed a biochemical assay that allows for the stabilization and quantification of t-loops in a cell.

Conditions that Yield Maximum Stabilization of T-loops were Determined by Oligo Models

At the ends of telomere is a ss 3' overhang that strand invades into the ds region resulting in a lariat, loop-like structure called t-loop, which is a secondary structure that is crucial in protecting the ends of chromosomes being recognized as ds breaks and preventing inappropriate DNA damage repair machineries. Yet, very little is known about t-loops since the only method that have been used to prove their existence is done by transmission electron microscopy, a highly difficult method that require large amounts of starting DNA material and special expertise in the EM field. Thus, we have developed a novel t-loop assay based on biochemical approaches such that intact t-loops can be isolated and analyzed.

We have used oligo model system to determine the conditions in which intact t-loops can be isolated based on the theory of branch migration, where ds DNA slides back and forth until one strand completely displaces another strand of DNA. Modifying temperature, different salt concentrations, and DNA binding dyes, the conditions that are best for isolating maximum amount of t-loops (minimizing branch migration) are: keeping samples at 4°C, 25 mM $MgCl_2$, 50 mM NaCl, and 5 ug/mL of EtBr. However, we substituted NaCl with LiCl due the fact that Na^+ highly promotes formation of G-quadruplex at the end of ss 3' overhang (need reference here) such that it inhibits Exo I digestion (supplementary data). We have also found that the maximum concentration of LiCl that Proteinase K is still sufficiently functional at 4°C is 600 mM, and that restriction enzyme (Alu I) is can still digest genomic DNA sufficiently at is 150 mM. Thus, the buffer used for cell lysis and Proteinase K digestion contains 600 mM LiCl, 100 mM Tris, and 100 mM EDTA (Quick Prep Buffer). The buffer used for Alu I and Exo I digestion contains 150 mM LiCl, 10 mM Tris, 25 mM $MgCl_2$, and 1 mM DTT. All of which are

conditions that we optimized for in order to isolate intact t-loops without the need of psoralen crosslinking.

T-loop Assay Shows a Two-fold Increase of T-loops Compared with Linear Telomeres

The basis of our t-loop assay uses a 3→5' ss Exonuclease (Exo I) to distinguish between t-loops and linear telomeres. In t-loops, the 3' overhang is protected from Exo I digestion via strand invasion into the ds region of the telomeres. In linear telomeres, the 3' overhang is exposed and allow for Exo I digestion. Thus, using a radioactive P32- telomere specific probe for the C-rich strand using Southern blotting under native conditions, t-loops will retain the overhang/D-loop signal in even in presence of Exo I, and linear telomeres will show a decrease in overhang signal due to digestion by Exo I. We have shown that an almost two fold difference in overhang signal was achieved in comparing t-loop (Pro K digestion at 4°C) vs. linear telomere (Pro K digestion at 55°C) samples. Attempts to increase the difference between t-loop and linear telomere samples were made, but increasing enzyme concentration does not yield a higher digestion above background at 4°C and increasing temperature of Exo I digestion results in spontaneous t-loop unfolding due to increase in branch migration in presence of Exo I. But the consistency and high reproducibility of experiments with various cell lines for t-loop samples yielding an almost 2 fold higher overhang signal than linear telomere samples provide enough evidence to distinguish between the two samples.

EM Analysis Provide Validation of T-loop Assay that Shows a High Enrichment of T-loops

To validate our t-loop assay that we are indeed isolating intact t-loops, both t-loop and linear telomere samples were visualized by EM. Since EM provides very high resolution images

to all substances in a given sample, we purify and enrich for only telomeric DNA using our method of telomere purification via streptavidin beads and biotinylated oligo that contains complementary sequences to the 3' overhang. Psoralen-crosslinking was done after Proteinase K digestion such that any t-loops present would be stabilized for the duration of subsequent procedures. A typical telomere purification conducted at 4°C results in average telomere yield of 10-15%. Although the yield is lowered to 4-8% after G-25 column clean-up (a critical step done to remove any leftover globular impurities present in the sample), we can still visualize large amounts of DNA strands/molecules using the procedures developed by the Griffith Laboratory (as described in experimental procedures). In two independent experiments, 13 and 16% t-loops were seen in t-loop sample and only 2 and 1% of t-loops were observed in linear telomere samples. This provides very strong evidence that what we isolated for our t-loop assay is enriched with t-loops. Although the percentage of t-loops may be lower than what the Griffith lab is able to achieve, this is due to the reason that we psoralen crosslink after cell lysis (including nuclei) and deproteinization where the stability of t-loop is entirely depended on DNA-DNA interactions that can differ by temperatures and salt concentrations.

T-loops Remain in Folded State throughout Cell Cycle

After validation of our t-loop assay that we are indeed looking at authentic t-loops, the analysis of t-loop presence/absence throughout cell cycle can now be achieved. There exists the question that asks whether t-loops remain unfolded after telomere replication/telomerase extension before C-strand fill-in at late S/G2 phase to achieve mature overhang size, or do they refold soon after replication is completed and unfold again later for the rest of end-processing events. Analyzing overhang signal by the t-loop assay at different time points of cell cycle

showed that there is no high amount of net change in t-loops throughout. This suggest that there is no single prolong period of time in which majority of t-loops remain unfolded under normal cell cycle progression. This result lies parallel with the idea that t-loops plays an important role in protecting ends of telomeres from being recognized as ds breaks. If t-loops were to remain unfolded for prolong period of time, one can imagine that it would require more processes and protein binding factors inhibit the ends from being recognized as DNA damage and activation of subsequent repair machineries. It would be much simpler if t-loops were to remain folded, or the protected state, unless unfolding becomes necessary for replication and end-processing to occur.

T-loops are Less Stable when Overhang Sizes are Shorter than 30 nts in Length

Another further experiment we have done to analyze t-loop characteristics is with BJ foreskin fibroblast cells. BJ cells are known to have leading strand overhangs (~30-40 nts) that are almost three times shorter than lagging strand overhangs (~90-120 nts). Going back to our previous experiments with oligo model system, we found that it is much more difficult to keep a 30-bp complex from branch migration than a 155-bp complex. Thus, we hypothesized that leading strand overhangs should result in t-loops that are much less stable than lagging strand overhangs such that one would see a decrease in the amount of t-loops in leading strands using our t-loop assay. After separation of leading and lagging strands via CsCl gradients, our data shows that there is a large difference in overhang signal between leading (39%) and lagging (73%) strands. Thus, this further provide evidence that our t-loop assay is able to distinguish between t-loops and linear telomeres

T-loops Stability is Highly Dependent on DNA Length by the Theory of Branch Migration

One of the caveats in our t-loop assay by Exo I was that there is only a consistent ~20% signal difference between intact t-loops and linear telomere samples due to the amount of background signal that is left in the presence of Exo I in the linear telomere samples. We have two possible explanations: 1) the enzymatic activity of Exo I is limited by the low temperature in which the digestion is conducted, and 2) there exists a portion of telomeres in t-loops with longer overhangs that cannot be unfolded/linearized even at 55°C for 3 hours. In attempts to troubleshoot the first theory, we digested t-loops with Exo I at slightly higher temperatures, 16 and 25°C, (Fig. 2-11) compared to the optimal temperature at 37°C. We predicted that enzymatic activity would be increased at slightly higher temperatures such that the background signal in presence of Exo I for linear telomeres would be decreased but yet able to keep t-loops from unfolding significantly. Unfortunately, results indicated that as the signal for linear telomere decrease, t-loop signal also decreased dramatically. This goes back to the idea that branch migration increases with any increase in temperature where the overhang melts away from the double stranded telomere region resulting in unfolding of t-loops. In addition, the overhang can also melt at the opposite 3' end (Fig. 2-1B) for Exo I to bind and initiate digestion thus contributing to the rapid unfolding of t-loops. We have also tried to increase the amount of enzymes to digest at 4°C, but results showed that there is no significant difference in the amount of digestion after 20U of enzyme (Fig. 2-13), which was already the amount we were using in our t-loop assay.

In efforts to support our second theory, we are currently going back to our oligonucleotide system of branch migration. Telomere overhangs range in length such that an average size is usually given for a specific cell type. For example, telomere overhangs in Hela cells exhibit a smear over a range of sizes from as short as 10nts to as long as 300 nts (Zhao et al.,

2008) with an average size of 74 nts. By the oligonucleotide system, we have shown that a complex made with 30 bps rapidly branch migrates even at 4°C unless stabilized by addition of Mg^{2+} and EtBr given that it was a 4-stranded structure. A 150 bps complex would branch migrate slower, but a portion still unfolds at 37°C unless stabilized by incorporating additional salt conditions. The question would then be what happens with 200, 250, or 300 bps? Are they stabilized to a point where even at 55°C for 3 hours complete branch migration does not occur thereby stabilizing the t-loop structures? Thus, we are currently generating oligos the range in different lengths from 60 to 350 bps arms of branch migration to test this hyopothesis. Expected results would be that the complexes formed by shorter oligos will undergo rapid branch migration possibly even at 4°C, and the rate will decrease with increasing lengths of oligos to a point where the complex is stable even at higher temperatures for extended amount of incubation time. This will provide an explanation to why we consistently see a 30-40% background that may still be in t-loop conformations after Exo I digestion of linear telomeres and in combination of inadequate enzymatic activity at 4°C.

T-loops are Folded into 3- vs. 4-Stranded Structures

T-loops are formed by insertion of the 3' overhang into the ds region of telomeres, but a structural question is whether only the 3' G-rich overhang binds to the telomere (3-stranded structure) or if the C-rich strand also migrates to bind to the D-loop region of the telomere (4-stranded structure) (Fig. 2-4). An interesting fact that provides a way to distinguish between the two structure is that Mg^{2+} can bind to 4-stranded structures to stabilize the complex and prevent branch migration. If the complex was a 3-stranded structure, Mg^{2+} will not provide stabilization from branch migration. This theory is based on the special property of magnesium cations being

able to stabilize the base stacking in ds DNA in 4-stranded complexes. We can provide evidence for this theory with our oligonucleotide system such that we will have complexes that are either formed by 4 strands of oligos vs. 3 strands of oligos. Their rate of branch migration can be measured with increasing temperatures in presence and absence of Mg^{2+} to observe whether the complex can be stabilized. The expected result would be that there will be little to no branch migration in 4-stranded structures in presence of Mg^{2+} at higher temperatures while no such effect can be seen in 3-stranded structures. Once the described hypothesis is established, we can apply the same experimental conditions to authentic t-loops in our biochemical assay to infer whether they are in 3- or 4-stranded structures. The experimental strategy would be to melt t-loops at higher temperatures showing that in absence of Mg^{2+}, t-loops falls apart (decrease in overhang signal). In the presence of Mg^{2+} however, if t-loops cannot be stabilized and still falls apart, then it provides strong evidence that t-loops are in 3-stranded structures. If the opposite result is obtained, t-loops are stabilized and prevented from branch migration, then we infer with confidence that t-loops are likely to be in 4-stranded structures.

Shelterin Proteins that are Essential in Formation of T-loops

The six protein components of the shelterin complex altogether contribute in function to preserve the capping of telomeric ends (Palm and de Lange, 2008). There is strong evidence *in vitro* that TRF2 may play an essential role in forming t-loops by promoting strand-invasion of the 3'overhang into the double stranded region of telomeres (Griffith et al., 1999). *In vivo,* TRF2 has been shown to function in protection of chromosomal ends from end-to-end fusions (Amiard et al., 2007). Thus, one of the first targets we would like to test is whether knockout/knockdown or any functional mutation of TRF2 in NHEJ deficient cells (to prevent end-to-end fusions)

affects the amount of t-loops that would be present. If TRF2 does indeed play a key role in the strand invasion to form t-loops, then we would expect a significant decrease in the amount of t-loops in absence of TRF2. If no change in the amount of t-loops is observed, then the absence of TRF2 may not be sufficient/necessary in the formation of t-loops. For example, other components of the shelterin complex either in combination or only one subunit are enough to assist in formation of t-loops. The same process can be done to the rest of the telomere binding proteins, TRF1 and Pot 1, and their interconnected proteins—Tin2, TPP1, and Rap1, to assess their role in t-loop formation.

Summary:

Understanding t-loop dynamics and structure provides important information about telomere biology that can lead to improvements to existing cancer treatments and/or discover new potential targets for other drug therapies. Yet, only a minimal amount of information is currently known about t-loops due to the difficulty in isolating intact authentic t-loops. Our development of a novel biochemical t-loop assay will allow for the study of crucial mechanistic details of t-loop structure and dynamics under different cellular conditions. A tremendous amount of new information and questions can be addressed with this assay without the necessity of difficult imaging techniques such as EM.

BIBLIOGRAPHY

Allers, T., and Lichten, M. (2000). A method for preparing genomic DNA that restrains branch migration of Holliday junctions. Nucleic acids research *28*, e6.

Amiard, S., Doudeau, M., Pinte, S., Poulet, A., Lenain, C., Faivre-Moskalenko, C., Angelov, D., Hug, N., Vindigni, A., Bouvet, P., *et al.* (2007). A topological mechanism for TRF2-enhanced strand invasion. Nature structural & molecular biology *14*, 147-154.

Basenko, E.Y., Cesare, A.J., Iyer, S., Griffith, J.D., and McEachern, M.J. (2010). Telomeric circles are abundant in the stn1-M1 mutant that maintains its telomeres through recombination. Nucleic acids research *38*, 182-189.

Bianchi, A., Smith, S., Chong, L., Elias, P., and de Lange, T. (1997). TRF1 is a dimer and bends telomeric DNA. The EMBO journal *16*, 1785-1794.

Bryan, T.M., Englezou, A., Dalla-Pozza, L., Dunham, M.A., and Reddel, R.R. (1997). Evidence for an alternative mechanism for maintaining telomere length in human tumors and tumor-derived cell lines. Nature medicine *3*, 1271-1274.

Cesare, A.J., Groff-Vindman, C., Compton, S.A., McEachern, M.J., and Griffith, J.D. (2008). Telomere loops and homologous recombination-dependent telomeric circles in a Kluyveromyces lactis telomere mutant strain. Molecular and cellular biology *28*, 20-29.

Cesare, A.J., Quinney, N., Willcox, S., Subramanian, D., and Griffith, J.D. (2003). Telomere looping in P. sativum (common garden pea). The Plant journal : for cell and molecular biology *36*, 271-279.

Chow, T.T., Zhao, Y., Mak, S.S., Shay, J.W., and Wright, W.E. (2012). Early and late steps in telomere overhang processing in normal human cells: the position of the final RNA primer drives telomere shortening. Genes & development *26*, 1167-1178.

Gilson, E., and Geli, V. (2007). How telomeres are replicated. Nature reviews Molecular cell biology *8*, 825-838.

Gottschling, D.E., and Zakian, V.A. (1986). Telomere proteins: specific recognition and protection of the natural termini of Oxytricha macronuclear DNA. Cell *47*, 195-205.

Griffith, J., Bianchi, A., and de Lange, T. (1998). TRF1 promotes parallel pairing of telomeric tracts in vitro. Journal of molecular biology *278*, 79-88.

Griffith, J.D., Comeau, L., Rosenfield, S., Stansel, R.M., Bianchi, A., Moss, H., and de Lange, T. (1999). Mammalian telomeres end in a large duplex loop. Cell *97*, 503-514.

Hanson, C.V. (1979). Photochemical inactivation of deoxyribonucleic and ribonucleic acid viruses by chlorpromazine. Antimicrobial agents and chemotherapy *15*, 461-464.

Hockemeyer, D., Sfeir, A.J., Shay, J.W., Wright, W.E., and de Lange, T. (2005). POT1 protects telomeres from a transient DNA damage response and determines how human chromosomes end. The EMBO journal *24*, 2667-2678.

Horvath, M.P., Schweiker, V.L., Bevilacqua, J.M., Ruggles, J.A., and Schultz, S.C. (1998). Crystal structure of the Oxytricha nova telomere end binding protein complexed with single strand DNA. Cell *95*, 963-974.

Jacob, N.K., Skopp, R., and Price, C.M. (2001). G-overhang dynamics at Tetrahymena telomeres. The EMBO journal *20*, 4299-4308.

Jady, B.E., Richard, P., Bertrand, E., and Kiss, T. (2006). Cell cycle-dependent recruitment of telomerase RNA and Cajal bodies to human telomeres. Molecular biology of the cell *17*, 944-954.

John Wiley & Sons, I. (2003). Support Protocol 3: Synthesis of a high-specific acitivty telomeric repeat probe. In Current Protocols in Cell Biology Online.

Karlseder, J., Broccoli, D., Dai, Y., Hardy, S., and de Lange, T. (1999). p53- and ATM-dependent apoptosis induced by telomeres lacking TRF2. Science *283*, 1321-1325.

Kleinschmidt, A.K., and Zahn, R.K. (1959). Z Naturforsch *146*.

Klobutcher, L.A., Swanton, M.T., Donini, P., and Prescott, D.M. (1981). All gene-sized DNA molecules in four species of hypotrichs have the same terminal sequence and an unusual 3' terminus. Proceedings of the National Academy of Sciences of the United States of America *78*, 3015-3019.

Konishi, A., and de Lange, T. (2008). Cell cycle control of telomere protection and NHEJ revealed by a ts mutation in the DNA-binding domain of TRF2. Genes & development *22*, 1221-1230.

Larrivee, M., LeBel, C., and Wellinger, R.J. (2004). The generation of proper constitutive G-tails on yeast telomeres is dependent on the MRX complex. Genes & development *18*, 1391-1396.

Makarov, V.L., Hirose, Y., and Langmore, J.P. (1997). Long G tails at both ends of human chromosomes suggest a C strand degradation mechanism for telomere shortening. Cell *88*, 657-666.

Mokbel, K. (2003). The evolving role of telomerase inhibitors in the treatment of cancer. Current medical research and opinion *19*, 470-472.

Munoz-Jordan, J.L., Cross, G.A., de Lange, T., and Griffith, J.D. (2001). t-loops at trypanosome telomeres. The EMBO journal *20*, 579-588.

Murti, K.G., and Prescott, D.M. (1999). Telomeres of polytene chromosomes in a ciliated protozoan terminate in duplex DNA loops. Proceedings of the National Academy of Sciences of the United States of America *96*, 14436-14439.

Paeschke, K., McDonald, K.R., and Zakian, V.A. (2010). Telomeres: structures in need of unwinding. FEBS letters *584*, 3760-3772.

Palm, W., and de Lange, T. (2008). How shelterin protects mammalian telomeres. Annual review of genetics *42*, 301-334.

Panyutin, I.G., and Hsieh, P. (1994). The kinetics of spontaneous DNA branch migration. Proceedings of the National Academy of Sciences of the United States of America *91*, 2021-2025.

Price, C.M. (1997). Synthesis of the telomeric C-strand. A review. Biochemistry Biokhimiia *62*, 1216-1223.

Randall, A., and Griffith, J.D. (2009). Structure of long telomeric RNA transcripts: the G-rich RNA forms a compact repeating structure containing G-quartets. The Journal of biological chemistry *284*, 13980-13986.

Rhodes, D., and Giraldo, R. (1995). Telomere structure and function. Current opinion in structural biology *5*, 311-322.

Sfeir, A.J., Chai, W., Shay, J.W., and Wright, W.E. (2005). Telomere-end processing the terminal nucleotides of human chromosomes. Molecular cell *18*, 131-138.

Shay, J.W. (1997). Telomerase in human development and cancer. Journal of cellular physiology *173*, 266-270.

Shay, J.W., and Wright, W.E. (2002). Telomerase: a target for cancer therapeutics. Cancer cell *2*, 257-265.

Shay, J.W., and Wright, W.E. (2006). Telomerase therapeutics for cancer: challenges and new directions. Nature reviews Drug discovery *5*, 577-584.

Simonsson, T. (2001). G-quadruplex DNA structures--variations on a theme. Biological chemistry *382*, 621-628.

Smogorzewska, A., and de Lange, T. (2004). Regulation of telomerase by telomeric proteins. Annual review of biochemistry *73*, 177-208.

Stansel, R.M., de Lange, T., and Griffith, J.D. (2001). T-loop assembly in vitro involves binding of TRF2 near the 3' telomeric overhang. The EMBO journal *20*, 5532-5540.

Tang, J., Kan, Z.Y., Yao, Y., Wang, Q., Hao, Y.H., and Tan, Z. (2008). G-quadruplex preferentially forms at the very 3' end of vertebrate telomeric DNA. Nucleic acids research *36*, 1200-1208.

Tomlinson, R.L., Ziegler, T.D., Supakorndej, T., Terns, R.M., and Terns, M.P. (2006). Cell cycle-regulated trafficking of human telomerase to telomeres. Molecular biology of the cell *17*, 955-965.

Verdun, R.E., and Karlseder, J. (2006). The DNA damage machinery and homologous recombination pathway act consecutively to protect human telomeres. Cell *127*, 709-720.

Zaug, A.J., Podell, E.R., and Cech, T.R. (2005). Human POT1 disrupts telomeric G-quadruplexes allowing telomerase extension in vitro. Proceedings of the National Academy of Sciences of the United States of America *102*, 10864-10869.

Zhao, Y., Hoshiyama, H., Shay, J.W., and Wright, W.E. (2008). Quantitative telomeric overhang determination using a double-strand specific nuclease. Nucleic acids research *36*, e14.

Zhao, Y., Sfeir, A.J., Zou, Y., Buseman, C.M., Chow, T.T., Shay, J.W., and Wright, W.E. (2009). Telomere extension occurs at most chromosome ends and is uncoupled from fill-in in human cancer cells. Cell *138*, 463-475.